Spatial and Temporal Variability in Zooplankton-Fish Interactions in Freshwater Communities

A DISSERTATION
SUBMITTED TO THE FACULTY OF THE GRADUATE SCHOOL
OF THE UNIVERSITY OF MINNESOTA
BY

Beth Victoria Holbrook

IN PARTIAL FULFILLMENT OF THE REQUIREMENTS
FOR THE DEGREE OF
DOCTOR OF PHILOSOPHY

Donn K. Branstrator and Thomas R. Hrabik, Advisers

June 2011

Acknowledgements

I would like to thank my advisers, Dr. Tom Hrabik and Dr. Donn Branstrator for their time, knowledge, and professional guidance over the course of my graduate career. On a personal note, I would also like to thank them for their patience and understanding as I attempted to finish my doctorate while raising a young family. They both know from personal experience the challenges associated with attempting to write coherently while severely sleep deprived.

Also a big thank you to all the collaborators, field assistants, and lab mates who helped me out along the way. It would take me several pages to thank everyone that assisted me while bringing my dissertation to fruition, but I would especially like to acknowledge Brad Ray, Meghan Brown, Dan Yule, Ed Verhamme, and John Schwalbe for assisting me with the field work associated with my third chapter.

I would also like to acknowledge my parents, Mary and John, who provided countless hours of free childcare so I could finish my dissertation. And finally, I am extraordinarily grateful to my husband, John Sandberg, for his field assistance, encouragement, and support. And of course for watching the kids so I could write.

For my sons, Paul and Kyle

Abstract

Abiotic and biotic factors interact at multiple scales to create heterogeneity in the distribution of zooplankton and zooplanktivorous fish in the pelagic area of freshwater lakes. In this dissertation, I explored the predator-prey relationship between these trophic levels in four studies conducted at a variety of spatial and temporal scales. The objective was to identify the processes that may structure spatial heterogeneity in these populations. At the smallest scales in the laboratory, I simulated light and temperature conditions similar to those found in an oligotrophic lake and observed interactions between age-0 lake trout (*Salvelinus namaycush*) and mysids (*Mysis diluviana*), and determined that the intake rate of age-0 lake trout (mg min^{-1}) could be modeled as a function of mysid biomass (mg m^{-2}). I then applied this model to field data collected at intermediate scales at a spawning shoal in Lake Superior and determined that age-0 lake trout distributed in a spatially predictable pattern based on maximizing their growth rate potential. I also explored the more general relationship between pelagic zooplankton biomass and fish density at intermediate spatial scales in three north temperate lakes. In all six depth strata that I analyzed, there was consistent and significant autocorrelation in the distribution of zooplankton biomass, but spatial structure in the distribution of fish density was weaker and more variable. I also detected a significant bottom-up influence of zooplankton biomass on the spatial structure of fish density in three of the six depth strata that I analyzed, but I did not detect any top-down influences of fish density on the spatial structure of zooplankton biomass. Finally, I explored the influence of surface temperature and mesoscale eddies on the distribution of epilimnetic zooplankton biomass

and fish density at large scales in Lake Superior. Circulation patterns associated with prevailing wind conditions could explain some of the spatial patterns in zooplankton biomass, but epilimnetic fish distributions showed no pattern during both years of the study.

Table of Contents

List of Tables

List of Figures

Chapter 3:

Chapter 4:

Chapter 5:

Forward

This is a doctoral dissertation submitted as partial fulfillment of the degree of Doctor of Philosophy in Water Resources Science at the University of Minnesota. Chapters 2, 3, 4, and 5 are papers prepared for publication with coauthors, so the collective "we" is used instead of "I". Coauthors of Chapter 2 are Tom Hrabik, Donn Branstrator, and Allen Mensinger. Coauthors of Chapter 3 are Tom Hrabik, Donn Branstrator, Steve Schram, and Dan Yule. Coauthors of Chapter 4 are Tom Hrabik, Donn Branstrator, and Meghan Brown. Coauthors of Chapter 5 are Donn Branstrator and Tom Hrabik.

Chapter 1: Introduction to Thesis

Understanding the causes and consequences of spatial and temporal heterogeneity has become a primary objective in the study of ecology (Shaver 2005, Hobbs 2006). Identifying processes that create spatial structure is important for understanding the structure and function of ecological systems (White and Brown 2005), for developing accurate models that incorporate spatial patterning (Turner and Chapin 2005, Franklin 2005), and for sampling ecological populations accurately (Ludovisi et al. 2005). A combination of abiotic and biotic processes interacting across multiple spatial and temporal scales can create patchiness in the distributions of organisms (Turner et al. 2001, Franklin 2005, White and Brown 2005, Hobbs 2006), which has been shown to increase coexistence of competing species (Hanski 1983, Bascompte and Sole 1995), to influence predator-prey interactions (Hastings 2001), and to enhance ecosystem productivity (Rovinsky et al. 1997, Brentnall et al. 2003).

Zooplankton and fish comprise two trophic levels in the pelagic region of aquatic ecosystems. Both of these trophic levels are subject to temporal and spatial heterogeneity as a result of abiotic and biotic processes, although processes that occur at longer temporal scales also generally occur at larger spatial scales (Fig. 1). In zooplankton, processes that cause large-scale spatial patterns (> 1 km) may include seasonal periodicity, currents, and upwellings, while processes that cause small-scale spatial patterns (10-1,000 m) may include thermal stratification, inshore-offshore thermal gradients, swimming capacity, food resources, and fish predation (Malone and McQueen1983, Pinel-Alloul 1999). Different processes also may be important for structuring vertical heterogeneity compared to horizontal heterogeneity. Avois et al. (2000) determined that during daylight hours, abiotic factors largely structured vertical heterogeneity in zooplankton populations while a combination of abiotic and biotic factors structured horizontal heterogeneity.

Vertical and horizontal patterns in fish populations are largely influenced by food availability, predator avoidance, and temperature tolerance (Rose and Leggett 1990, Ciannelli et al. 2002). Although predators often concentrate in areas of greater prey

density, mobile prey will attempt to avoid predation (Krebs 1978). Therefore, Sih (1984) hypothesized that positive spatial correlation between predators and prey will only result if prey cannot avoid areas of greater predator density, and that negative spatial correlation will result if prey are mobile and capable of seeking a refuge. Zooplankton have developed behavioral mechanisms to avoid fish predation such as diel vertical migration (Gabriel and Thomas 1988, Ringelberg 1999) or diurnal horizontal migration (Davies 1985, Masson et al. 2001). However, zooplankton are also influenced by food availability and may be subject to predation particularly at night when zooplankton move upward in the water column to feed.

The ability to detect horizontal spatial correlations between fish and zooplankton is highly dependent upon the scale of analysis (Rose and Leggett 1990). If the scale of analysis is too similar in size to the scale of predator-prey aggregations, otherwise positively correlated spatial patterns may appear weakly correlated or non-correlated (Rose and Leggett 1990). For example, at very small space and time scales, predators may be tightly associated with their prey only while actively foraging, so that there is a low probability of detecting this correlation. However, as the scale of analysis is increased, predators are more likely to be located in the general vicinity of the prey, even if not actively foraging, so that detecting this correlation becomes more probable. Additionally, another important consideration for studying spatial patterns in fish and zooplankton communities is that heterogeneity often increases with the size of the sampling area (Pinel-Alloul et al. 1988, Avois et al. 2000). The application of more recent technological innovations, such as hydroacoustics, has enabled the rapid assessment of large volumes of water at relatively fine resolutions. These and other remote sensing technologies are proving to be powerful in assessing questions about scale and spatial heterogeneity in aquatic populations.

Because the technology has only recently become available to survey fish and zooplankton populations simultaneously at fine resolutions, there remain many unanswered questions about spatial correlations between these trophic levels, particularly in freshwater ecosystems. Several marine studies have indicated that there is a tight spatial coupling between trophic levels such that changes in plankton biomass likely propagate up the trophic web and impact higher-order consumers (Richardson and

Schoemann 2004, Ware and Thomson 2005). Few freshwater studies have examined the horizontal spatial relationship between fish and zooplankton. Of those that have, there is evidence that these trophic levels are negatively correlated, suggesting that fish predation may act as a constraint on the distribution of zooplankton through predation or predator-avoidance behavior (George and Winfield 2000, Masson et al. 2001, Romare et al. 2003).

The objective of this dissertation was to examine the spatial correlation between fish and zooplankton using four studies at a variety of spatial and temporal scales (Fig. 2) to identify processes that may structure heterogeneity between these trophic levels in freshwater lake ecosystems. Beginning at the smallest spatial and temporal scales (centimeters and minutes, Chapter 2), I modeled predator-prey interactions in the laboratory between a zooplanktivorous fish (age-0 lake trout, *Salvelinus namaycush*) and their preferred zooplankton prey (mysids, *Mysis diluviana*). I applied this model to field measurements that were made at intermediate spatial and temporal scales (tens of kilometers and months, Chapter 3) to determine whether age-0 lake trout distributed in a spatially predictable pattern based on mechanisms associated with maximizing foraging opportunities on mysids. In Chapter 4, I examined spatial correlations between pelagic zooplankton biomass and fish density in three north temperate lakes at intermediate spatial and temporal scales (thousands of meters and hours) to determine whether fish generally locate in areas of greater zooplankton abundance. And finally, I examined the spatial distributions of zooplankton and fish at large spatial and temporal scales (hundreds of kilometers and days, Chapter 5) in a large lake to determine the effects of broad-scale temperature patterns caused by upwelling and eddies.

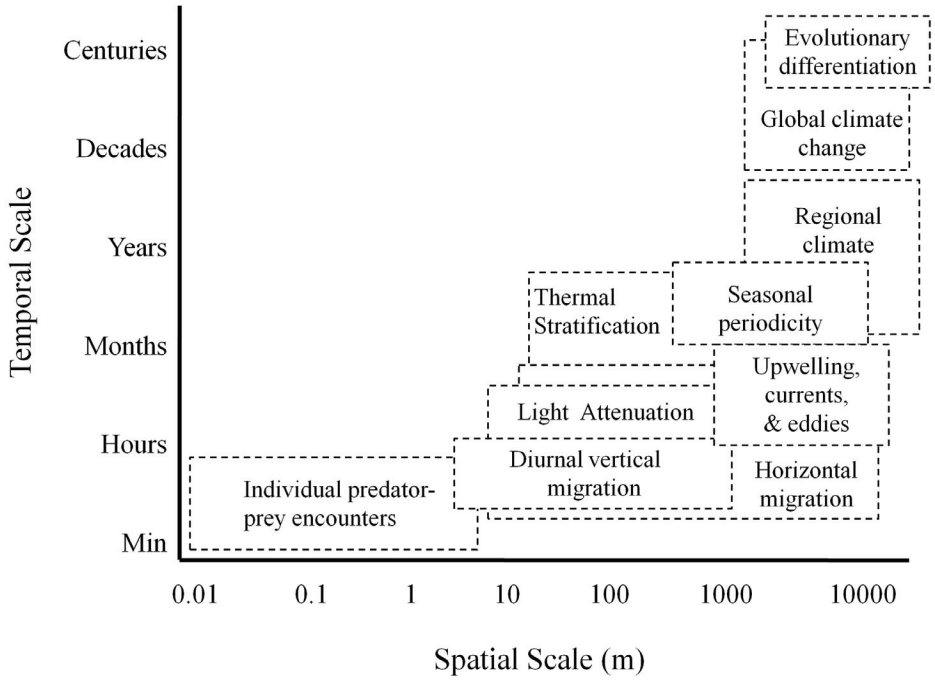

Fig. 1. Abiotic and biotic processes that influence spatial and temporal heterogeneity in freshwater zooplankton and fish populations.

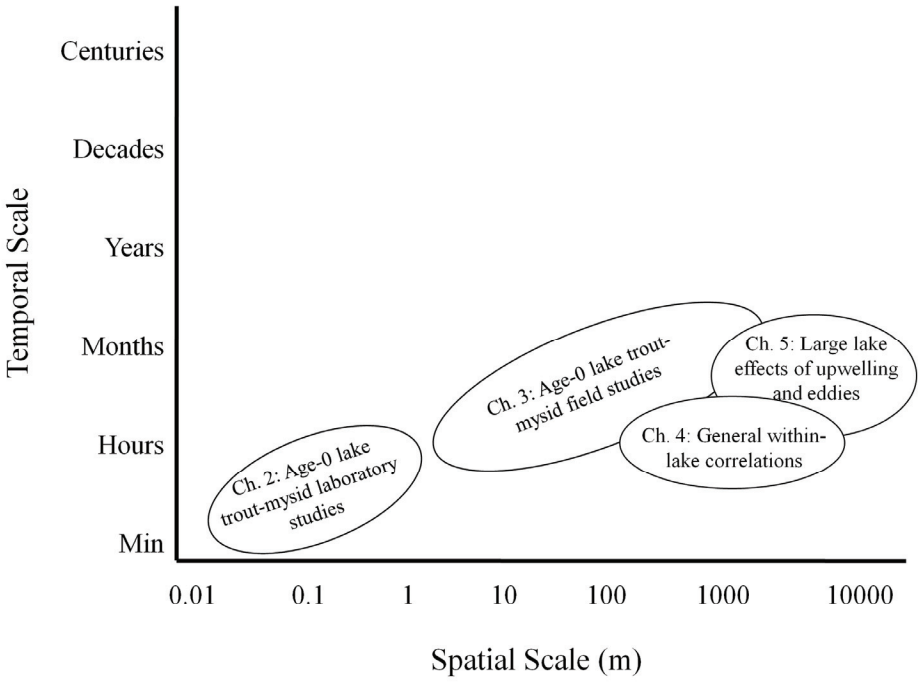

Fig. 2. The spatial and temporal scales and associated processes examined in the four data chapters of this dissertation.

Chapter 2: Foraging Mechanisms of Age-0 Lake Trout (*Salvelinus namaycush*)

Introduction

Lake trout (*Salvelinus namaycush*) is a long-lived, slow-growing top salmonid predator in oligotrophic northern lakes and reservoirs. Lake trout was once an important species to the commercial fishing industry of the Laurentian Great Lakes. Annual catches averaged between 3 and 6 million pounds each in Lakes Huron, Michigan, and Superior prior to the 1940s (Smith 1968). By the 1960s, a combination of sea lamprey predation, overharvesting, and habitat degradation eliminated lake trout from Lakes Michigan, Erie, and Ontario, and severely reduced populations in Lakes Superior and Huron (Smith 1972, Lawrie and Rahrer 1972, Christie 1974). Although restoration efforts have been underway since the 1950s and have been successful in establishing adult lean lake trout populations throughout the Great Lakes, most populations still rely heavily on introductions of hatchery raised fish (Zimmerman and Krueger 2009).

Currently, natural recruitment of lake trout is common only in Lake Superior and parts of Lake Huron (Bronte et al. 2003, Riley et al. 2007, Morbey et al. 2008). Despite decades of failure, reestablishing self-sustaining native lake trout populations throughout the Great Lakes remains a management goal (Zimmerman and Krueger 2009). Mortality during the age-0 life stage has been identified as one of the primary factors impeding rehabilitation of native stocks (Holey et al. 1995, Zimmerman and Krueger 2009). Early Mortality Syndrome caused by thiamine deficiency and predation upon age-0 lake trout have been two factors identified as significant sources of early life stage mortality (Krueger et al. 1995, Tillitt et al. 2005, Zimmerman and Krueger 2009). Recent research also has indicated that in addition to acute morality, thiamine deficiency causes reductions in age-0 lake trout visual acuity, prey capture rates, and specific growth rates (Carvalho et al. 2009, Fitzsimons et al. 2009). The influence of these factors on age-0 lake trout survival are not well understood and are difficult to assess without the development of a baseline foraging model.

The development of a foraging model also may be valuable, particularly when combined with temperature and bioenergetics modeling, for assessing factors that influence age-0 lake trout distribution on spawning shoals. Previous research has indicated that age-0 lake trout are often heterogeneously distributed across spawning shoals and "nursery areas", but the controlling factors have not been determined (Bronte et al. 1995). Identifying the most important factors influencing age-0 lake trout distribution may be useful for assessing the rehabilitation potential of spawning shoals throughout the Great Lakes. Therefore, our objectives were to: 1) determine the foraging parameters of age-0 lake trout, including reaction distances under various light regimes, angles of attack, swimming speeds, and overall foraging success; 2) measure intake rate under various light regimes and prey densities, and model these intake rates using a foraging model and Michaelis-Menten function; and 3) quantify daily consumption rates. Each objective was addressed using data collected in foraging arenas in a carefully controlled laboratory setting.

Methods

Collection and culture

Age-0 lake trout—Approximately 80 hatchery-raised age-0 lake trout averaging 3.0-cm in total length (TL) were received from the Les Voight Hatchery operated by the Wisconsin Department of Natural Resources (Bayfield County, WI) in mid February 2007. Lake trout were housed at the University of Minnesota Duluth (Duluth, MN) in a mechanically and chemically filtered recirculating 150-L system. The tank was maintained in a cold room where the temperature was held constant at 8ºC and the light was varied according to a 14 h light : 10 h dark photoperiod. Age-0 lake trout were fed a mixture of commercial trout pellets (increasing from size-0 to size-3 as the fish grew). To acclimate fish to live prey, lake trout were also fed freshwater oligochaetes (*Lumbriculus variegatus*) and amphipods (*Hyalella azteca*) twice daily until satiated. *L. varigegatus* and *H. azteca* were received from the Mid-Continental Division of the U.S. Environmental Protection Agency (USEPA, Duluth, MN). All experiments conformed to the University of Minnesota animal care protocol.

Prey—Diet analyses of age-0 lake trout captured from Lakes Superior and Huron have indicated that these fish feed primarily on *Mysis diluviana* (formerly *M. relicta,* Hudson et al. 1995, Roseman 2009). In our experiments, we used amphipods (*H. azteca*) as prey in feeding trials until mysids could be captured in the field. Amphipods were received from the USEPA (see above), maintained at room temperature (~50 animals per 3.25 L aerated tank at 20ºC), and fed a mixture of fermented trout pellets, cereal leaves, and yeast (YCT, 20 mL per 3.25 L tank, three times per week). Amphipods were acclimated to a temperature of 8ºC for a minimum of 24 hours prior to use in foraging trials. Amphipods used in foraging trials averaged 3.3 (± 1.0 SD) mm length.

Mysids were captured using a Wisconsin net (50-cm diameter opening, 250-µm mesh) from Lake Superior (St. Louis County, MN) on 17 May 2007 and 28 May 2007 and from Greenwood Lake (Cook County, MN) on 2 June 2007 and 17 June 2007. Mysids were maintained in 38 L aerated tanks (approximately 30 animals per tank) in a cold room at 5ºC and fed upon zooplankton that were captured concurrently during their collection. Mysids used in foraging trials averaged 14.7 (± 2.9 SD) mm length.

Daphnia magna were used for a subset of experiments to compare with results from a previous study on juvenile lake trout foraging (Confer et al. 1978). *D. magna* were received from Carolina Biological Supply Company, Burlington, NC and maintained in a 38 L tank at room temperature (20ºC). *D. magna* were fed 250 mL of YCT and 250 mL of green algae three times per week. Daphnids used in foraging trials averaged 3.0 (± 0.4 SD) mm length

Foraging experiments

Experimental set-up—Trials were conducted beginning on 5 March 2007 and ending on 27 July 2007. The three prey species were used at different times: *H. azteca* from early March until early June (lake trout size: 3.5-7.5 cm TL); *M. diluviana* from mid May through early July (lake trout size: 4.5-8.5 cm TL); and *D. magna* from early through late July (lake trout size: 7.0-9.0 cm TL). Two circular arenas (0.29-m and 0.65-m diameter) were used and water depth was maintained at 7.5 cm. This shallow depth was used to minimize vertical movements of the lake trout within the water column so that measurements of distance and swimming speed could be accurately made using an

overhead digital video camera. Experiments were conducted in a variable temperature dark room where the temperature was maintained at 8ºC and all external ambient light was eliminated. Additionally, a black fabric enclosure was used around the foraging arena to shield fish from any movement of the observer.

Electroretinograms indicated that age-0 lake trout were most sensitive to wavelengths between 490-550 nm with peak sensitivity at 500 nm (B. Holbrook, unpublished data). These wavelengths also comprise the majority of light in deep, clear, oligotrophic lakes inhabited by lake trout. For example, in Lake Superior, wavelengths between 490-550 nm comprise more than 70% of light at a depth of 15 m and more than 90% of light at depths greater than 35 m (S. Green, personal communication).

We simulated oligotrophic lake conditions in a laboratory setting by using cyan light-emitting diode (LED) lights (Cree XLamp XR Series, Durham, North Carolina) ranging from 450-550 nm with peak spectral power at 500 nm. Four light engines with six LEDs each arranged in a pentagonal pattern were mounted 18 cm above the water surface on the corners of the arena to provide diffuse light. The intensities of the LED lights were controlled by using a driver dimmer (IRIS LED driver dimmer, Power Vector, Waterloo, Ontario) and a DMX controller (Elation SCD-6 DMX Controller, Los Angeles, CA). Black mesh filters were used to further reduce light intensity at the two lowest non-zero light levels. Light levels were measured using two light meters (microeinsteins: LI-COR 1400 datalogger, Lincoln, NE; lux: Sper Scientific Ltd. 840020, Scottsdale, AZ). Light intensities used in the foraging trials included 0, 0.007, 0.02, 0.09, 0.6, 4, and 19 $\mu E\ m^{-2}\ s^{-1}$ (equivalent to 0, 0.4, 2.5, 8, 55, 340, and 1965 lx, respectively), which were selected to simulate a range of light conditions under which age-0 lake trout might forage.

Feeding trials were videotaped overhead using a Sony DCR-TRV250 digital video camera recorder (30 fps). The camera had a built-in infrared capacity that was used to record feeding trials conducted at light levels less than 0.02 $\mu E\ m^{-2}\ s^{-1}$. Fish used in foraging trials were separated from the main tank and housed in 9-L tanks that were maintained at 8ºC. All food was withheld for a minimum of 24 hours before experimental trials. Prior to each trial, fish were acclimated to experimental light conditions for a minimum of 30 minutes.

Foraging parameters—To measure foraging parameters, the smaller arena was used for amphipod prey until lake trout grew to approximately 4.5 cm length and then the larger arena was used. The larger arena was used throughout trials where mysids and *D. magna* were used as prey. A 5-mL pipette was modified to provide a larger opening (7 mm) to insert prey into the foraging arena opposite the orientation of the fish. Prey were replaced sequentially as they were consumed. A trial was terminated after 20 minutes or once the lake trout consumed three prey items.

Video was imported digitally using Windows MovieMaker (Microsoft, v. 5.0). ImageJ software (v. 1.38, National Institute of Health) was used to measure the total lengths of the lake trout, the total lengths of the prey, reaction distances, and angles of attack. The reaction distance and angle of attack were measured at the moment a fish oriented towards a prey. The reaction distance was measured between the midpoint of the eyes of the fish and the midpoint of the body of the prey. The angle of attack was calculated as the location of the prey off-axis, with the axis being oriented longitudinally along the head of the fish. DLTdataviewer2 (Hedrick 2008) was used in MATLAB (v. 7.4.0.287, Mathworks Inc., Natick, MA) to estimate the swimming speed of the lake trout and their prey prior to the moment at which the fish oriented towards its prey. The burst attack speed of the lake trout and the burst escape speed of mysids were also measured as the speeds achieved during pursuit (lake trout) and avoidance (mysids) during an attack after which a fish oriented towards its prey.

Intake rate experiments (see below) also were analyzed for reaction distances, angles of attack and swimming speeds if mysid densities were less than 9 m^{-2}, because this density corresponded with three mysids per the large foraging arena, which was a manageable number to track simultaneously.

A subset of data was used to estimate average foraging success, which was defined as the individual probabilities of a fish successfully locating, pursuing, attacking, and retaining amphipods and mysids that were encountered during trials. These probabilities were calculated using methods described in Richmond et al. (2004). Additionally, the amount of time that mysids and amphipods actively moved around the

foraging arena were measured and compared to the amount of time that prey remained stationary.

Intake rate—Prey intake rate (number min^{-1}) for lake trout was evaluated at various light levels (0.007, 0.02, 0.09, and 4 μE m^{-2} s^{-1}) and prey densities (3, 6, 9, 15, 45, 157, and 392 m^{-2} for amphipods; 3, 6, 9, 24, and 157 m^{-2} for mysids). Mysid prey densities corresponded to densities (individuals m^{-2}) observed near a lake trout spawning shoal in Lake Superior (Holbrook 2011). The size of the foraging arena used was dependent on prey density. Trials were conducted for 10 minutes each. Prey that was consumed was replaced so that the total prey density remained constant during a trial. Data were imported digitally (see *Foraging parameters* above). ImageJ software was used to measure the total length (cm) of lake trout in each trial. Numeric intake rates (number min^{-1}) were converted to a biomass intake rates (mg min^{-1}) using an average dry weight (mg) estimate for each prey species based on dry weight measurements in the laboratory (amphipods, 0.66 mg) or on average length measurements and the application of a length-weight relationship (mysids, 3.7 mg; E. Isaac, USGS unpublished data).

Daily maximum consumption—To determine the maximum amount of prey that lake trout could consume in one day, trials were conducted in which lake trout were placed in the smaller (0.29-m) foraging arena and provided unlimited food for 24 hours at 8ºC. Light levels were kept constant at 8.6 μE m^{-2} s^{-1} (800 lx) for the entire 24 hours. Amphipods were used in trials until mysids were available, and the total number of prey consumed was recorded at the end of each trial. Trials were recorded using a 1-sec interval time lapse DVR (Lorex L154SG). Video was used to measure total lake trout length (cm) and to determine the average evacuation rate for mysid trials. This rate was calculated by measuring the amount of elapsed time between consumption of the first mysid and evacuation of fecal matter. It was too difficult to distinguish between fecal matter and amphipods so the evacuation rate was not calculated for amphipod trials.

To estimate the maximum specific feeding rate (C_{max}, mg mg^{-1} wet weight day^{-1}), lake trout length measurements were converted to weight measurements using a general length-weight equation for age-0 lake trout in Lake Superior (B. Holbrook, unpublished

data). Numeric consumption (number day^{-1} was converted to biomass consumption (g dry weight day^{-1}) using an average dry weight estimate for each prey species (see *Intake rate* above). Dry weight biomass of prey species was then converted to wet weight biomass using dry-wet mass relationships reported in the literature (amphipods: Cummins and Wuychuck 1971; mysids: Downing and Rigler 1984).

Statistical analysis and modeling

Statistical analysis—The data on light and reaction distance measured in the foraging parameter trials did not fulfill the requirements of normality. Therefore, data were transformed using Box-Cox transformations (powerTransform) in the Rcmdr package (v. 1.6-2) within the R environment (R 2.11.1, R Development Core Team 2011) prior to conducting statistical analyses. We made multiple measurements for the same fish in response to amphipods and mysids during parameter trials, but individual fish were not identified so repeated measures ANOVA could not be used. Therefore, mixed effect models were used in the nlme package (v. 3.1-97) and the most appropriate model was selected using the likelihood ratio test as the model selection criteria. Post-hoc pairwise comparisons were conducted using Tukey's all-pair comparisons (glht) in the multcomp package (v. 1.2-4) within the R environment to test for significant differences between main effects, or using the contrast package (v. 2.2-1) to test for significant differences between interaction effects. $P<0.05$ was used throughout this study as a cutoff to infer statistical significance.

Modeling—We compared lake trout measured intake rate with two models, a Michaelis-Menten function and a foraging rate model. The Michaelis-Menten function took the form:

$$I = \frac{I_{max} N_p}{\alpha + N_p} \qquad (1)$$

where I is the predicted intake rate (number min^{-1} or biomass min^{-1}), I_{max} is the maximum intake rate (number min^{-1} or mg min^{-1}) when prey density is unlimited, α is the half-

saturation constant (number min^{-1} or mg min^{-1}), and N_p is prey density (number m^{-2} or biomass m^{-2}). The parameters I_{max} and α were estimated using Gauss-Newton nonlinear least-squares methods (nls) in the Rcmdr package within the R environment.

The foraging model was calculated using an encounter rate model of the volume of water searched (Z, m^{-3}) developed by Gerritsen and Strickler (1977):

$$Z = \left(\frac{\pi {R_d}^2}{3}\right)\left(\frac{3v^2 + u^2}{v^2}\right)N_P \qquad (2)$$

where R_d is the reaction distance of the lake trout (cm), v is the swimming speed of the lake trout (cm s^{-1}), u is the swimming speed of the prey (cm s^{-1}), and N_p is the prey density (number cm^{-3}). The encounter rate model assumes that fish use a conical search area when foraging for prey. Therefore, it was inappropriate to calculate prey density using the actual water depth in the foraging arenas (7.5-cm) because the reaction distance of lake trout in response to amphipods and mysids was greater than this depth. Additionally, the encounter rate model was developed for use at a prey density scale of approximately one cubic meter (Gerritsen and Strickler 1977). Therefore, we assumed that the measured areal prey density (number m^{-2}) was equivalent to a three dimensional prey density (number m^{-3}). Amphipods and mysids exhibited primarily benthic behavior at light intensities greater than 0 µE m^{-2} s^{-1}, as did lake trout when they were actively searching for prey. At light intensities of 0 µE m^{-2} s^{-1}, we did not detect successful foraging behavior of lake trout.

To estimate foraging rates on amphipods and mysids (number min^{-1}), Z was multiplied by the cumulative probability (C_p) that a fish would undergo a series of chronological predation events where a prey item would be located, pursued, attacked, and retained (Wright and O'Brien 1984). However, we determined that R_d varied significantly depending on whether prey was mobile or stationary. Therefore we modified equation (2) so that the final foraging model (F, number min^{-1}) took the form:

$$F = \left({R_{di}}^2 P_i + {R_{da}}^2 P_a\right)\left(\frac{\pi}{3}\right)\left(\frac{3v^2 + u^2}{v^2}\right)N_p C_p \qquad (3)$$

where R_{di} was the reaction distance in response to inactive prey, P_i was the proportion of time prey was inactive, R_{da} was the reaction distance in response to moving prey, and P_a was the proportion of time prey moved.

Results

Foraging Parameters

Reaction distances—Foraging trials conducted at 0 μE m^{-2} s^{-1} (0 lx) were excluded from multifactor ANOVA analyses, since there was only one successful capture of an amphipod at 0 cm at this light intensity. When controlling for prey type, prey movement, and light intensity, there was no significant effect of arena size (likelihood ratio test, mixed effect models) so data were combined for both foraging arenas. Analyses conducted on the combined dataset indicated that the most appropriate model included the effect of prey type and prey movement but not the effect of fish length, or light intensity (Fig. 1) on lake trout reaction distance (likelihood ratio test, mixed effect models). Post-hoc comparisons indicated that lake trout reaction distance in response to stationary amphipods versus stationary mysids was statistically insignificant, but that there was a significant increase in reaction distance in response to mobile mysids compared to all other prey groups (Fig. 2). There was no significant relationship between amphipod length and reaction distance, but there was a significant positive relationship between mysid length and reaction distance (Spearman rank correlation coefficient, $\rho=0.16$, $p<0.01$). An analysis of prey movement indicated that amphipods were active on average 55% the duration of a foraging trial while mysids were active on average 30% the duration of a foraging trial.

To determine the effect of using LED lighting that simulated the deepwater aquatic spectrum, reaction distance experiments were also conducted with *D. magna* to compare with previous results published by Confer et al. (1978). The results of our experiments (Fig. 3) indicated that there was a significant difference between reaction distances at the light level of 0.007 μE m^{-2} s^{-1} (0.4 lx) compared with all other light levels (mixed effect models, Tukey's comparisons, $p<0.05$). Reaction distances were similar between our study and Confer et al. (1978) at light levels ≤ 0.09 μE m^{-2} s^{-1} (8 lx).

However, at light intensities ≥ 0.6 μE m^{-2} s^{-1} (55 lx), Confer et al. (1978) measured higher average reaction distances than we did

Horizontal angle of attack—More than half of all events in which lake trout oriented towards prey occurred at angles ±0-60º from longitudinal axis (64% of located amphipods; 56% of located mysids, Fig. 4). Foraging lake trout oriented towards very few prey located posterior to the fish at angles ±150-180º from longitudinal axis (2% of located amphipods and mysids, Fig. 4).

Swimming speeds—The average swimming speed of lake trout was greater than that of either amphipods or mysids (Fig. 5). There was a significant effect of both prey species and prey movement on the burst swimming speed of lake trout after fish located their prey (likelihood ratio test, mixed effect models). Post-hoc comparisons indicated that lake trout had a significantly greater burst speed in response to mobile prey than stationary prey, and in response to mobile mysids compared with mobile amphipods (data not shown). Lake trout burst swimming speeds were positively correlated with the swimming speeds of their prey prior to an attack event (Spearman rank correlation coefficient; amphipods: $\rho=0.46$, $p<0.001$; mysids: $\rho=0.50$, $p<0.001$). In contrast to amphipods, mysids appeared to attempt to avoid capture by quickly propelling themselves forward when a lake trout approached. This may have been the result of mysids sensing a pressure wave from an approaching lake trout. Mysid escape burst speed was significantly greater than the burst speed of an attacking lake trout (Fig. 5; mixed effect models, Tukey's comparison, $p<0.001$).

Foraging success—Age-0 lake trout had an overall average foraging success of 42% for amphipods and 25% for mysids. The low foraging success for amphipods was due in part to a 63% retention rate (Fig. 6). Age-0 lake trout often successfully captured the amphipod in their buccal cavity only to reject the prey. The rejected prey was often recaptured multiple times until it was finally retained. In contrast to amphipods, lake trout had a high mysid retention rate (94%, Fig. 6). However, lake trout only

successfully attacked 31% of mysids that were encountered, located, and pursued (Fig. 6).

Intake rate

At the four light levels that we tested (0.007, 0.02, 0.09, and 4 μE m^{-2} s^{-1}), there were no significant effects of light intensity on the intake rate of lake trout that consumed amphipods (ANOVA, $p>0.05$) or mysids (ANOVA, $p>0.05$). When the intake rates (number min^{-1}) were combined across all light levels for each prey species, there was a significant effect of prey density on intake rates for both amphipods and mysids (ANOVA, $p<0.001$, Fig. 7). Corresponding biomass intake rates (mg min^{-1}) for both prey species are displayed in Fig. 8. There was no significant relationship between fish length and intake rate for amphipods, but there was a correlation for mysids (Spearman rank correlation coefficient; amphipods: $\rho=0.07$, $p>0.05$; mysids: $\rho=0.62$, $p<0.001$).

Measured intake rates (number min^{-1}, mg min^{-1}) were modeled using the Michaelis-Menten function (Eq. 1, Table 1) and the foraging model (Eq. 3, Table 2). Foraging models predicted intake rates similar to measured intake rates at the lowest prey densities. However, foraging models did not include a satiation mechanism to limit consumption at higher prey densities. In contrast, Michaelis-Menten functions closely modeled measured intake rates at both low and high prey densities. Results indicated that there was a maximum intake rate beyond which consumption did not increase. Observations indicated that this functional response was likely the result of satiation due to consuming large-bodied prey.

When plotted on the same scale using biomass estimates, lake trout intake rates (mg min^{-1}) at the lowest prey densities were similar between both prey species (Fig. 8). However, age-0 lake trout had a higher maximum intake rate of mysids compared with amphipods (Fig. 8).

Daily consumption

The maximum daily consumption on a per weight basis (mg mg^{-1} day^{-1} wet weight) decreased as the fish grew in weight (Fig. 9). Based on the maximum daily consumption and the modeled intake rate (Fig. 8), age-0 lake trout apparently need very

little foraging time to achieve maximum consumption. For example, consider a 1000 mg lake trout that our data indicate would consume a maximum of 113 mg wet weight day^{-1} (Fig. 9). At high prey densities, the maximum lake trout intake of mysids was 1.38 mg dry weight min^{-1} (Table 1, Fig. 8), or the equivalent of 8.6 mg wet weight min^{-1} (Downing and Rigler 1984). According to this calculation, a 1000 mg lake trout would only need to forage for approximately 13 minutes per day to achieve the maximum intake rate. However, this might not be obtainable in one meal. Our results indicated that age-0 lake trout consume a maximum of 86 mg wet weight during a 10 minute trial before becoming satiated, and that the estimated time between consumption and evacuation of mysids was approximately 5.25 hours at 8ºC. Therefore, we predict that age-0 lake trout that prey selectively on mysids would likely need to undergo between 1-3 foraging bouts per day at high prey densities, depending on their weight, to satisfy their energetic needs.

Discussion

The results of our trials suggest that age-0 lake trout can forage effectively under very low light but have reduced foraging rates under no light. A minimum reaction distance of 0 cm under no light conditions has also been recorded for adult lake trout (Mazur and Beauchamp 2003). Due to the limitations of our equipment, we did not test non-zero light levels lower than 0.007 $\mu E\ m^{-2}\ s^{-1}$ (0.4 lx), so we were unable to determine the minimum light level under which age-0 lake trout reaction distance might be compromised. However, there are several indications that nighttime foraging by age-0 lake trout may be a relatively minor component of their overall daily intake. First, mysids undergo diel vertical migration at night (Bowers 1988, Gal et al. 1999), so prey densities would become more diffuse. Secondly, light levels at night are much lower than those that were tested in this study. Even under full-moon conditions, the light intensity at the water's surface during summer months in northern latitude lakes is approximately 0.007 $\mu E\ m^{-2}\ s^{-1}$ (0.4 lx, Janiczcek and DeYoung 1987). Using a vertical extinction coefficient of 0.14 measured midsummer at a lake trout spawning shoal in Lake Superior (B. Holbrook, unpublished data), light intensity at the depths of 15-40 m at

which age-0 lake trout are captured (Bronte et al. 1995) would range between $8.4E^{-4}$ μE m^{-2} s^{-1} and $2.5E^{-5}$ μE m^{-2} s^{-1} (0.05 lx and $0.001E^{-4}$ lx). Thirdly, our studies indicate that in areas with high prey density, age-0 lake trout would only need to forage for less than 10 minutes 1-3 times per day to reach their daily maximum consumption. Thus, it is likely that foraging during daylight hours alone could easily maximize age-0 lake trout intake needs. Moreover, during day, mysids would be more abundant on the sediment surface and lake trout reaction distance potentially less compromised by light.

There were some significant differences between the two prey species used in the foraging parameter trials. We selected amphipods for use in trials until we could capture mysids in the field because amphipods are visible, mobile, benthic, and could withstand 8ºC temperatures used in the trials. Although the two prey species had similar average swimming speeds (Fig. 5) and the reaction distances of age-0 lake trout in response to stationary prey were similar (Fig. 2), lake trout had a much longer reaction distance in response to moving mysids compared with moving amphipods (Fig. 2). Increased reaction distance in response to increased prey mobility has been documented in other fish foraging studies (Wright and O'Brien 1982, Howick and O'Brien 1983, Holmes and Gibson 1986). In contrast to amphipods, mysids also had a rapid escape response (Fig. 5) which resulted in a low probability of successful attacks by age-0 lake trout (Fig. 6). This quick, jerky escape response has also been observed in Euphausiids (O'Brien 1987) and marine mysids (O'Brien and Ritz 1988, Rademacher and Kils 1996). The maximum mysid escape speeds that we recorded (63 cm s^{-1}) were similar to reported maximum escape speeds recorded for the marine mysid *Neomysis interger* (80 cm s^{-1}) which in that study resulted in an overall foraging success of 25% for the fifteen-spined stickleback (*Spinachia spinachia*, Rademacher and Kils 1996), similar to the foraging success we measured in our mysid trials.

In contrast to their relatively low attack success rate for mysids, age-0 lake trout had a high attack success rate for amphipods, but the retention rate was lower (Fig. 6). Age-0 lake trout often attacked, captured, and rejected the same amphipod repeatedly. Although most amphipods were eventually retained successfully, we counted all successful captures of previous rejected prey as non-retentions according to methodology reported by Richmond et al. (2004). It is unclear why age-0 lake trout rejected

amphipods at such a high rate. It seems unlikely that the size of the amphipod (~0.3 cm) was too large to retain, given that age-0 lake trout as small as 3.5 cm caught on spawning shoals in Lake Superior consumed mysids averaging 0.9 cm in length (B. Holbrook, unpublished data). Although it is possible that the low retention rate was due to foraging inexperience, we fed lake trout live prey daily. Additionally, age-0 lake trout continued to have problems successfully retaining amphipods after two months of experimental trials. One possibility to explain the low retention rate may be the presence of dorsal tergite spines on *H. azteca*. The presences of similar morphological spines on the amphipod *Gammarus roeseli* was identified as a antipredator defense causing reduced ingestion rates for brown trout (*Salmo trutta*, Bollache et al. 2006). Although *G. roeseli* was much larger than the *H. azteca* that we used in our study, the amphipods in both studies were approximately 10% the total length of the respective fish species. Another possibility may be that *H. azteca* are unpalatable; however, this species is frequently consumed by other fish species (Cooper 1965, Wellborn 1994) and were cultured using a similar food mixture as *D. magna,* which was readily consumed in our foraging trials.

Despite significant differences in the foraging behavior of age-0 lake trout in response to amphipods and mysids, the foraging model (Eq. 3, Table 2) predicted similar intake rates at low biomass prey densities for the two prey species when we converted numeric intake rates (Fig. 7) to dry weight biomass intake rates (Fig. 8). Although the foraging model was fairly accurate at low prey densities, the linear predictions of the model were inappropriate at higher prey densities. Therefore, for this model to be useful for estimating age-0 lake trout consumption, it would be important to incorporate a functional response or a satiation mechanism at higher prey densities. Similar to the foraging model predictions, measured biomass intake rates at low biomass prey densities were similar between the two prey species (Fig. 8). However, at high biomass prey densities the measured intake rates were higher for mysids than for amphipods. This difference in maximum intake rate (mg min^{-1}, Table 1) may have been a result of prey preference for mysids, although results from the daily consumption trials suggest that it may also be an effect of using larger fish on average when conducting trials with mysids. Age-0 lake trout averaged 4.9 cm in length during amphipod intake rate trials and 6.1 cm in length during mysid intake rate trials. When conducting intake rate trials, we did not

detect a relationship between fish length and amphipod intake rate, but we did detect a relationship between fish length and mysid intake rate. Unfortunately, time was a constraint while conducting intake rate trials, and we were unable to eliminate the effect of lake trout growth while attempting to test multiple combinations of light levels and prey densities.

Age-0 lake trout are atypical among young zooplanktivorous fish in that they consume primarily large-bodied macrozooplankton in the wild (Hudson et al. 1995, Roseman 2009). During intake rate trials, particularly at higher prey densities, we often observed lake trout that became satiated within10 minutes and no longer actively sought prey. Even at the lowest mysid density of 3 individuals m^{-2} that we tested, the Michaelis-Menten model (Eq. 1, Table 1) indicated that age-0 lake trout would become satiated within 30 minutes, suggesting that they would only need to forage for 30 to 90 minutes each day, depending on their weight, to achieve their daily maximum consumption. The Michaelis-Menten model also predicts that only at mysid densities less than 0.1 m^{-2} would age-0 lake trout need to forage constantly during daylight hours. One caveat in this prediction is that we did not test for indirect effects of intraspecific competition (Hansson et al. 2001). To have an effect, our results imply that intraspecific competition would have to be strong enough to greatly reduce local mysid density. Nonetheless, it would be useful to examine this effect because age-0 lake trout tend to aggregate on spawning shoals and nursery areas during summer months (Bronte et al. 1995).

Collectively, results from foraging parameter, intake rate, and daily consumption trials indicated that age-0 lake trout are more similar in their foraging mechanisms to piscivorous fish than to zooplanktivorous fish (Breck 1993). Similar to piscivores (Breck 1993), age-0 lake trout consumed only a few, large prey daily (Fig. 9) and had a relatively low probability of overall capture success (Fig. 6). Additionally, age-0 lake trout handling time per prey item was inconsequential compared with time involved in gastric evacuation and digestion. Breck (1993) has hypothesized that piscivores are susceptible to large variability in growth due to the small number of prey consumed daily. Therefore, it is possible that cohorts of age-0 lake trout may experience greater variability in growth compared with other zooplanktivorous fish as a result of small daily variations in prey size and prey consumption.

One of our more unusual findings was that there was no reduction in reaction distance for age-0 lake trout at the lowest non-zero light levels for both amphipods and mysids. This is particularly interesting given that previous studies on adult lake trout have found a reduction in reaction distance at light levels less than 18 lx (Vogel and Beauchamp 1999, Mazur and Beauchamp 2003). Similarly, Confer et al. (1978) found that both age-0 lake trout (7-9 cm) and juvenile lake trout (11 cm) had reduced reaction distances at light levels of 0.9 and 8 lx. Two possible explanations for the difference in our results may be that we used benthic prey (which reduced the number of escape directions for prey), and that we used blue-green LED lighting that more closely resembled the spectrum in the underwater habitat that lake trout occupy.

To determine the effect that LED lighting may have had on our results, we conducted reaction distance experiments using *D. magna*, a pelagic zooplankton species, to compare with results previously published by Confer et al. (1978). Although the length of the age-0 lake trout (7-9 cm) and *D. magna* (0.3 cm) were the same in both studies, there were significant differences in the maximum reaction distances measured at light levels greater than 0.6 $\mu E\ m^{-2}\ s^{-1}$ (55 lx, Fig. 3). One possible explanation for this discrepancy was that at low light levels, only photoreceptors within the peak spectral sensitivity were activated, causing reaction distances to be similar between both experiments, but as the brightness of multispectral lighting was increased in trials conducted by Confer et al. (1978), secondary photoreceptors sensitive to wavelengths outside the peak spectral sensitivity may also have become activated, resulting in increased visual acuity. Although age-0 lake trout were most highly sensitive to wavelengths between 490-550 nm, sensitivity was also measured for wavelengths between 550-600 nm (B. Holbrook, unpublished data). However, Utne-Palm and Bowmaker (2006) demonstrated that the maximum reaction distance of the two-spotted goby (*Gobiusculus flavescens*) increased when the light spectrum used in foraging experiments was most similar to the maximum spectral sensitivity of the photoreceptors.

A second possible explanation for enhanced visual acuity caused by multispectral lighting may be the effect of increased contrast (Lythgoe 1984). As the intensity of multispectral lighting is increased, wavelengths outside the blue-green spectrum may have the visual effect of creating greater contrast between *D. magna* and the aquatic

environment. Longer wavelengths have been documented as creating greater contrast between zooplankton prey and their surroundings (Utne-Palm 1999, White et al. 2005). A third possibility is that multispectral lighting that includes longer wavelengths may increase a fish's sensitivity to motion (Schaerer and Neumeyer 1996, Krauss and Neumeyer 2003). Because age-0 lake trout are very sensitive to prey movement (Fig. 2), improved perception of motion could cause an increase in reaction distance. Although we are unsure of the precise mechanism, our study in conjunction with previous research (Downing and Litvak 2001, White et al. 2005, Utne-Palm and Bowmaker 2006) suggests that reaction distances and foraging rates may be strongly dependent on the light spectrum used in the experiments. We encourage future researchers to use lighting that more closely resembles the underwater light spectrum experienced by fish, as this methodology would likely reduce biases in measured parameters and predictions made by foraging models.

In summary, our study suggests that even at the lowest mysid densities that we tested (3 individuals m^{-2}), age-0 lake would quickly become satiated and would need to forage only intermittingly during daylight hours to achieve their maximum daily consumption. We estimate that mysid densities would need to be less than 0.1 individuals m^{-2} for age-0 lake trout to forage constantly during daylight hours. Therefore, as long as mysids are present, even in relatively low densities, our results suggest that food availability is unlikely a limiting factor influencing age-0 lake trout survival as long as visual acuity is unimpaired by thiamine deficiencies (Carvalho et al. 2009, Fitzsimons et al. 2009). Edsall et al. (2003) made similar conclusions after determining that age-0 lake trout were highly resistant to starvation upon hatching and that food shortages were unlikely to be a major cause of mortality. However, food availability may still be an important factor in determining the spatial distribution of age-0 lake trout on and near spawning shoals, which are likely to have large fluctuations in prey density due to depth and substrate variability. The development of an age-0 lake trout Michaelis-Menten foraging function lays the groundwork for evaluating whether food abundance, in conjunction with temperature and bioenergetic growth data, may be useful in predicting spatial patterns in age-0 lake trout distribution.

Table 1. Variables used in the Michaelis-Menten models (Eq. 1).

	Intake rate (# min^{-1})		Intake rate (mg min^{-1})	
	Amphipods	Mysids	Amphipods	Mysids
I_{max}	0.99	0.37	0.67	1.38
α	3.7	4.6	3.5	17.0

Table 2. Variables used in the foraging models (Eq. 3). RD = reaction distance, P(L,A,C,I) represents the overall probability that an encountered prey would be located, attacked, captured, and ingested.

	Amphipod Model	Mysid Model
Lake trout RD – moving prey (cm)	7.8	19.2
Lake trout RD – stationary prey (cm)	5.8	6.7
Proportion of time prey moved	0.55	0.30
Lake trout swimming speed (cm s^{-1})	6.1	6.1
Prey swimming speed (cm s^{-1})	1.5	2.2
P(L,A,C,I)	0.42	0.25

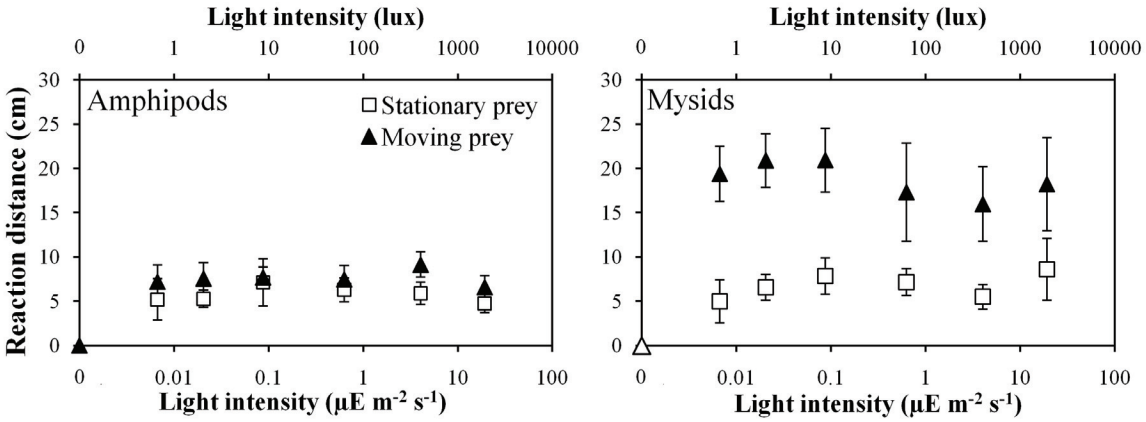

Fig. 1. Lake trout reaction distance in response to amphipods (left panel) and mysids (right panel). Error bars are ±2 SE. On the left panel, the closed triangle located at a light intensity of 0 µE m^{-2} s^{-1} (0 lx) represents one successful lake trout capture of an amphipod at 0 cm (out of *n*=11 trials). On the right panel, the open triangle located at a light intensity of 0 µE m^{-2} s^{-1} (0 lx) represents zero successful captures of mysids at this light intensity even though multiple trials were conducted (*n*=13).

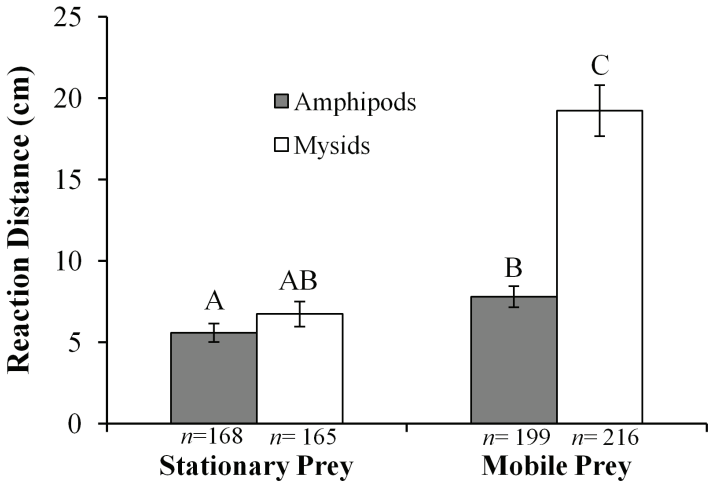

Fig. 2. The average reaction distance (cm) of lake trout in response to stationary and mobile amphipods and mysids. Common letters above the bars represent means that are not statistically different based on Tukey's post-hoc comparisons. Error bars are ±2 SE.

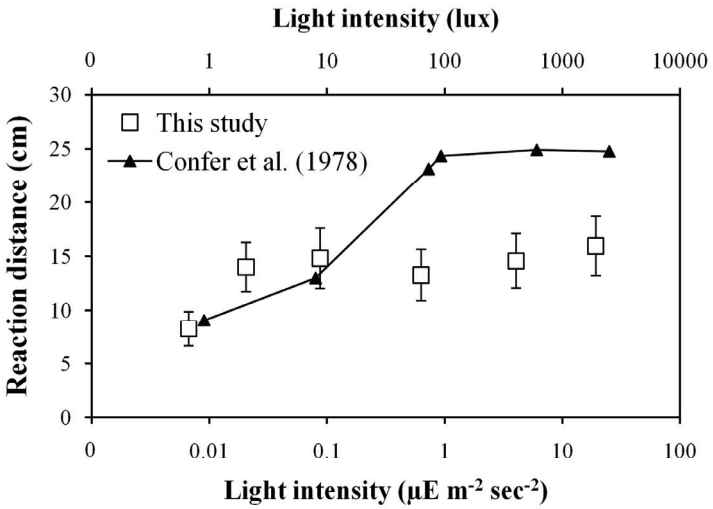

Fig. 3. Reaction distance of age-0 lake trout (7-9 cm) in response to *Daphnia magna* (0.3 cm). Results of our study are compared with Confer et al. (1978) to determine the potential effects in our study of using LED lights to simulate the deepwater light spectrum. Error bars are ±2 SE.

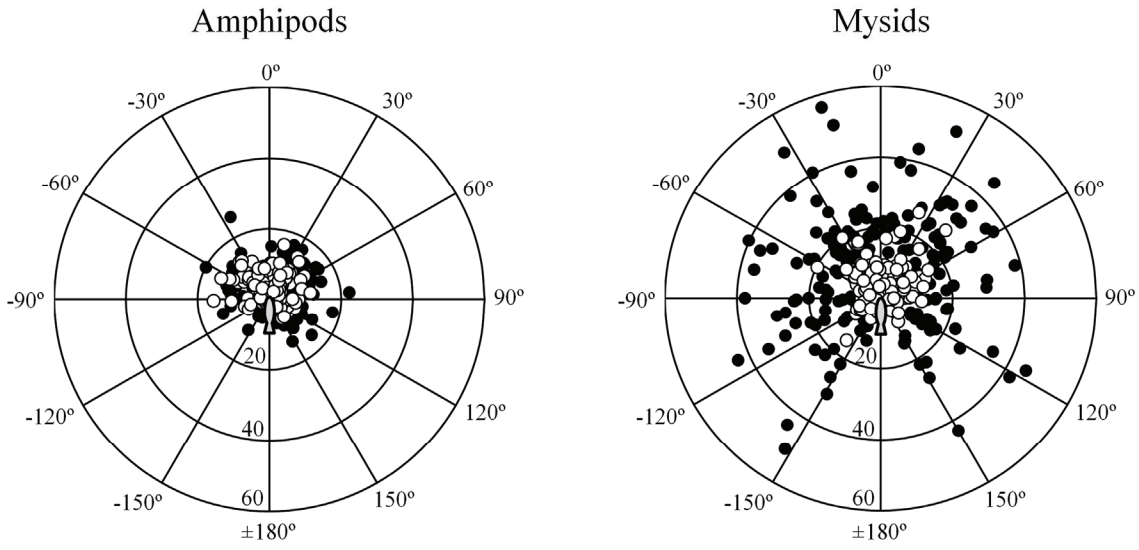

Fig. 4. Simultaneous representation of attack angle and reaction distance for lake trout in response to amphipods (*n*=338, left panel) and mysids (*n*=381, right panel). Closed circles represent moving prey and open circles represent stationary prey. The gray shaded figure in the middle represents the orientation of the fish. Each concentric circle represents a distance of 20-cm.

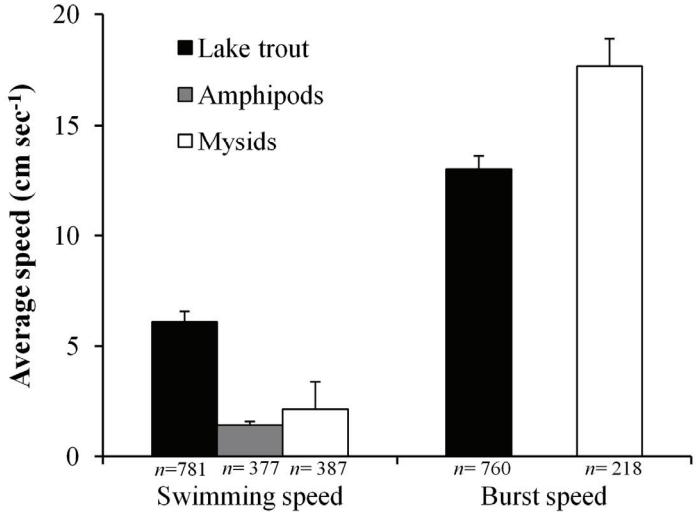

Fig. 5. Average and burst swimming speeds (cm s^{-1}) for lake trout, amphipods, and mysids. Amphipods did not have a burst escape speed. Error bars are ±2 SE.

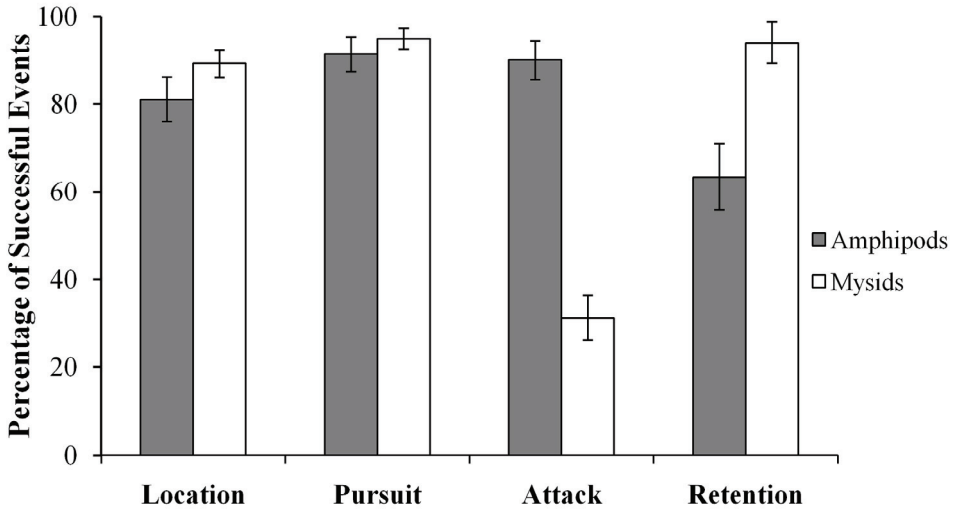

Fig. 6. The average probability that a lake trout successfully located, pursued, attacked, and retained either amphipods or mysids that were encountered during foraging trials. The overall percentage of lake trout foraging success was 42% for amphipods and 25% for mysids. Error bars are ±2 SE.

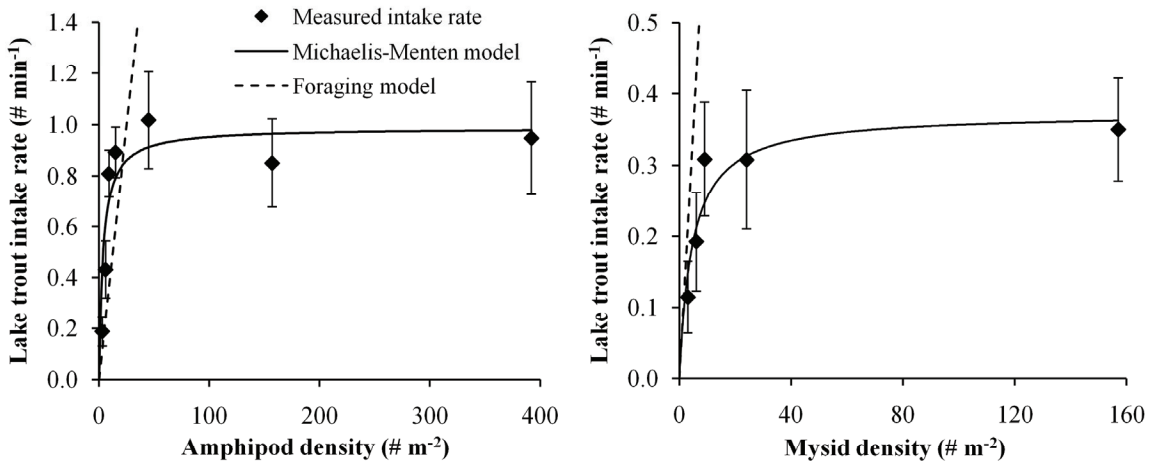

Fig. 7. Measured and modeled numeric intake rates (number min^{-1}) for amphipods (left panel) and mysids (right panel). Variables used in the models are listed in Tables 1 and 2. Error bars are ±2 SE.

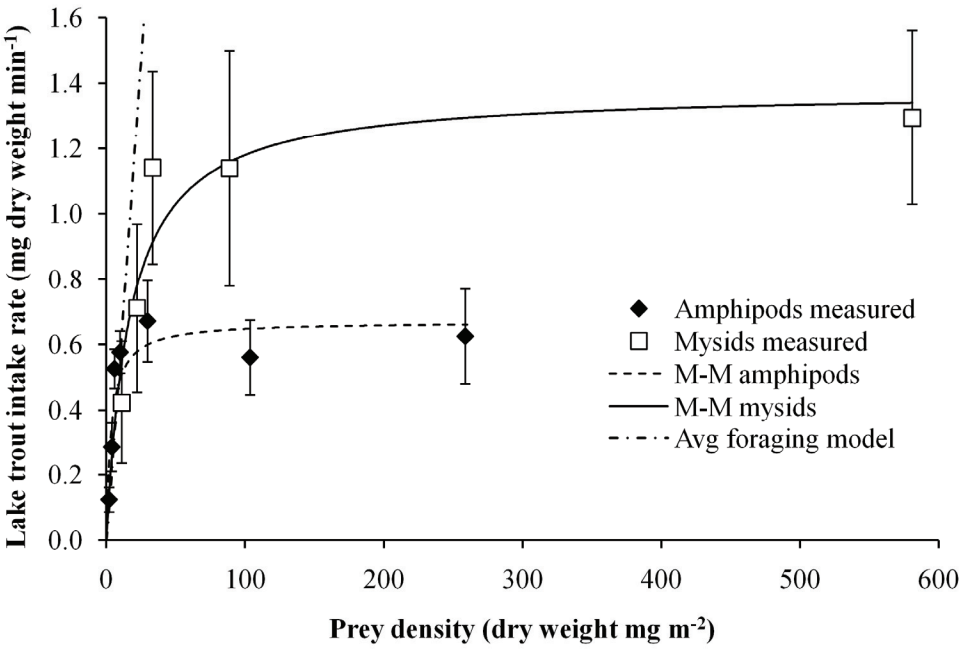

Fig. 8. Measured and modeled biomass intake rates (mg dry weight min^{-1}) for amphipods and mysids. Foraging model biomass estimates were very similar for amphipods and mysids (Table 2), so they were combined into one overall average foraging model. Michaelis-Menten functions were modeled separately (Table 1). Error bars are ±2 SE.

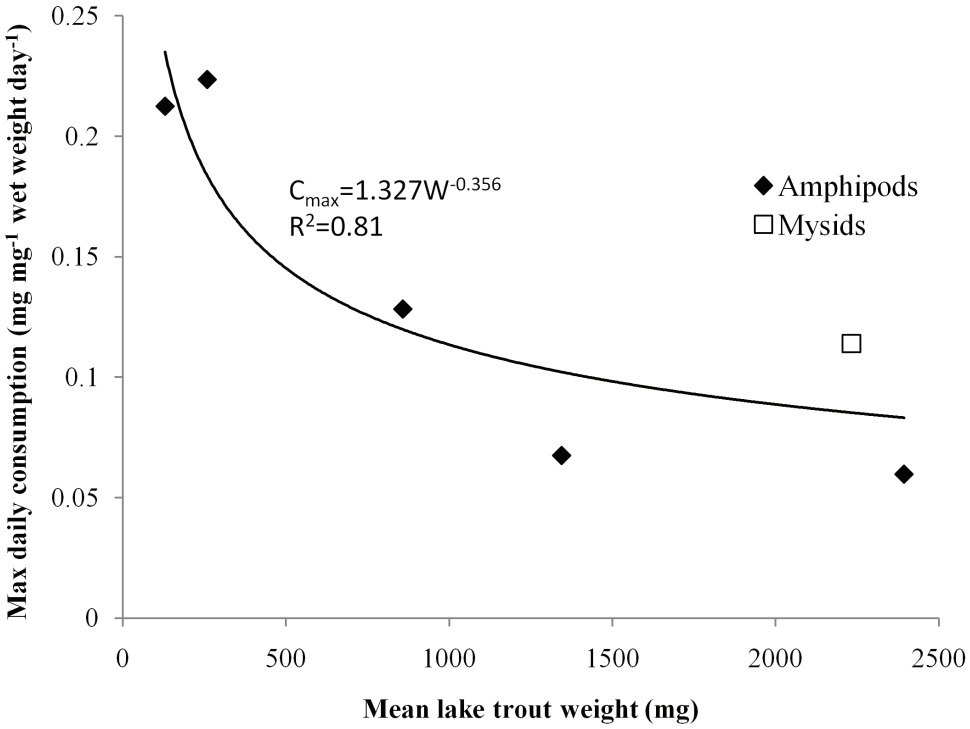

Fig. 9. Maximum daily lake trout consumption (mg mg^{-1} wet weight day^{-1}). Each point represents a composite of two or three 24-hour trials. The regression includes trials involving both mysids and amphipods.

Chapter 3: Modeling the spatial and temporal variability of Age-0 Lake Trout (*Salvelinus Namaycush*) at spawning shoals in Lake Superior

Introduction

Lake trout (*Salvelinus namaycush*) were the top native salmonid predator in the Great Lakes prior to the 1940s and 1950s, at which time a combination of fishing exploitation, sea lamprey predation, and habitat degradation caused extirpation of the species in Lakes Erie, Ontario, and Michigan, and greatly reduced stocks in Lakes Huron and Superior (Smith 1972, Lawrie and Rahrer 1972, Christie 1974). Despite over fifty years of management intervention, self-sustaining populations of lake trout exist only in Lake Superior and parts of Lake Huron (Reid et al. 2001, Zimmerman and Krueger 2009). Great attention has been paid to early life stages as a potential bottleneck that impedes recruitment and hinders recovery of the species in the Great Lakes (RESTORE 1995, Zimmerman and Krueger 2009).

After eggs hatch in the spring, age-0 lake trout are demersal and spend several weeks absorbing their yolk sac before beginning to actively forage (Swedberg and Peck 1984). Several studies have indicated that age-0 lake trout are distributed heterogeneously on spawning shoals before moving off the shoal during their first summer (DeRoche 1969, Peck 1982, Bronte et al. 1995). Habitat that age-0 lake trout occupy after leaving spawning substrates has been described as "nurseries", loosely characterized by a sand substrate, deeper water, and presumably higher prey densities. (Schram et al. 1995, Bronte et al. 1995). Although several mechanisms have been proposed to explain this movement, research has not been conducted to test which factor(s) might explain the patchy spatial distributions of age-0 lake trout on spawning shoals and nursery areas.

Understanding factors that influence the spatial distribution of age-0 lake trout would be useful for assessing the quality of spawning shoals and nursery areas and determining areas best capable of supporting this early life stage. This information would be particularly useful in light of recent research that has determined that thiamine

deficiencies in larval lake trout, resulting from the consumption of alewives (*Alosa pseudoharengus*) by parental stocks, are associated with reduced visual acuity and specific growth rates in individuals that survive Early Mortality Syndrome (Carvalho et al. 2009, Fitzsimons et al. 2009). Because the effects of thiamine deficiency on foraging capabilities would likely be amplified in environments with marginal or poor habitat, targeting management efforts towards rehabilitating spawning shoals and nursery areas with quality habitat may be key for successful recruitment of lake trout in Great Lakes that contain populations of alewives.

The objective of this study was to evaluate a well-known, productive lake trout spawning shoal, Gull Island Shoal, in the Apostle Island region of Lake Superior to evaluate factors which may influence age-0 lake trout spatial distribution throughout their first summer. We evaluated the effects of sculpin abundance, mysid abundance, temperature, foraging potential, and bioenergetic growth rate potential using spatially-discrete modeling techniques and compared these models with the distribution of age-0 lake trout determined from trawl data. A second spawning shoal in the Apostle Island Region of Lake Superior also was evaluated using the model developed on Gull Island Shoal to better understand whether food availability or other factors might explain the lower abundance of age-0 lake trout detected there.

Methods

Study Site

Field collections were conducted at two lake trout spawning shoals in the Apostle Island Region of Lake Superior (Fig. 1). Gull Island Shoal (46.94 N, -90.39 W) was located 7 km northeast of Michigan Island. Shallow depths < 17 m extended southwest from the shoal to Michigan Island, gradually increasing to 25 m depth east of the island before dropping off to > 60 m depth approximately 3 km from the southeast side of the island. On the west side of Michigan Island, depths increased rapidly to > 70 m within 1 km of the island. Gull Island Shoal was sampled from June until October in 2003 and from May until September in 2004.

Sand Cut Shoals (46.73 N -90.69 W) were located approximately 7.5 km east of Madeline Island. The shoals were shallow (<10 m) and depths gradually increased north

and northeast of the shoals to approximately 40 m at the deepest part of the study site. Sand Cut Shoals was sampled from May until September in 2004.

Fish Sampling

Gill nets - Multimesh cotton gill nets (12.5-, 16-, 19-, 25-, 38-, 51-, 64-, 89-, and 127-mm stretch mesh) were set in four gangs over two days and each gang was deployed for approximately 24 h a minimum of once per month at each location (Table 1). Gill nets were deployed at depths ranging between 11 m and 27 m. Fish captured in gill nets were identified, counted, measured (mm), and weighed (g). If more than 20 fish of a single species were caught per mesh size, then a representative sample of 20 fish were measured and weighed. Stomachs were removed from up to 20 fish from each species per mesh size, and frozen until a stomach analysis could be conducted in the laboratory (see *Stomach analysis* below). Additional stomach samples were provided by the Wisconsin Department of Natural Resources from lake trout, lake whitefish, and round whitefish captured at Sand Cut Shoals on 7 Jul 2004. Because cotton gill nets are less efficient than the nylon monofilament gill nets that are more commonly used to sample Great Lakes fishes (Pycha 1962, Henderson and Nepszy 1992), we estimated an index of relative abundance corrected for sampling effort to compare densities of lake trout, lake whitefish (*Coregonus clupeaformis*), and round whitefish (*Prosopium cylindraceum*) between sampling locations and dates.

Trawling - Beam trawls were used to sample age-0 lake trout, deepwater sculpin (*Myoxocephalus thompsoni*), slimy sculpin (*Cottus cognatus*), and spoonhead sculpin (*Cottus ricei*) a minimum of once per month at each sampling site (Table 1). Beam trawls were based on the design described by Stauffer (1981). A 1.2-m wide trawl was used in June and July 2003, and a 2.0-m wide trawl was used for all subsequent sampling, with the exception being trawls that were conducted by the United States Geological Survey Lake Superior Biological Station (USGS-LSBS, Table 1). Trawls used by the USGS-LSBS included a 3/4 Yankee bottom trawl (11.9-m headrope, 15.5-m footrope, 2.2-m wing lines, 9.4-m average wingspread) and a 3-m wide beam trawl based on the design described by Stauffer (1981). The 1.2-m and 2-m beam trawl were towed at an

average of 2.5 km h^{-1}, and the bottom trawl and 3-m beam trawl were towed at an average of 3.5 km h^{-1}. Beam and bottom trawls were conducted at depths ranging between 6 m and 60 m.

At Gull Island Shoal, trawls were conducted in similar locations as those described by Bronte et al. (1995). Additionally, we sampled the west side of Michigan Island in 2003. No age-0 lake trout were captured, and the steep drop-off and silt-like substrate made beam trawling exceedingly difficult. Subsequently, these trawls were excluded from analyses and only the north and east sides of Michigan Island were sampled in 2004.

Samples from the 1.2-m and 2.0-m beam trawl often contained large numbers of mysids that made it difficult to quickly sort and identify fish. Consequently, ethanol was used as a preservative until they could be sorted and processed in the laboratory. All fish captured in the 3-m beam trawl were frozen until they could be processed. All age-0 lake trout captured in the bottom trawl and up to 20 individuals of other fish species were frozen until they could be processed. In the laboratory, fish were measured (to nearest mm), weighed (0.01 g), and stomach contents were analyzed (see *Stomach analysis* below). The remaining fish captured in the bottom trawl were measured individually (mm) but were grouped by species to estimate biomass (g).

Stomach analysis – Stomach contents from lake trout, lake whitefish, and round whitefish were analyzed individually. Up to 15 stomachs from rainbow smelt captured in the same trawl or gill net mesh size were combined and analyzed at one time. Contents were removed, identified, counted, and measured. Fish that were consumed as prey were identified to species when possible, measured to the nearest 1 mm, dried for 24 h at 60ºC, and weighed to the nearest 0.01 g to estimate dry weight biomass. Macroinvertebrates, including mysids, were sorted, and identified to order, except for Chironomidae which were identified to family, amphipods (*Diporeia* spp.) which were identified to genus, and mysids (*Mysis diluviana*, formerly *M. relicta*) which were identified to species. Macroinvertebrates were measured to the nearest 0.1 mm at 8× using an Olympus dissecting microscope, dried for 24 h at 60ºC, and weighed to the nearest 0.001 g. If stomach contents were highly mixed with multiple taxonomic groups, 10% of the sample

was drawn off randomly, and taxon were identified, measured, weighed and compared to the total dry weight of the remaining stomach contents to estimate diet proportions. If zooplankton were present, other prey items were removed and zooplankton were subsampled quantitatively so that a minimum of 10% of the overall sample was counted. Organisms were identified to species, except for *Diaptomus* which was identified to genus. Ten individuals of each taxonomic group were measured to the nearest 0.1 mm at 50×. Numerical estimates were converted to dry weight biomass estimates using published length-weight regressions.

Age-0 Lake Trout Growth

Regression analyses were conducted for length at a given date for age-0 lake trout by calculating an average length for each trawl and averaging these estimates by sampling date. This methodology was applied to incorporate spatial variability in length estimates and reduce the influence of a single trawl when a large number of lake trout were caught. Length measurements were converted to weight estimates using length-weight regressions that were developed using data collected during the survey (Table 2). Length-weight regressions were developed individually for each year at Gull Island. Since only five age-0 lake trout were captured at Sand Cut Shoals in 2004, a composite length-weight regression was applied using data from all locations. This composite length-weight regression was also used to compare body condition for age-0 lake trout captured at each sampling location. A positive residual indicated more weight per length and a more robust body condition, while a negative residual indicated less weight per length.

In the laboratory, sagittal otoliths were extracted from age-0 lake trout captured on 12 and 13 Jul 2004 at Sand Cut Shoals and Gull Island Shoal. Otoliths were prepared using the method outlined by Bergstedt et al. (1990) with modifications made by Negus (1999). Otoliths were ground on one side to the mid-sagittal plane and were continually checked during the grinding process to retain the maximum amount of microstructure detail. Growth increments were assumed to be daily formations (Brothers 1990). Daily growth increments were counted at 400-1,000× using a compound light microscope and

were averaged for age-0 lake trout captured at each sampling location. Back-calculation was used to estimate hatching dates.

Zooplankton Sampling

Zooplankton net tows were conducted concurrently with hydroacoustic surveys at night (at least 1 h after sunset and 2 h before sunrise) to estimate mysid populations in each survey area. All vessel lights were turned off during sampling. A Wisconsin net (50-cm diameter opening, 250-μm mesh) was towed from approximately 1 m off the lake bottom to the surface at a maximum retrieval speed of 1 m s^{-1}. When weather and time allowed, replicate tows were conducted at each sampling site. Between two and six sampling sites around the shoals were sampled on each date. Zooplankton net tows were conducted at depths ranging between 7 m and 50 m.

When replicate tows were conducted, they were combined into a single sample. All samples were preserved in ethanol (75%, final volume). In the laboratory, mysids were counted and measured from the tip of the rostrum to the cleft in the telson at 8× with an ocular micrometer on a Leica dissecting microscope. All individuals were measured if fewer than 10 mysids were present in the sample; otherwise a representative sample of 10 mysids was measured.

Mysid areal density (individuals m^{-2}) was calculated for each sample and converted to areal dry weight biomass (mg m^{-2}) by converting individual length measurements to individual biomass estimates using a length-weight regression developed for mysids in Lake Superior (E. Isaac, USGS unpublished data), and then averaging these biomass estimates.

Hydroacoustic Data

Hydroacoustic surveys were conducted in a zig-zag pattern across the shoals using a Biosonics DT6000 unit (Biosonics Inc., Seattle, Washington), except on 18 and 19 July 2004 when a Biosonics DTX unit (Biosonics Inc., Seattle, Washington) was used. Split-beam 120-kHz (7.3º circular beam) and 430-kHz (6.5º circular beam) transducers mounted on the same towbody (Biofin, Biosonics Inc.) were towed alongside the research vessel at approximately 7.4 km h^{-1} and alternating pulse transmissions were used, except

on 17 and 18 August 2003 when the 120-kHz transducer was unavailable and data were collected with the 430-kHz transducer. Both units were periodically calibrated using standard tungsten-carbide spheres, and the target strengths never varied significantly (<±1 dB) from the known target strength of the spheres. Configurations of the transducers and data collection parameters are listed in Table 3. Sampling dates during which hydroacoustic data were collected are listed in Table 1. All hydroacoustic data were analyzed with Echoview postprocessing software (v. 4.10, Myriax Software Pty., Hobart, Tasmania). Backscatter from bottom sediments was eliminated by manually defining the lake bottom in each file.

To develop a hydroacoustic-mysid biomass regression that could be used to spatially estimate patterns in mysid biomass across the shoals, hydroacoustic data were collected at the site of each zooplankton net tow. Backscatter from the 430-kHz transducer was analyzed down to the maximum depth of each zooplankton net tow. A threshold of -85 dB was applied to the data and fish targets were manually excluded prior to analysis. A correction factor for noise-at-depth was also applied because ambient noise files indicated that the DT6000 began detecting noise at 35 m depth and the DTX began detecting noise at 13 m depth. Nonlinear regression was used to predict mysid biomass (mg dry weight m^{-2}) from corrected hydroacoustic backscatter (Nautical Area Scattering Coefficient, m^2 $n.mi^{-2}$) using the equation:

$$y = B_0 x^{B_1} \quad (1)$$

where B_0 and B_1 were the nonlinear regression coefficients. Nonlinear regression was conducted using the nonlinear least-squares method (nls) in the Rcmdr package (v. 1.6-2) within the R environment (R 2.11.1, R Development Core Team 2011).

The entire 430-kHz hydroacoustic transect from each sampling date was also divided into 75 m horizontal cells and the NASC was analyzed. A maximum threshold was applied to minimize backscatter from fish. This threshold was determined by manually eliminating fish targets from five regions of the dataset from each sampling date and then determining the average maximum threshold that corresponded with

backscatter from fish targets (Table 4). A correction factor for noise-at-depth was applied and mysid biomass for each 75 m cell was estimated using equation (1).

Backscatter from the 120-kHz transducer was used to estimate densities of rainbow smelt (*Osmerus mordax*) on each shoal. At Gull Island Shoal, analysis of trawl data (*see Fish Sampling above*) indicated that age-0 lake trout were present east of Michigan Island. Therefore, estimates of rainbow smelt were made only for this area of the shoal. At Sand Cut Shoals, the entire hydroacoustic transect was analyzed for rainbow smelt densities. Average mean backscatter for rainbow smelt was estimated by conducting a split-beam analysis of single targets using a -55 dB threshold and target detection parameters described by Yule et al. (2006). To determine the size range of single targets likely to be rainbow smelt, length distributions from gill net data (*see Fish Sampling above*) were converted to estimates of target strength using a standard equation for rainbow smelt (Rudstam et al. 2003). The proportion of rainbow smelt-sized targets was calculated using single target analyses and an average mean backscatter was estimated, which varied from -43.0 dB to -46.3 dB depending on the sampling date and location. The proportion of adult lake trout sized single targets was also estimated by converting length distributions from gillnets to estimates of target strength using a standard equation (Love 1977) and an overall mean backscatter was estimated for the remaining proportion of single fish targets excluding those identified as likely to be rainbow smelt and lake trout. Proportions and average mean backscatter for rainbow smelt, lake trout, and all other species was then used to convert echo squared integration data to estimates of density. A minimum threshold value of -65 dB was applied during post-processing analysis of the echo squared integration data.

Spatial Modeling

Bathymetry - Hydroacoustic files from each sampling date were combined into one file for each shoal. Data were divided and analyzed at 10 m horizontal increments. Depth was estimated from the transducer surface to the depth at which the lake bottom was defined using Echoview post processing software. Georeferenced horizontal spatial estimates of depth were analyzed using GS+ 9.0 software (Gamma Design Software, Plainwell, Michigan) and the software was used to fit a spherical or exponential model

(Table 5). Data were modeled so that the number of distance classes multiplied by the lag distance represented approximately half the distance of the two furthest data points.

Georeferenced depth data were imported into a geographic information system (GIS, ESRI ArcMap 9.3). The geostatistical analyst extension was used to fit the same variogram model to the data that was identified using GS+ software. Ordinary kriging was used to create a spatial coverage raster from point data using 10-m cell size. Ordinary kriging parameters included using a standard searching neighborhood where at least two neighbors and a maximum of five neighbors were included and a four sector type was used with a 45º offset.

Temperature - Temperature profiles were conducted a minimum of once per month at multiple locations throughout the study sites using an Alec Electronics ABT-1 depth temperature probe (Table 1). A composite profile was developed for each date by averaging the temperature from multiple sampling locations around each shoal. A mathematical function was used to model the composite temperature profile for each date, and the spatial analyst extension in GIS was used to estimate the temperature at the lake bottom using the depth raster previously developed (see *Bathymetry* above).

Mysid abundance – Previous research has indicated that age-0 lake trout likely forage most effectively during the day (Holbrook 2011). Because hydroacoustic assessments of prey were conducted at night and mysids undergo diel vertical migration (Bowers 1988, Gal et al. 1999), we assumed that nighttime mysid biomass was the equivalent of daytime biomass (mg m^{-2}) within 1 m of the lake bottom. Daytime zooplankton tows confirmed that mysids were absent from the water column.

Georeferenced estimates of mysid biomass predicted from 430-kHz backscatter (see *Hydroacoustic data* above) were fit with an exponential or spherical model using GS+ software (Table 4). A natural log transformation was applied to mysid biomass estimates to normalize the data prior to fitting a variogram model. Data were modeled so that the number of distance classes multiplied by the lag distance represented approximately half the distance of the two furthest data points.

Similar to the development of a spatial depth raster (see *Bathymetry* above), georeferenced natural log-transformed mysid biomass estimates were imported into GIS and the geostatistical analyst extention was used to fit the same variogram model as was identified using GS+ software. The data were kriged using 75-m cell size and the same parameters as for the spatial depth raster (see *Bathymetry* above). The spatial analyst extension in GIS was then used to backtransform estimates of mysid abundance (mg m^{-2}).

Bioenergetics growth rate potential – Bioenergetics equations are based on metabolic energy costs that depend on water temperature, fish weight (wet weight g), and consumption. We used age-0 lake trout length-at-date relationships and length-weight regressions (see *Age-0 lake trout growth* above) to calculate an average weight for lake trout for each sampling date during which hydroacoustics were conducted. The bioenergetics equation for consumption (C, g $g^{-1}day^{-1}$, Kitchell et al. 1977) takes the form:

$$C = C_{max} * P * f(T) \quad (2)$$

where C_{max} is the maximum specific feeding rate as a function of mass at an optimum water temperature (g g^{-1} day^{-1}), P is the proportion of maximum consumption, and $f(T)$ is an exponential temperature dependent function specific to lake trout (Stewart et al. 1983). The proportion of maximum consumption was estimated using a Michaelis-Menten model developed for age-0 lake trout (Holbrook 2011). Two different estimates were used: the proportion of maximum consumption based on intake rate per min (P_{MM}) and the proportion of maximum consumption based on intake rate per day (P). P_{MM} was estimated from a model of intake rate (dry weight mg min^{-1}) based on mysid abundance (dry weight mg m^{-2}, Holbrook 2011). Spatial models of P_{MM} were created by calculating the intake rate (dry weight mg min^{-1}) based on date-specific spatial estimates of mysid biomass (see *Prey abundance* above) and dividing by a maximum theoretical intake rate of 1.38 dry weight mg min^{-1} (Holbrook 2011).

Spatial models of the proportion of maximum consumption based on intake rate per day (P) were calculated in GIS by applying a model of intake rate (dry weight mg

min^{-1}) based on mysid abundance (dry weight mg m^{-2}, Holbrook 2011) and multiplying by minutes of daylight for each hydroacoustic sampling date. Daily intake rate was converted to wet weight (g day^{-1}, Downing and Rigler 1984) and multiplied by a correction factor for the energy density of mysids (3600 J g^{-1}, Cummins and Wuycheck 1971, Rudstam 1989) divided by the energy density of age-0 lake trout (4625 J g^{-1}, Johnson et al. 1999). Corrected daily intake rates (wet weight g day^{-1}) were then divided by date-specific age-0 lake trout weight (g) to estimate daily consumption (g g^{-1} day^{-1}) and divided by maximum consumption (C_{max}) to estimate P. If P was greater than one, then a value of one was assigned.

In GIS, spatial models of growth rate potential (G, g g^{-1} day^{-1}) were calculated for each hydroacoustic sampling date using the energy budget equation (Winberg 1956):

$$G = C - (R + S + E_g + E_x) \quad (3)$$

where C is consumption (g g^{-1} day^{-1}), S is the proportion of assimilated energy lost to specific dynamic action, R is the specific rate or respiration (g g^{-1} day^{-1}), Eg is waste losses due to egestion (g g^{-1} day^{-1}), and E_x is waste losses due to excretion (g g^{-1} day^{-1}). To estimate S, R, E_g, and E_x, physiological parameters were used (Hanson et al. 1997) that were developed for lake trout (Stewart et al. 1983), with the exception that E_g and E_x were calculated as a function of water temperature and consumption without making corrections for indigestible prey. Spatial estimates of temperature and P_{MM} or P were used in conjunction with date-specific estimates of age-0 lake trout weight to estimate growth rate potential.

Data and Statistical Analyses

Age-0 lake trout presence/absence from trawl data were paired with date-specific spatial models of temperature, mysid abundance, P_{MM}, P, growth rate potential calculated from P_{MM} (GP_{MM}) and growth rate potential calculated from P (GP). Data pairings are listed in Table 1. For each trawl, the spatial analyst extension in GIS was used to calculate an average value of each of the aforementioned variables. Data collected in May and June were excluded from this analysis for two reasons: 1) age-0 lake trout were

not captured at either shoal until July, so we could not determine a weight estimate for June hydroacoustic sampling dates; and 2) because we did not capture any age-0 lake trout in June, we could not perform a diet analysis to verify that age-0 lake trout were actively foraging. Age-0 lake trout have been observed to continue to absorb their yolk sac until they reach approximately 30 mm in length (Swedberg and Peck 1984). Additionally, Edsall et al. (2003) found that food can be withheld from lake trout for up to 21 days at 7ºC once they begin to forage without experiencing a reduction in growth or an increase in mortality. Temperatures at or below 7ºC were common at both shoals at depths greater than 10 m throughout most of the month of June.

Several trawling dates occurred approximately halfway between hydroacoustic sampling dates (28 Jul 2004 and 30 Aug 2004 at Gull Island; 28 Jul 2004 at Sand Cut). These trawls were paired with spatial models of bottom temperature and mysid abundance that were averaged for the two nearest hydroacoustic sampling dates. P_{MM} and P were calculated based on the composite mysid abundance spatial model. Spatial models of GP_{MM} and GP were calculated using the composite temperature model and date-specific estimate of weight based on age-0 length-at-date and length-weight regressions.

A classification tree was applied using the rpart package (v. 3.1-48) within the R environment to evaluate the most significant variables explaining the presence/absence of age-0 lake trout from trawl data. Presence/absence data were used rather than estimates of age-0 lake trout density because it is likely that catch efficiencies varied between sampling dates due to differences in trawling equipment, trawling speeds, and bottom substrates that were sampled. The classification tree statistical method is a nonparametric approach that is well-suited for habitat models that include complex interactions among variables (McCune and Grace 2002). The classification tree technique involves recursively partitioning the data into increasingly homogenous subsets. The first step involves growing a maximal tree and the second step involves pruning the tree to avoid overfitting. We used a cost-complexity criterion (cp) and 10-fold cross-validation to prune the tree to an optimum size (Therneau and Atkinson 1997). Variables entered into the analysis included: temperature (ºC), mysid biomass (mg m^{-2}), P_{MM}, P, GP_{MM} (g g^{-1} day^{-1}), GP (g g^{-1} day^{-1}), and sculpin density (individuals m^{-2}), which included all three

species of sculpin present on the shoals. We conducted two classification tree analyses: one where data from Sand Cut Shoal was excluded and one where data from Sand Cut Shoal was included. Misclassification results were estimated using a full jackknife cross-validation (McCune and Grace 2002).

Results

Age-0 lake trout length varied based on sampling date for Sand Cut Shoals and both years at Gull Island Shoal (Fig. 2). Some of this variability was likely due to differences in hatching date because otolith analysis from age-0 lake trout captured in 2004 indicated that the hatch date at Sand Cut Shoals was significantly earlier than at Gull Island Shoal (t-test, $p<0.001$, $t=-11.4$). May 24 was the estimated average hatch date for age-0 lake trout at Gull Island in 2004 and April 27 was the estimated average hatch date for age-0 lake trout captured at Sand Cut Shoals in 2004 (Fig. 3). Accounting for differences in hatch date, the growth rate at Sand Cut Shoals appeared to be slower compared to Gull Island in 2004 (Fig. 3).

Sampling location was a significant factor explaining differences in body condition (ANOVA, $p<0.001$, $F=18.9$, Fig. 4). Post-hoc comparisons indicated that age-0 lake trout at Gull Island in 2004 were significantly heavier per length than at Gull Island in 2003 (Tukey's HSD, $p<0.001$). There was no statistical difference between the means of residuals for age-0 lake trout captured at Sand Cut compared with those captured at Gull Island in 2003 or in 2004.

Stomach analysis of age-0 lake trout indicated that mysids were the predominant prey by proportion of dry weight biomass (Fig. 5). Greater than 85% of age-0 lake trout diets were composed of mysids during all months at all three sampling locations. To estimate the spatial distribution of mysids using hydroacoustics, a regression was developed to convert 430-kHz hydroacoustic backscatter (Nautical Area Scattering Coefficient, m^2 $n.mi^{-2}$) to mysid dry weight biomass (mg m^{-2}). A nonlinear regression explained 95% of the variability in mysid dry weight biomass (Fig. 6).

Vertical temperature profiles from each of the sampling locations indicated that water temperatures were warmer during the months of June at Sand Cut and Gull Island 2004 compared with Gull Island 2003. Strong summer stratification occurred at all three sampling locations by July and the temperature profiles were similar. In August, however, Gull Island 2004 had lower surface temperatures but a deeper thermocline compared to the other two sampling locations. In September, Sand Cut was the coldest of the three sampling locations (Fig. 7).

Classification tree analysis indicated that GP_{MM} (g g^{-1} day^{-1}) was the only significant variable explaining the presence/absence of age-0 lake at Gull Island Shoal in 2003 and 2004 (Fig. 8). The jackknife misclassification rate for the data was approximately 18%. When GP_{MM} was excluded from the analysis, the second most important variable determining the presence of age-0 lake trout was mysid biomass (mg dry weight m^{-2}). However, the jackknife misclassification rate of this dataset increased to 32% compared to 18% when GP_{MM} was the explanatory variable. When data from Sand Cut Shoals was included in the analysis, the pruned classification tree was identical to Fig. 8. The split value remained the same, but the jackknife misclassification rate increased to 39%. Maps displaying date-specific estimations of GP_{MM} overlaid with trawling transects are displayed in Fig. 9.

The application of the classification tree model to Sand Cut data indicated that age-0 lake trout should have been present in all but one of the trawl surveys. Growth data also indicated that age-0 lake trout captured at Sand Cut had lower growth compared to Gull Island in 2004 (Fig. 3). To investigate differences between shoals, we compared growth rates (GP_{MM}), proportion of maximum consumption per minute (P_{MM}), and temperature (ºC) for transects where age-0 lake trout were captured. We determined that differences in GP_{MM} at Sand Cut versus Gull Island were likely attributable to differences in July bottom temperatures since P_{MM} was greater at Sand Cut compared with Gull Island (Fig. 10).

We also compared differences in growth potential across the entire shoal at Sand Cut and Gull Island and found that the total area in hectares at each shoal where GP_{MM} exceeded 0.013 g g^{-1} day^{-1} was comparable at all three sampling locations for the month of July. In September, Sand Cut had roughly twice as much area where GP_{MM} exceeded

0.013 g g^{-1} day^{-1} compared with Gull Island in 2003 and three times as much as Gull Island in 2004 (Fig. 11). Quality of habitat, measured as average GP_{MM} for areas on each shoal where GP_{MM} exceeded 0.013 g g^{-1} day^{-1}, indicated that Sand Cut had a lower average GP_{MM} compared with Gull Island in 2003 and 2004 (Fig. 11), which corresponds with differences in observed age-0 lake trout growth rates (Fig. 2).

The lack of age-0 lake trout captured at Sand Cut could be partially explained by differences in lake trout spawning activity. The Wisconsin Department of Natural Resources has conducted an annual gillnet spawning assessment every mid-October for the past forty years at Gull Island Shoal and Sand Cut Shoal and has consistently estimated the spawning population at Sand Cut Shoals to be roughly a third the population of spawning lake trout at Gull Island Shoal, including during the fall spawning runs preceding our study (Wisconsin Department of Natural Resources, Lake Superior Office, unpublished data). However, differences in spawning activity were not due to the origination of the adult lake trout, since greater than 92% of spawning lake trout were wild rather than hatchery-reared fish at both shoals during the fall spawning runs preceding our study.

A diet analysis was conducted on potential predatory species, including rainbow smelt, round whitefish, lake whitefish, and adult lake trout. No age-0 lake trout were found in any of the diets (Fig. 12). Rainbow smelt, round whitefish, and lake whitefish consumed primarily macroinvertebrates, zooplankton, mysids, and amphipods. Adult lake trout consumed primarily sculpin, rainbow smelt, and mysids (Fig. 12). Population estimates of the four potential predatory species are displayed in Fig. 13. The population of rainbow smelt was significantly higher at Sand Cut compared with Gull Island in 2003 (paired t-test, $t=-5.6$, $p<0.05$) and compared with Gull Island in 2004 (paired t-test, $t= -5.2$, $p<0.05$). The relative abundance of other potential predatory species was variable and comparable between shoals (Fig. 13).

Discussion

Diet analyses of age-0 lake trout from this study were consistent with other studies conducted in the Great Lakes that have found a highly prey-specific relationship with mysids (Hudson et al. 1995, Roseman et al. 2009). However, Hudson et al. (1995)

and Roseman et al. (2009) captured age-0 lake trout earlier in the summer and found a stronger effect of seasonality, whereby age-0 lake trout diets in May and June were composed of up to 50% chironomids and calanoid copepods. Although we detected the presence of chironomid pupae in age-0 lake trout diets captured in July at all three sampling locations, this prey item comprised less than 5% of the overall dry weight biomass. Therefore, we felt it was accurate to develop foraging and bioenergetics models using mysids as the sole prey for age-0 lake trout for the months during which we conducted this study.

Our study also supported previous research that indicated Gull Island Shoal is a successful nursery area for age-0 lake trout. Bronte et al. (1995) documented large numbers of age-0 lake trout present around the shoal between 1990 and 1991, and Schram et al. (1995) found a positive relationship between the relative abundance of female spawning lake trout on the shoal and the density of age-0 lake trout the following summer between the years 1964-1992. Similar to the study conducted by Bronte et al. (1995), we documented the presence of age-0 lake trout east and southeast of Michigan Island, but we did not detect age-0 lake trout north of Michigan Island. Therefore, our data supported hypotheses forwarded by Bronte et al. (1995) that either age-0 lake trout hatched on or near Gull Island Shoal quickly moved off the shoal, or that the main source of lake trout egg deposition was more closely located to the northeast corner of Michigan Island.

Bronte et al. (1995) hypothesized that a sandy substrate was an important component of a nursery area for age-0 lake trout because it likely supported higher concentrations of mysids. Models of mysid distribution combined with detailed substrate maps at Gull Island Shoal (N. Wattrus, Large Lakes Observatory, unpublished data) generally supported this hypothesis for July sampling dates, but there was seasonal variability in August and September. During both years of this study, early in the summer we observed patterns of high mysid biomass over sandy substrates both in shallow nearshore regions and in deep offshore regions. However, as the summer progressed, areas of high mysid biomass were observed over deep sandy substrates at increasing distances offshore from Michigan Island. Although the movement of age-0 lake trout generally followed the seasonal pattern of mysid abundance, our classification

model indicated that growth potential (GP_{MM}, g g^{-1} day^{-1}) was the most important factor influencing the spatial distribution of age-0 lake trout at Gull Island Shoal. These results indicated that food availability in conjunction with temperature-influenced metabolic processes best explained the spatial distribution of age-0 lake trout at Gull Island Shoal.

One interesting facet of our model was that GP_{MM}, which was based on the proportion of maximum consumption per min (P_{MM}), was the most significant explanatory variable for the presence of age-0 lake trout rather than *GP*, which was based on the proportion of maximum consumption per day (*P*). *GP* was a poor predictor of age-0 lake trout presence, likely because age-0 lake trout need so few mysids throughout the day to reach their maximum consumption (Stewart et al. 1983, Holbrook 2011). Therefore, estimated daily consumption was the equivalent of the maximum consumption across the entire shoal for each sampling date. Changes in *GP* were therefore solely dependent on changes in temperature-influenced metabolic processes. Temperature alone was a poor predictor of age-0 lake trout distribution, so it was not altogether surprising that *GP* also performed poorly.

Our results suggest that age-0 lake trout avoided areas with low or negative GP_{MM}, which by proxy, suggests they also avoid areas with low prey availability. These results may seem unexpected given that even at low mysid densities, age-0 lake trout could relatively easily reach their maximum daily consumption (Holbrook 2011). However laboratory studies on foraging habits of age-0 lake trout have not examined the effect of intraspecific or interspecific competition (Confer et al. 1978, Holbrook 2011). Both of these factors may be important because we found that age-0 lake trout densities can reach 100 individuals $hectare^{-1}$ and often in conjunction with other species. Additionally, diet analyses of potential predators indicated that rainbow smelt, lake whitefish, and adult lake trout may be more likely to compete with age-0 lake trout than to prey upon them because all three fish species readily consumed mysids, particularly late in the summer. Therefore, estimates of intake rates from laboratory studies are likely optimistic and present a “best-case scenario”, which may be inflated when accounting for other factors such as competition.

Although competition may explain why P_{MM} and GP_{MM} more accurately reflected foraging and growth rate conditions than P and GP, our data also indicated that food availability was not likely to be a limiting factor during the months of this study. There was ample abundance of high quality growth rate potential across all three sampling locations during the months when we captured age-0 lake trout (Fig. 11). Although the growth rate at Sand Cut Shoals was lower compared with Gull Island Shoal 2003 and 2004 (Fig. 2), our data suggested that this difference in growth was likely due to variation in temperature (Figs. 7, 10). Furthermore, when sculpin densities were included in our classification model as a potential competitor species (Hudson et al. 1995), it was not identified as an important variable associated with the distribution of age-0 lake trout.

When data from Sand Cut Shoal were included in the classification model, the pruned model was identical to when the Gull Island data were used alone. However, the jackknife misclassification rate increased to 39% because the model predicted that age-0 lake trout should be present in many locations where we did not detect them. Because the quantity and quality of growth rate potential does not appear to be limiting age-0 lake trout growth at Sand Cut Shoals (Fig. 11), there are several other potential possibilities to explain the lack of age-0 lake trout at this sampling location: 1) fewer lake trout eggs are deposited; 2) egg mortality is higher; 3) predation rates upon lake trout fry are higher; 4) the primary nursery area went undetected during this study.

Of these four factors, there are data to address the first and third possibilities. Historically, and during the years of this study, the population of spawning lake trout at Sand Cut Shoals was approximately a third of the population at Gull Island Shoal (Wisconsin Department of Natural Resources, Lake Superior Office, unpublished data), which would likely indicate that the abundance of lake trout eggs was lower at Sand Cut Shoals. We also detected a greater abundance of rainbow smelt at Sand Cut Shoals compared with Gull Island Shoal (Fig. 13). Although we did not detect any age-0 lake trout in rainbow smelt diets (Fig. 12), the earlier hatch date at Sand Cut Shoals may have left lake trout fry vulnerable to rainbow smelt predation prior to our first gillnet sets. Other studies have found that rainbow smelt are an important predator on larval cisco (*Coregonus artedi*, Loftus and Hulsman 1986, Hrabik et al. 1998, Myers et al. 2009) and larval lake whitefish (Loftus and Hulsman 1986). Rainbow smelt have been observed to

prey on lake trout fry in other lakes (Hassinger and Close 1984); however predation rates were very low in that study, so it is uncertain whether rainbow smelt could inflict detectable mortality on lake trout fry.

We are unable to address the other two possibilities that may explain the absence of age-0 lake trout in areas where they would be predicted to occur at Sand Cut Shoals. Egg mortality has been indicated as a potential factor limiting age-0 lake trout survival (Jones et al. 1995, Perkins and Krueger 1995, Claramunt et al. 2005). Two major sources of mortality at this early life stage may include egg predation and physical disturbance (Fitzsimons et al. 2007). We did not design this study to assess egg predation, but there is evidence from Lake Michigan and Lake Huron that predators such as sculpin can inflict significant egg mortality (Fitzsimons et al. 2007).

Physical disturbance may include wave action that reduces egg survival through displacement or damage of eggs (Fitzsimons 1995, Perkins and Krueger 1995, Roseman et al. 2001), or fine-grained sedimentation that smothers eggs (Sly 1988, Ventling-Schwank and Livingstone 1994). Wind fetch has been used as an index to approximate physical disturbance (Fitzsimons et al. 2007), but we found that at Sand Cut Shoals, the wind fetch was less than that of Gull Island Shoal from all directions except the northeast, east, and southeast, which were similar in length. One potential difference between shoals may be that Sand Cut Shoals had higher turbidity earlier in the spring. In early June, we recorded a secchi depth of 3.0 m at Sand Cut compared with 13.0 m and 15.5 m at Gull Island in 2003 and 2004, respectively, which may have been the result of outflows from the Bad River and Chequamegon Bay. Age-0 lake trout at Sand Cut Shoals likely hatched over a month earlier than our June secchi depth measurements (Fig. 3), yet it is not known whether turbid conditions at Sand Cut Shoals existed prior to hatching, and whether increased turbidity also resulted in increased sedimentation rates at the shoal itself. Throughout the remainder of the summer, secchi depth measurements at Sand Cut Shoals were similar to those observed at Gull Island Shoal in 2003 and 2004.

Equipment malfunctions and weather conditions prevented us from conducting more extensive trawling at Sand Cut Shoals during many sampling dates. As a result, we may not have adequately detected the primary nursery area at Sand Cut Shoals, particularly during June trawling surveys. In later months, however, the trawls we did

conduct often coincided well with areas of the shoal determined to have high growth rate potential (Fig. 9). Therefore, although more research will need to be conducted at Sand Cut Shoals to determine the primary factors that may be limiting age-0 lake trout survival, preliminary results indicate that potential predation by rainbow smelt and negative effects of spring turbidity would be worth investigating further.

Because this research represents a first attempt at quantifying factors influencing the spatial distribution of age-0 lake trout at spawning shoals and nursery areas, it would be beneficial to further test and refine this model in subsequent studies. We did make several assumptions, which may introduce potential sources of error. For example, we assumed the hydroacoustic model that we developed provided an accurate estimate of daytime mysid biomass within 1 m of the lake bottom (Fig. 6), and we used geostatistical methods to estimate mysid abundance for areas of the shoal that we did not sample because hydroacoustic transects and trawling surveys did not always align well. However, it does appear that geostatistical methods were effective, since variogram models explained a high proportion of variability in the spatial pattern of mysid biomass (Table 4). For example, the lowest R^2 value was 0.89 (19 Jul 2004). Additionally, although two variogram models had a notable nugget effect (16 Sept 2003 and 14 Sept 2004), almost 95% and 91% of the respective variance was still spatially structured.

One weakness in this study is that we were unable to conduct more trawls around each shoal due to equipment failures and weather complications. During some sampling dates, trawl surveys were limited geographically (Fig. 9) and although we attempted to collect trawl data and hydroacoustic data at similar times, surveys were occasionally conducted up to 9 days apart (Table 2). Additionally, we conducted daytime trawls to compare with nighttime hydroacoustic data. Although Bronte et al. (1995) determined that bottom trawl densities of age-0 lake trout were higher during the day versus at night, at least two other studies successfully used nighttime beam trawl surveys to sample age-0 lake trout (Stauffer 1981, Peck 1982). Stauffer (1981) also tested day-night bottom beam trawl differences and determined that nighttime surveys were significantly more productive when conducted over a rough bottom substrate. Therefore, there remains some uncertainty about the best time of day by which to sample age-0 lake trout. Using

presence/absence data rather than density estimates when developing a classification tree model may have eliminated some of these problems associated with sampling efficiency.

In conclusion, this research presents one of the first attempts to assess factors influencing age-0 lake trout spatial distribution at spawning shoals and nursery areas. Statistical analyses indicate that GP_{MM} (g g^{-1} day^{-1}) was the most significant variable influencing age-0 lake trout distribution at Gull Island Shoal, a spawning and nursery area that has had a documented history of high spawner and age-0 lake trout abundance (Fig. 12, Schram et al. 1995). Since GP_{MM} can be easily calculated using estimates of prey abundance and measurements of temperature, this model can be applied to estimate the quality and quantity of habitat at historic lake trout spawning shoals. This information would be valuable for the following reasons: 1) managers could target rehabilitation efforts on shoals that have the greatest growth rate potential for supporting age-0 lake trout populations; 2) potential nursery areas could be identified, which would allow for a more targeted approach to sampling for the presence and abundance of age-0 lake trout populations; and 3) shoals with high quantity and quality of GP_{MM} would likely indicate that competition is not a factor influencing growth and survival of age-0 lake trout, allowing researchers to focus on other factors that may have a negative effect on this early life stage.

Table 1. Dates during which hydroacoustic, zooplankton net tows, trawling, and gill net sampling were conducted. Trawl types included beam trawls (B; 1.2 m, 2.0 m, and 3.0 m) and bottom trawls (BT; 9.4 m average wingspread). Sampling efforts listed on the same line were grouped for analyses (see Methods).

Shoal	Acoustics & Zooplankton	Trawls	Trawl Type	Gill nets	Temp Profiles
GI 2003	12 Jun	17 - 18 Jun[6]	1.2 B	12 - 14 Jun	18 Jun
	31 Jul - 1 Aug	28 - 29 Jul; 5-6 Aug	1.2 B; 2.0 B	14 - 17 Jul	29 Jul
	17 Aug - 18 Aug[1]			7 - 9 Aug	18 Aug
	16 Sep	13 - 14 Sep	2.0 B	15 - 16 Sep[3]	15 Sep
		16 Oct	BT		
GI 2004	27 May				28 May
	22 Jun	13 Jun[6]	2.0 B	4 - 5 Jun[4]	22 Jun
	18 Jul[2]	12 Jul	3.0 B; BT	30 Jun - 2 Jul	18 Jul
		28 Jul	2.0 B		
	12 Aug	14 Aug	2.0 B	1 - 3 Aug	12 Aug
		30 Aug	BT		
	14 Sep	22 Sept	BT	4 - 5 Sep[5]	14 Sep
SC 2004	28 May				29 May
	23 Jun	14 Jun[6]	2.0 B	3 - 5 Jun	23 Jun
	19 Jul[2]	12 Jul	BT	2 - 4 Jul	16 Jul
		28 Jul	2.0 B		
	9 Aug			3 - 5 Aug	9 Aug
	17 Sep	23 Sep	BT		14 Sep

[1] 120-kHz hydroacoustic data were unavailable
[2] DTX echosounder used during these dates
[3] Only 12.5 & 16 mm stretch gill nets set
[4] Only 12.5, 16, 19, 25, & 38 mm stretch gill nets set
[5] Only 51, 64, 89, & 127 mm stretch gill nets set
[6] Trawls excluded from the classification tree analysis due to an absence of age-0 lake trout

Table 2. Equations used to convert age-0 lake trout length (mm) to weight (g). Equations followed the general linear form $\ln(W) = \beta_0 + \beta_1 \ln(L)$ but a correction factor was applied to correct for bias in backtransformations (Miller 1984), so the general form of the equation was $W = e^{\beta_0} e^{\beta_1} e^{\frac{1}{2}\theta^2}$ where θ^2 was the mean square error of the regression. The equation used for Sand Cut Shoals included fish captured from Gull Island Shoal in 2003 and 2004 and the five fish captured at Sand Cut Shoals in 2004.

Site	B_0	B_1	$\frac{1}{2}\theta^2$	N	R^2
GI03	-15.424	3.797	0.009	42	0.98
GI04	-14.422	3.581	0.006	240	0.97
SC04	-14.865	3.686	0.008	287	0.97

Table 3. Configurations and data collection parameters for the transducers and echosounders used in this study.

System	DT6000		DTX	
Frequency (kHz)	120	430	120	430
Transducer beam angle	7.3º	6.5º	6.8º	6.6º
Source level (db//uPa)	222.0	219.0	220.6	218.0
Receive sensitivity (dBC/µPa)	-51.2	-54.0	-43.5	-63.5
Pulse length (ms)	0.4	0.2	0.4	0.2
Pings per second (pps)	1-2	1-2	2	2

Table 4. Variogram models used for creating spatial estimates of mysid biomass (mg m^{-2}) using ordinary kriging. Fish (dB) was the maximum threshold that was applied to remove backscatter from fish targets. Data were fit with either a spherical or exponential model, but in all cases a spherical (sph) model fit the data better. Backscatter (NASC) from the 430-kHz transducer was converted to mysid biomass using a regression (Fig. 6) and log-transformed prior to fitting a variogram model and kriging.

	Gull Island 2003			Gull Island 2004			Sand Cut 2004		
	31 Jul	18 Aug	16 Sep	18 Jul	12 Aug	14 Sep	19 Jul	09 Aug	17 Sep
Fish (dB)	-61	-62	-61	-63	-63	-63	-63	-62	-63
Model	Sph	Sph	Sph	Sph	Sph	Sph	Sph	Sph	Sph
Nugget	0.01	0.01	0.27	0.01	0.01	1.01	0.01	0.00	0.01
Sill	6.696	7.345	4.884	12.04	8.84	11.029	7.013	2.114	7.352
Range (m)	2440	3400	3720	9660	3840	11800	4655	4310	6250
Resid SS	1.30	5.51	1.51	27.7	12.3	3.97	9.67	0.68	2.25
R^2	0.97	0.93	0.95	0.90	0.91	0.95	0.89	0.92	0.97
Lag (m)	489	476	489	490	451	424	295	430	364
Lag #	15	15	15	15	15	15	15	15	15

Table 5. Variogram models used for creating spatial estimates of depth (m) using ordinary kriging at both sampling sites. Data were fit with either a spherical or exponential model, but in both cases a spherical (sph) model fit the data better.

	Gull Island	Sand Cut
Model	Sph	Sph
Nugget	12.5	0.10
Sill	243.1	97.7
Range (m)	4480	8240
Residual SS	1326	588
R^2	0.98	0.98
Lag interval	590	486
Lag number	15	15

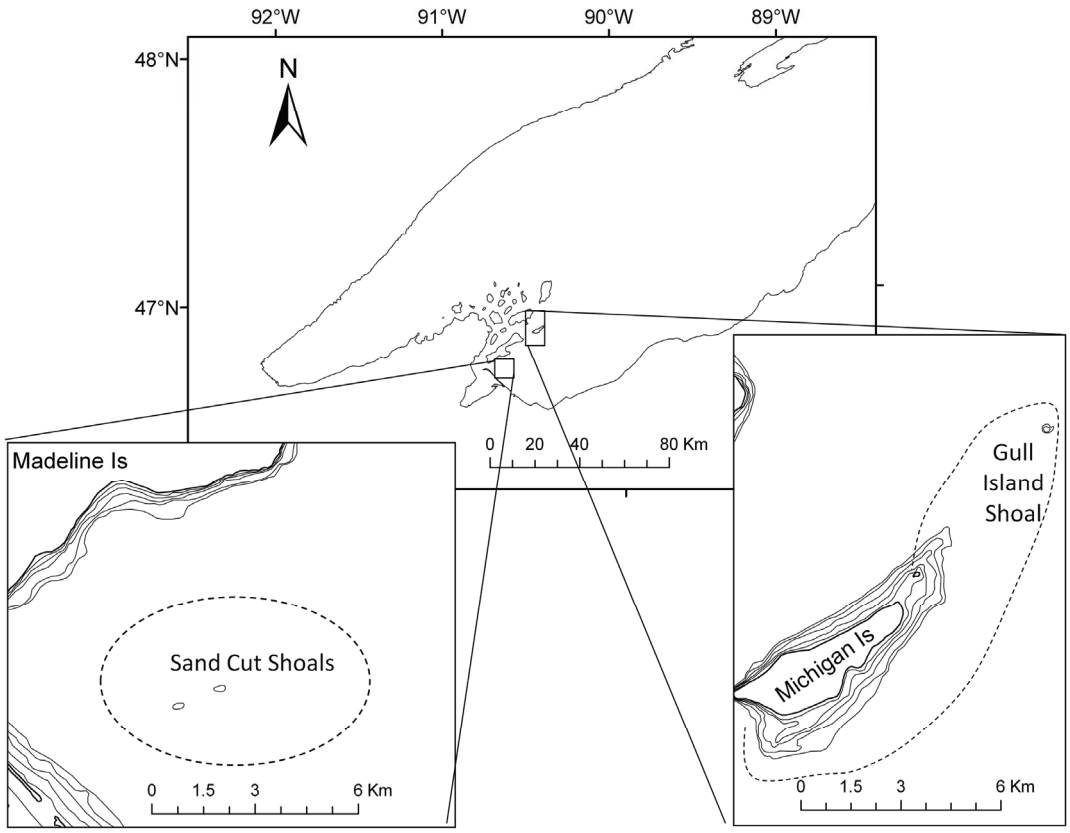

Fig. 1. Sampling sites in the Apostle Islands region of Lake Superior.

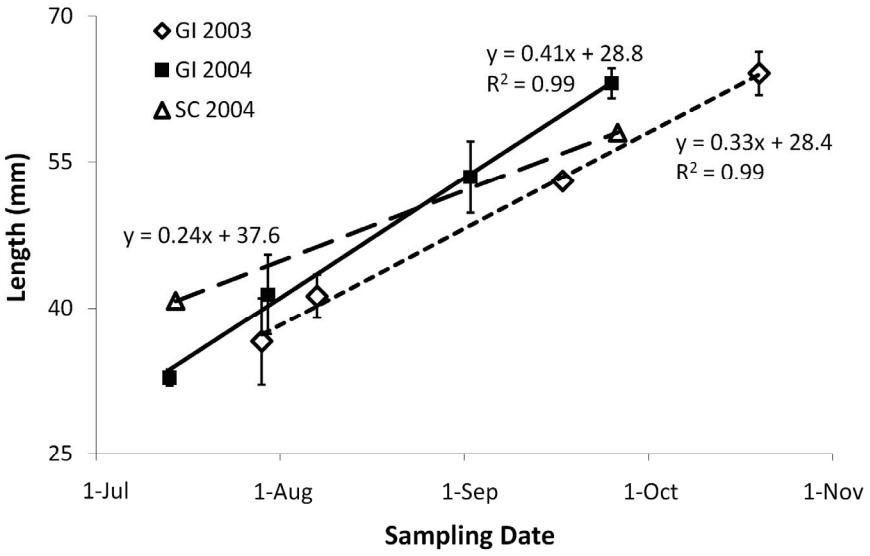

Fig. 2. Age-0 lake trout length by sampling date for each shoal (SC=Sand Cut, GI=Gull Island) and year at Gull Island Shoal. Length was averaged for lake trout captured during each trawl on each sampling date. Error bars are ±2 SE.

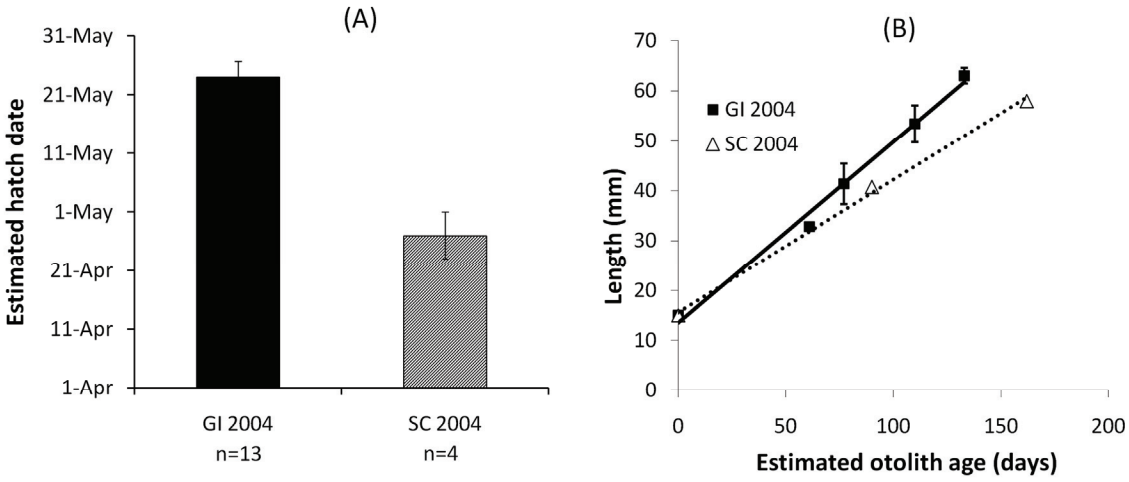

Fig. 3. Estimated hatch date (Fig. 3A) based on deposition of daily growth rings on otoliths for age-0 lake trout captured at Gull Island Shoal and Sand Cut Shoals on July 12-14, 2004, and the corrected length-at-age regression from Fig. 2 using the estimated hatch date as the starting date (Fig. 3B). Error bars are ±2 SE. Length at hatching was estimated to be 15 mm (Daly et al. 1962).

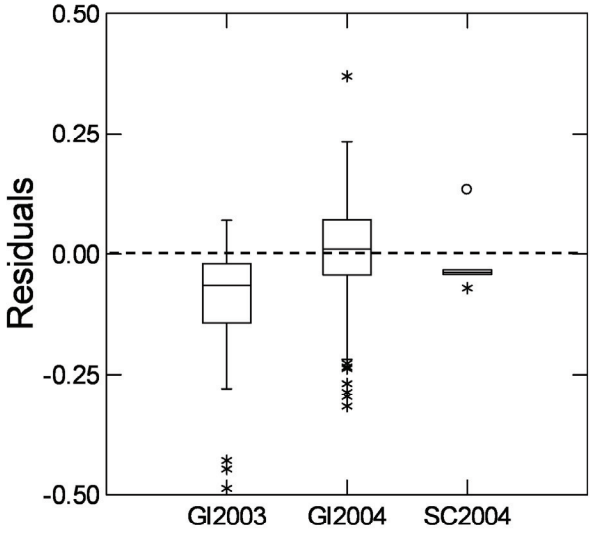

Fig. 4. Box and whisker plot displaying residuals associated with relative body condition of age-0 lake trout from each sampling location. The line represents the median, the box represents upper and lower quartile, and the whiskers represent ±1.5 inter-quartile range. Asterisks represent values that fall between ±1.5 inter-quartile range and ±3 inter-quartile range and open circles represent values that fall outside of the ±3 inter-quartile range. Positive residuals indicate more weight per length while negative residuals indicate less weight per length.

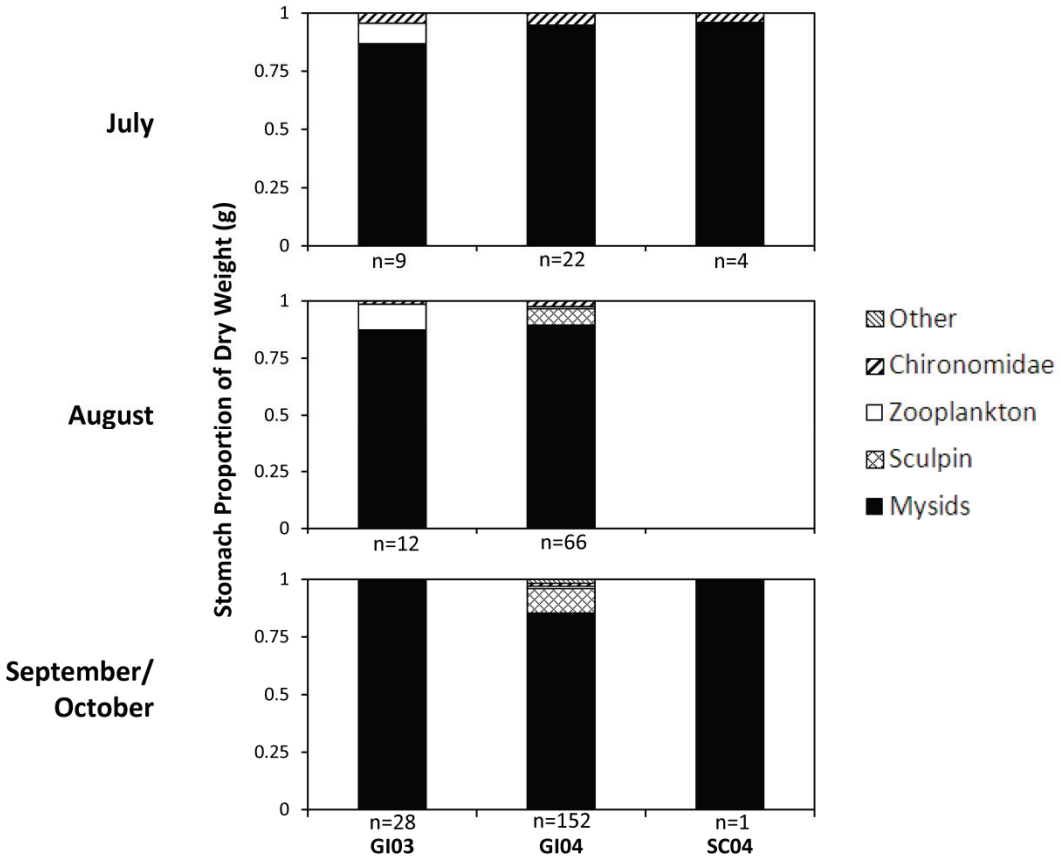

Fig. 5. Diet analysis of age-0 lake trout by sampling month. Mysids were the predominant prey item by proportion of dry weight (g) in the stomachs of lake trout captured at all months at all three sampling locations. The number of age-0 lake trout diets analyzed for each sampling date (*n*) is also reported.

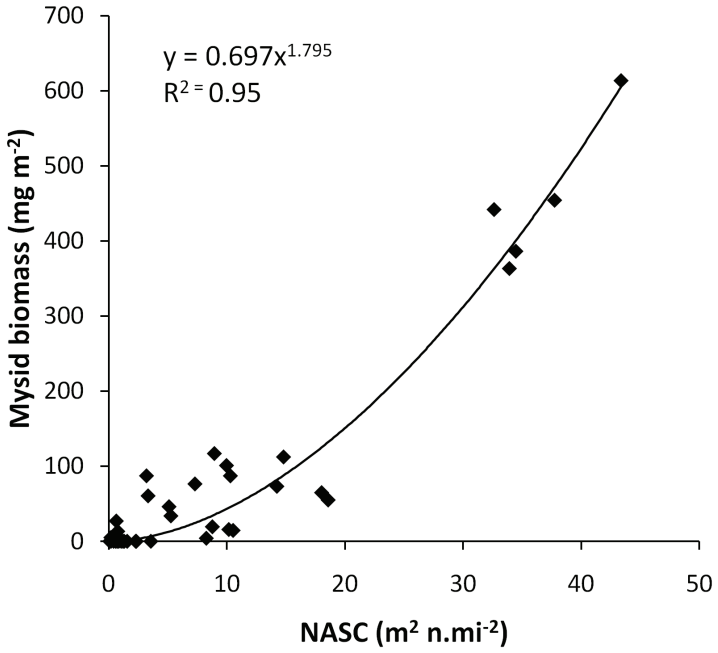

Fig. 6. Nonlinear regression between mysid biomass (dry weight mg m^{-2}) and 430-kHz hydroacoustic backscatter (Nautical Area Scattering Coefficient, m^2 $n.mi^{-2}$).

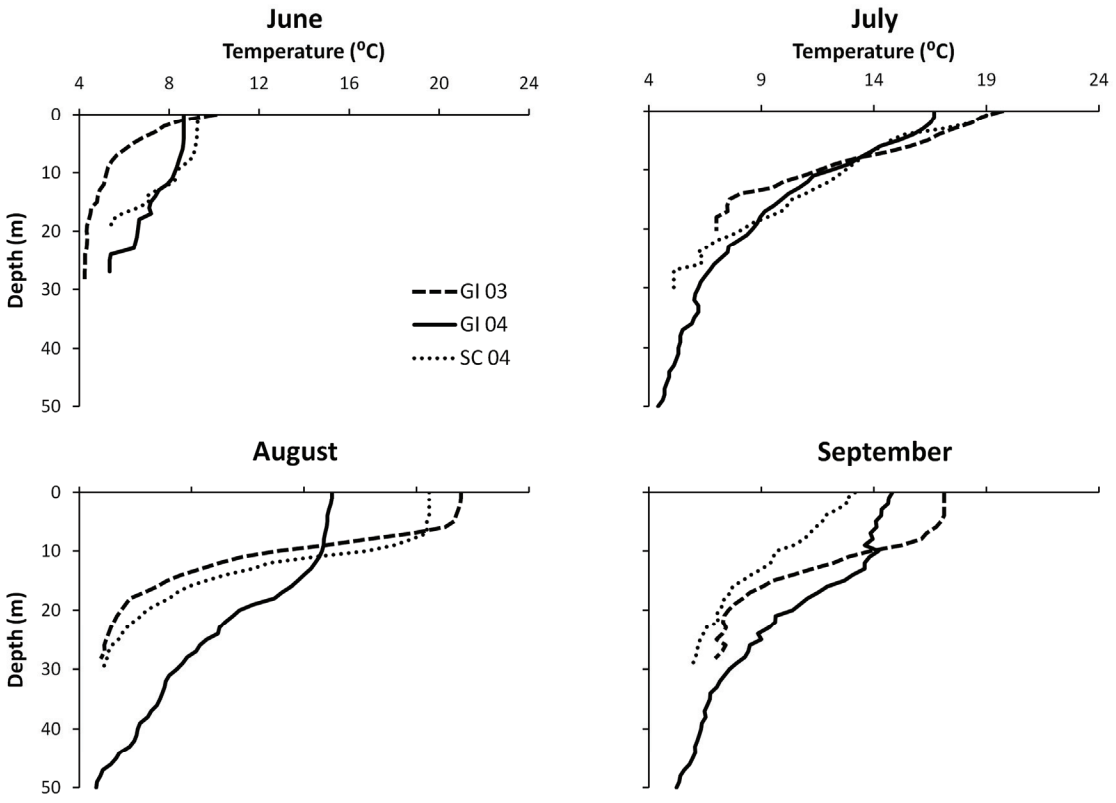

Fig. 7. Composite vertical temperature profiles for all three sampling locations by month.

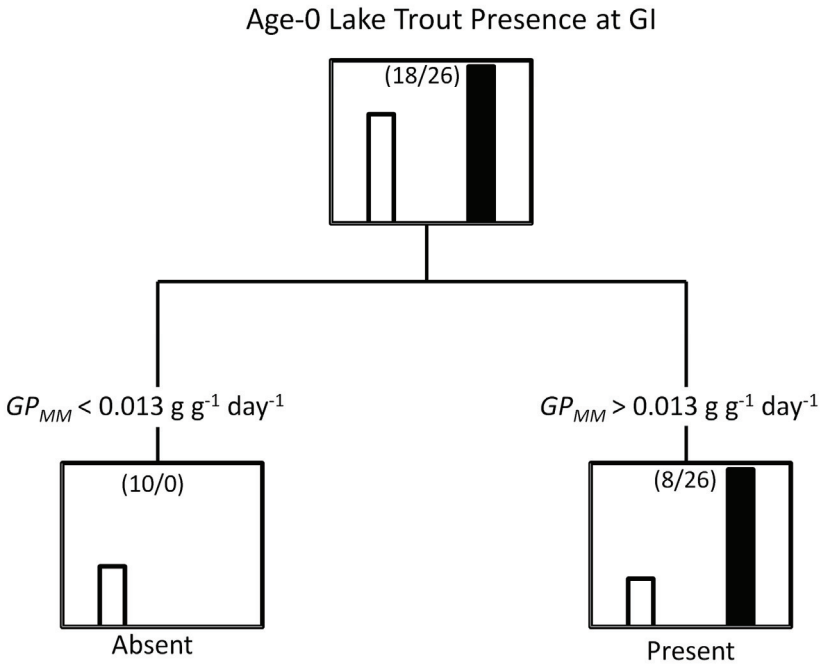

Fig. 8. Classification tree model for the presence of age-0 lake trout at Gull Island Shoal. Vertical bars represent the absence (white) and presence (black) at each node. Absence/presence values are also given in parentheses.

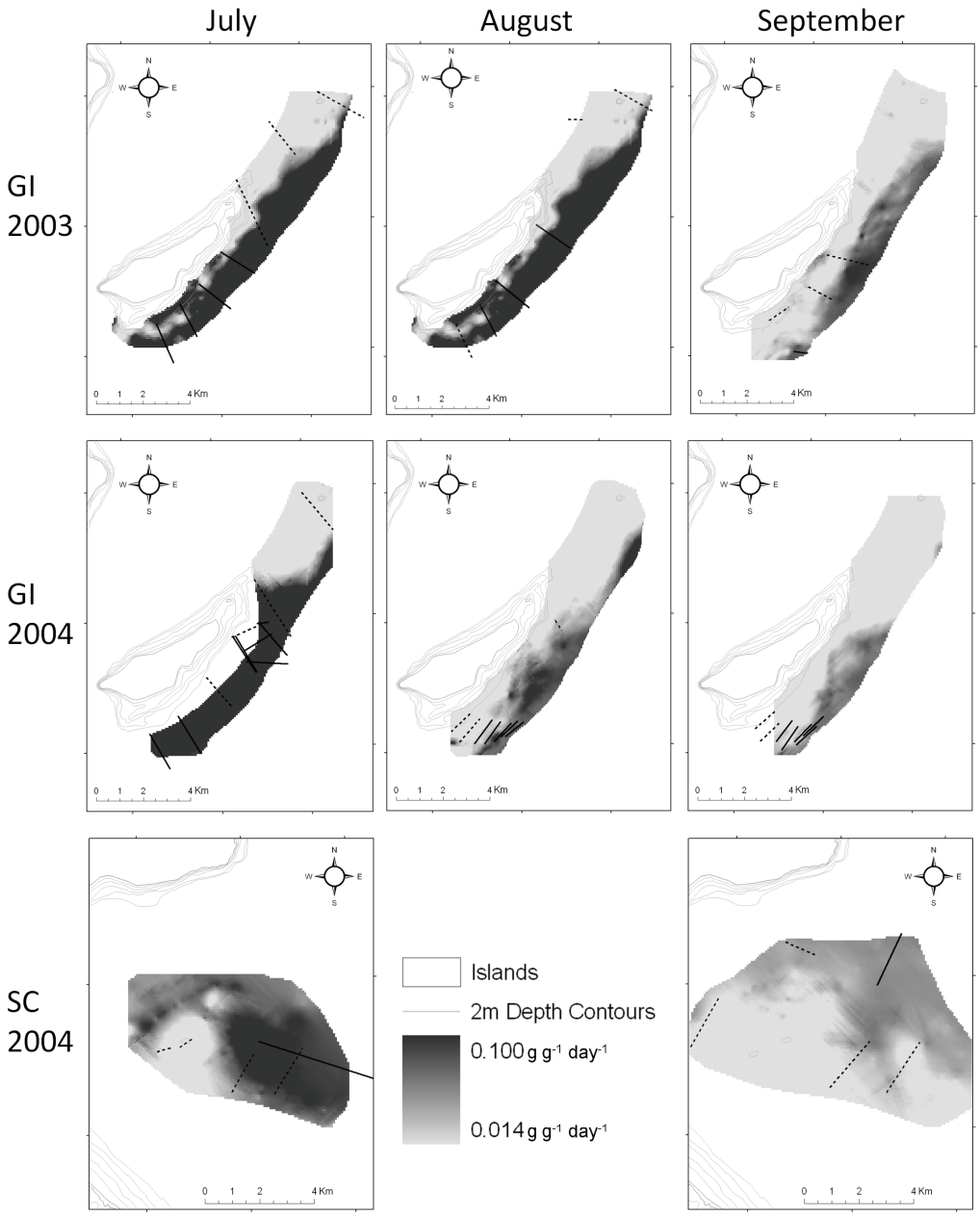

Fig. 9. Trawls where lake trout were present (solid) and absent (dashed) for July, August, and September at Gull Island Shoal in 2003 and 2004, and July and September at Sand Cut Shoals in 2004. Light gray shaded areas represent areas of low growth (0.014 g g^{-1} day^{-1}) and dark gray shaded areas represent high growth (0.100 g g^{-1} day^{-1}) estimated using bioenergetics modeling and the proportion of maximum consumption per minute (P_{MM}). Growth estimates and trawls from early and late July 2004 at Gull Island Shoal and Sand Cut Shoals were combined into one composite representation from each month.

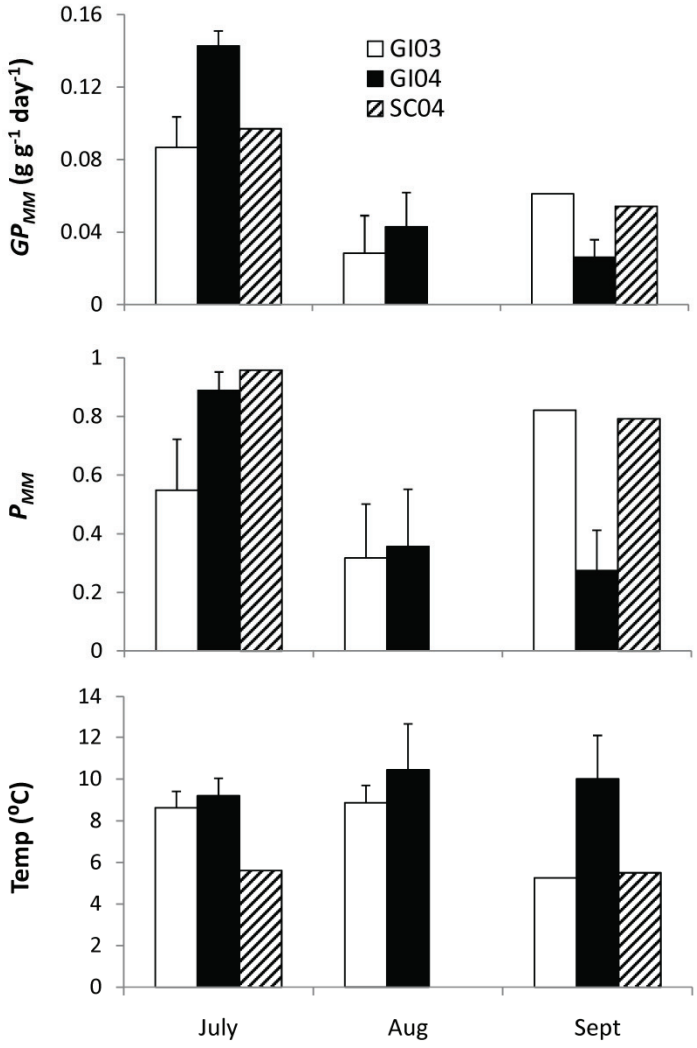

Fig. 10. Average potential growth (GP_{MM}, top panel), proportion of maximum consumption per minute (P_{MM}, middle panel), and temperature (lower panel) averaged for trawls where age-0 lake trout were captured, by sampling location and month. Error bars are ±2 SE. Bars where no error bars are present indicate that age-0 lake trout were only captured in one trawl on that sampling date.

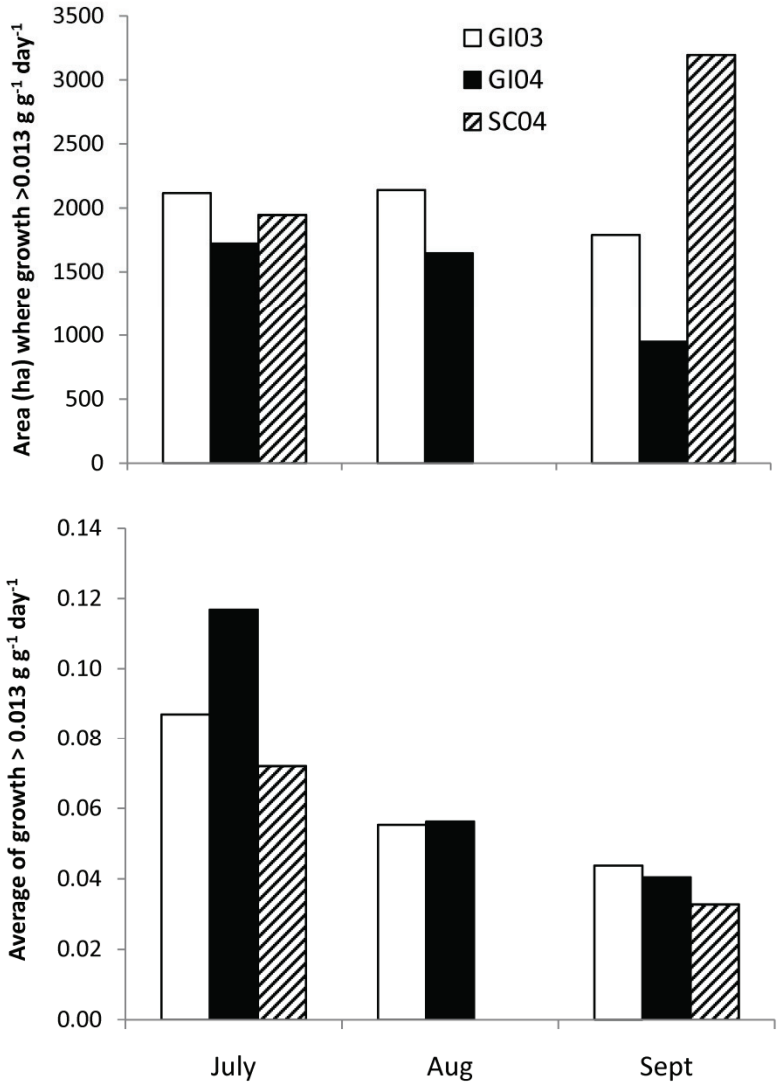

Fig. 11. Habitat quantity, calculated as area in hectares at each shoal where GP_{MM} > 0.013 g g^{-1} day^{-1}, for all three sampling locations by month (top panel); and habitat quality, calculated as the average of areas at each shoal where GP_{MM} > 0.013 g g^{-1} day^{-1} for all three sampling locations by month (bottom panel).

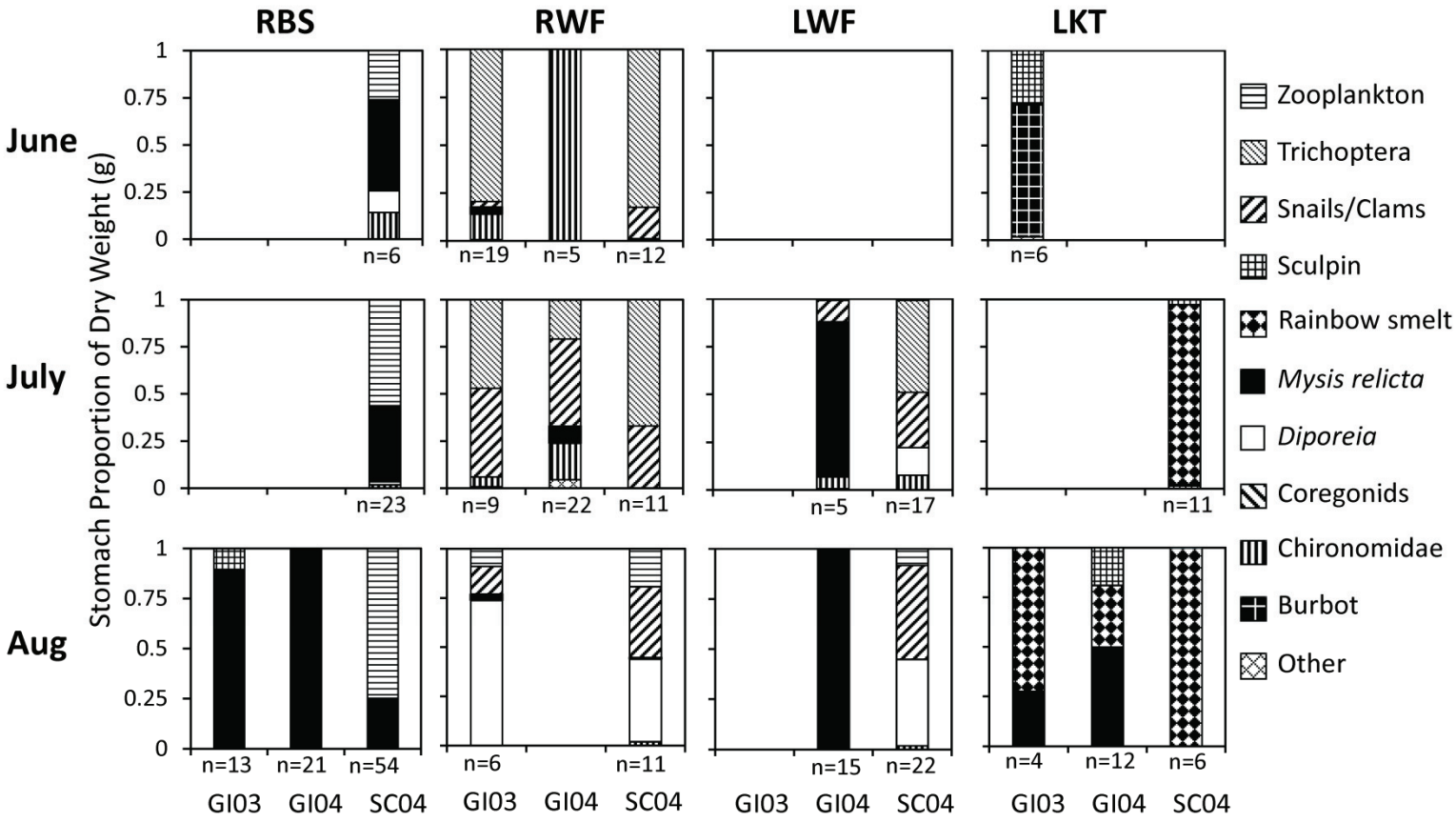

Fig. 12. Diet analysis by proportion of dry weight (g) for rainbow smelt (RBS), round whitefish (RWF), lake whitefish (LWF), and adult lake trout (LKT) for fish captured at each sampling location by month. Diets are shown from dates where the diets of >3 fish were analyzed. The number in each sample is shown (*n*). Empty stomachs were excluded from the sample number.

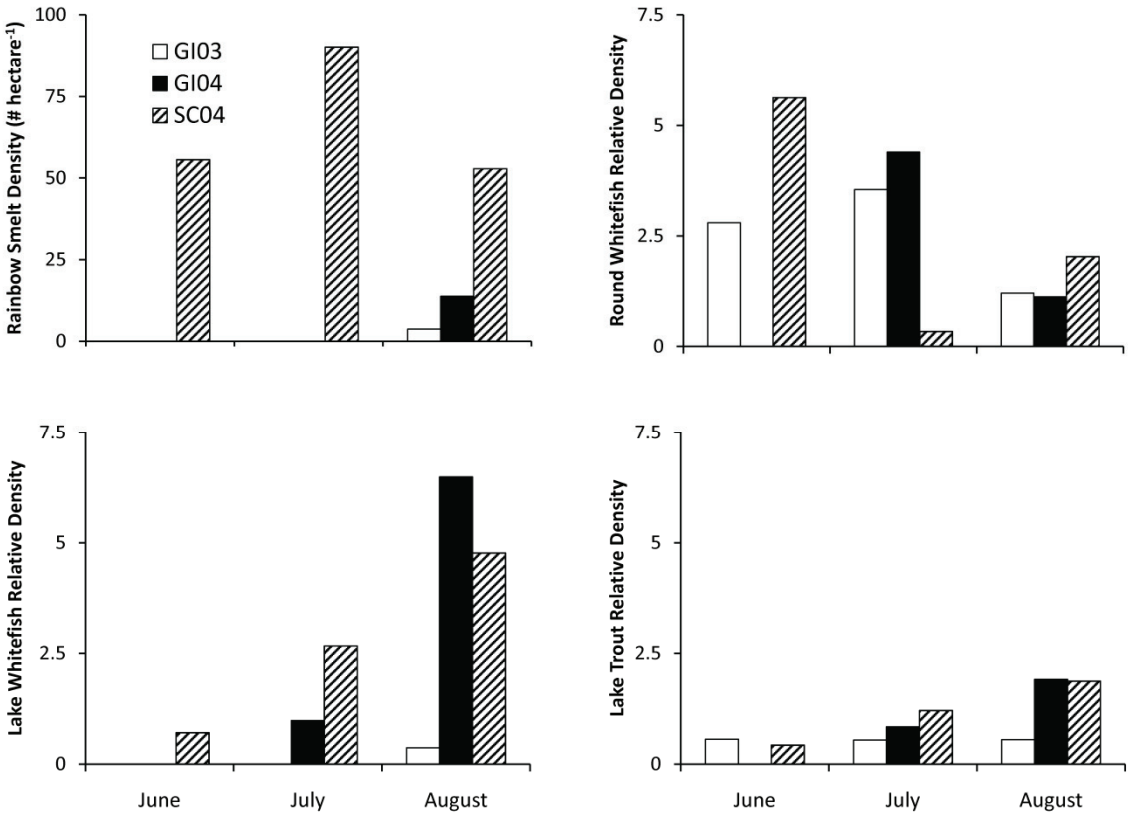

Fig. 13. The density of rainbow smelt (individuals hectare^{-1}, top left panel), and relative abundance of round whitefish (top right panel), lake whitefish (bottom left panel), and adult lake trout (bottom right panel). The 120-kHz transducer was unavailable in mid-August 2003 for estimating the density of rainbow smelt at Gull Island, so data from 31 Jul 03 were used instead. Relative abundance data were unavailable for Gull Island in June 2004.

Chapter 4: Using hydroacoustics to assess spatial distributions of mixed species zooplankton and fish assemblages

Introduction

Zooplankton populations are influenced by abiotic and biotic factors such as temperature, light intensity, wind-induced water movement, food, and predator avoidance that result in spatial aggregations and patchy distributions (Malone and McQueen 1983, Pinel-Alloul 1995, Folt and Burns 1999). High frequency hydroacoustic surveys increasingly have been used to assess spatial patterns in zooplankton populations because large volumes of water can be sampled continuously and rapidly, which enables zooplankton distribution to be assessed at a variety of spatial scales (Nero and Magnuson 1992, Pinel-Alloul 1995). However, hydroacoustic backscatter information must be quantitatively translated to estimate zooplankton density or biomass. Because the application of hydroacoustic technology to assess zooplankton in freshwaters is relatively undeveloped, research to determine the most appropriate quantitative method for converting hydroacoustic backscatter into biological units is necessary. The approach in most freshwater studies has been to use hydroacoustics to assess the distribution of a dominant taxonomic group such as amphipods (Trevorrow and Tanaka 1997), *Mysis diluviana* (formerly *M. relicta,* Rudstam et al. 2008), *Chaoborus* larvae (Knudsen et al. 2006), or *Daphnia pulicaria* (Hembre and Megard 2003). This approach has led to the estimation of species-specific target strengths for these taxonomic groups, any one or more of which may then be used to scale mean volume backscatter and estimate zooplankton density.

There are two main limitations to the approach of using species-specific target strengths to convert hydroacoustic backscatter information into zooplankton density in freshwaters. The first limitation is that zooplankton assemblages are typically multi-species and their compositions are temporally dynamic at short time scales (e.g., diel vertical migration). To accurately convert backscatter data, it thus becomes necessary to

know the relative contributions of several taxonomic groups at many points in time. Compounding this limitation is that species-specific target strength estimates for freshwater zooplankton can range greatly. For example, target strengths as low as -123 dB have been estimated for *Leptodiaptomus sicilis* (Megard et al. 1997) and as high as -61 dB have been estimated for *Chaoborus* (Knudsen et al. 2006). The second limitation is more problematic. The equation typically used to calculate zooplankton volumetric density (ρ_{vS}, individuals m^{-3}) is highly sensitive to large values of the linear mean volume backscattering coefficient (s_v, $m^2\ m^{-3}$):

$$\rho_{vS} = \frac{s_v}{10^{\frac{TS_s}{10}}} \quad (1)$$

where TS_s is the expected target strength returned from an individual of species *S*. In productive freshwater lakes where zooplankton densities are typically high, even small uncertainty in the expected target strength can introduce a large amount of uncertainty into zooplankton density estimates. Within-species target strength estimates can vary 5 dB or more due to individual differences in length, orientation within the beam, and the frequency used to collect the data (Wiebe et al. 1990, Knudsen et al. 2006, Rudstam et al. 2008). In some of the more productive lakes that we surveyed in this study, estimates of zooplankton density (ρ_{vS}) using Eq. 1 could differ by several orders of magnitude when using target strength estimates varying by less than 3 dB.

An alternative approach to convert hydroacoustic backscatter data in a mixed zooplankton assemblage is to develop a model to correlate backscatter with zooplankton density or biomass obtained from net tows. This method has produced relationships that explained 93% and 68% of the variability in total zooplankton densities when *Chaoborus* spp. were absent from an assemblage using backscatter from an Acoustic Doppler Current Profiler (Lorke et al. 2004, Rinke et al. 2007), and 76% of the variability in dry weight biomass for a copepod-dominated mixed zooplankton assemblage using backscatter from a 430-kHz transducer (Holbrook et al. 2006). There may be limitations to applying a mixed species model in marine systems where gas-bearing organisms such as siphonophores and elastic shelled organisms such as gastropods do not return the same amount of backscatter per unit biomass compared with fluid-like zooplankton such as

copepods or euphausiids (Stanton et al. 1994, Martin et al. 1996). However, this limitation may not apply in freshwaters where most zooplankton are classified similarly as fluid-like scatterers (Stanton et al. 1994). Additionally, taxonomic-specific differences due to morphology may be minimized if backscatter is measured using integrated return echoes from a vertical acoustic beam (Stanton and Chu 2000).

Establishing accurate, widely applicable tools for converting hydroacoustic data into biological units for mixed species assemblages of zooplankton is a worthwhile objective for two main reasons. First, as noted above, most zooplankton assemblages are inherently multi-species. Second, hydroacoustics offers a means to obtain data with fine-scale resolution over large spatial distances and short time intervals. Traditional net-tow techniques, by comparison, often sacrifice spatial resolution for taxonomic resolution and are more time and labor intensive at estimating zooplankton density and biomass. When hydroacoustic data are coupled with information on abiotic (e.g., temperature, light, wind) and/or biotic (e.g., fish density, phytoplankton fluorescence) characteristics, a variety of interesting top-down versus bottom-up interactions can be studied at large spatial scales.

One biotic interaction that can be addressed is the relationship between zooplanktivorous fish and zooplankton. Even though this is a main consumer-resource link in pelagic food webs, few studies have addressed the horizontal distributions fish and zooplankton simultaneously. Of the few freshwater studies that have been conducted, there is some evidence that negative correlations exist, suggesting that fish predation or predation risk may act as a top-down constraint on the horizontal distribution of zooplankton through mortality or predator-avoidance behavior (George and Winfield 2000, Masson et al. 2001, Romare et al. 2003). Other studies, however, have found positive spatial correlations between these trophic levels, suggesting that zooplankton abundance has a bottom-up influence on the distribution of fish (Malinen et al. 2001, Rinke et al. 2009). Given the small number of freshwater studies on the topic, there is a need for additional research. Hydroacoustic technology offers a compelling approach because of its ability to survey large volumes of water rapidly and cover large spatial scales with high resolution.

Our objectives in this study were to: 1) establish a general regression to convert hydroacoustic backscatter to zooplankton dry weight for mixed zooplankton assemblages using data from a variety of north temperate lakes, 2) evaluate the mixed species regression with additional hydroacoustic data from the north temperate lakes, 3) compare predictions of density and biomass made using the mixed species regression to those made using published species-specific estimates of target strength, and 4) apply the mixed species regression in an examination of spatial correlations between zooplanktivorous fish and zooplankton in three north temperate lakes.

Methods

Study locations

Data were collected on multiple lakes of varying size and trophic status (Table 1). We sampled 6 inland lakes in Minnesota and Wisconsin, and 3 locations in the Wisconsin waters of Lake Superior. In Lake Superior, the sampling locations were near Michigan and Long Islands, and in Chequamegon Bay, which is a shallow bay on the southern shore of the lake (Fig. 1, Table 1). Two of the lakes (Sparkling and Trout) and a location in the Western Arm of Lake Superior were sampled on additional dates to assess within-lake spatial correlations between zooplankton biomass and fish density (Fig. 1, Table 2).

Zooplankton net tow data

Zooplankton net tows were collected concurrently with hydroacoustic data on all dates noted in Table 1. Net tows were conducted at night, at least 1 h after sunset and 2 h before sunrise to accommodate organisms participating in diel vertical migration. Additionally, vessel lights were turned off during sampling to avoid compromising the collection of highly light-sensitive species such as *Chaoborus* spp. and *M. diluviana*. Zooplankton were collected with a Wisconsin net (50-cm diameter opening, 250-µm mesh; except in Island Lake where a 25-cm diameter opening, 80-µm mesh net and a 50-cm diameter opening, 500-µm mesh net were used). All collections were made by towing the nets from approximately 1 m off the lake bottom to the surface at a retrieval speed of 1 m s^{-1}. In the inland lakes, 3 replicate tows were collected at 3 sampling sites.

In Chequamegon Bay and the 2 other sampling locations in Lake Superior, 2 replicate tows were collected from either 4 or 5 sampling sites. Thus, on each date roughly the same number of collections (8-10) was made on each inland lake and at each site location in Lake Superior. Lakes and sampling locations on Lake Superior were sampled once except for locations near Michigan and Long Islands which were each sampled twice (Table 1).

Replicate zooplankton tows from each sampling site were combined into one sample for preservation (75% ethanol, final volume). GPS location and depth were recorded for each sample to match the net tows with the hydroacoustic data. In the lab, all *M. diluviana, Chaoborus*, chironomids, and other macroinvertebrates were counted and up to 10 individuals of each taxonomic group were measured for body length at 8× with an ocular micrometer on a Leica dissecting microscope. The remaining zooplankton were sub-sampled quantitatively, and more than 100 individuals were counted for each subsample. Organisms were identified to species, except for *Alona, Chaoborus,* and *Diaptomus* which were identified to genus and Macrothricideae which were identified to family. Ten individuals of each taxonomic group were measured for body length to the nearest 0.1 mm at 50×. Total volumetric densities (individuals m^{-3}) for each taxonomic group were calculated from the subsamples. In Island Lake, an average density for the two sized nets used for collection was calculated for each taxonomic group. Zooplankton density was converted to volumetric dry weight biomass (mg m^{-3}) by using published length-weight regressions (Table 3) to calculate an average biomass for each taxon based on length measurements.

Hydroacoustic backscatter – mixed species biomass regression (Objective 1)

Hydroacoustic data were collected with a Biosonics DT6000 unit (Biosonics Inc., Seattle, Washington), except in 2006 when a Biosonics DTX unit (Biosonics Inc., Seattle, Washington) was used. Split-beam 120-kHz and 430-kHz transducers mounted on the same towbody (Biofin, Biosonics Inc.) were towed alongside the research vessel at approximately 7.4 km h^{-1} and alternating pulse transmissions were used, except in Island Lake when the 120-kHz transducer was unavailable. Both units were periodically calibrated using a standard tungsten-carbide sphere, and the target strength never varied

significantly (<±1 dB) from the known target strength of the sphere. Configurations of the transducers are listed in Table 4. All hydroacoustic data were analyzed using Echoview 4.10 (Myriax Software Pty., Hobart, Tasmania).

To establish a general regression to convert hydroacoustic backscatter to zooplankton dry weight for the mixed zooplankton assemblages, hydroacoustic data from the 430-kHz transducer were analyzed at the GPS location and down to the maximum depth of each zooplankton tow. A minimum threshold of -75 dB was applied to echo squared integration data from the 430-kHz hydroacoustic data after a preliminary analysis indicated that this threshold eliminated ambient noise while providing the strongest relationship between backscatter and zooplankton biomass from net tows. Fish targets were manually excluded from the 430-kHz hydroacoustic data prior to analysis. The mean volume backscattering coefficient (S_v, dB re m^2 m^{-3}) was compared with the average of the natural log of volumetric zooplankton biomass (dry weight mg m^{-3}) from net tows for each lake or sampling location on Lake Superior to create a general regression to convert hydroacoustic backscatter to dry weight biomass (y) for mixed species assemblages. The regression model took the form:

$$y = e^{\beta_0} \times e^{\beta_1 x} \times e^{1/2\sigma^2} \quad (2)$$

where β_0 and β_1 were the regression coefficients, x was the mean volume backscattering coefficient (S_v, dB re m^2 m^{-3}), and σ^2 was the mean square error of the regression, which was necessary to avoid systematic bias when applying a reverse transformation to log-transformed response variables (Miller 1984). In equation (2), σ^2 was equal to 0.151. We used the linear model (lm) function in the Rcmdr package (v. 1.5-3) within the R environment (R 2.8.1, R Development Core Team 2009) to conduct the regression analysis.

Evaluation of the mixed species regression (Objective 2)

To evaluate the applicability of the mixed species regression for assessing overall mean zooplankton biomass, estimates from net tows were compared with mean biomass estimates calculated from hydroacoustic data collected at 430-kHz from each lake or

location in Lake Superior (Table 1). We avoided incorporating hydroacoustic data near each zooplankton net tow site to prevent using the same data that were used to develop the regression model. Excluding these data, the entire hydroacoustic dataset was used in the analysis. Hydroacoustic data were partitioned in 25 m horizontal increments, except in Lake Superior where data were partitioned in 75 m increments because the overall zooplankton biomass was much lower. Backscatter from fish was minimized by applying a maximum threshold to the 430-kHz data, which was determined by manually eliminating fish targets from five regions of the overall dataset and then determining the average maximum threshold that corresponded with backscatter from fish targets (Table 1). Hydroacoustic backscatter was then converted to zooplankton dry weight biomass using Eq. 2. Nonparametric statistic tests were conducted in SYSTAT (v. 13.00.05) to compare estimates from net tows with estimates using the regression because the data on zooplankton biomass did not fulfill the requirements of normality.

Comparing the mixed species regression to species-specific target strength estimates (Objective 3)

We compared calculations of zooplankton density and biomass from net tows to estimates predicted from a) published species-specific target strengths and b) our mixed species regression. For analysis, we divided taxa into three classification groups: 1) large scatterers (*Chaoborus* larvae, *M. diluviana*, amphipods, and chironomid larvae); 2) large scatterers and large copepods (*Limnocalanus macrurus* and *Epischura lacustris* in addition to the organisms listed in classification group 1); and 3) all scatterers for which target strength estimates have been published (*Daphnia* spp., *Diaptomus* spp., and Cyclopoida in addition to the organisms listed in classification group 2).

Net tows – Zooplankton density estimates (individuals m^{-3}) for each taxon were calculated from individual net tows (see above) and then averaged for each lake or location in Lake Superior. Biomass estimates (mg m^{-3}) for each taxon were calculated from individual net tows by converting density estimates to biomass using published length-weight regressions (see above) (Table 3) and then averaged for each lake or location in Lake Superior. Overall density and biomass estimates were then summed according to the taxa represented in each of the three classification groups.

Species-specific target strengths – Zooplankton density (ρ_{vS}, individuals m^{-3}) was calculated for each taxon *S* using the equation:

$$\rho_{vS} = \frac{p_S}{\sum_{S=0}^{N_S-1}\left(p_S 10^{\frac{TS_S}{10}}\right)} s_v \qquad (3)$$

where p_S was the expected proportion of the total number of zooplankton belonging to taxon *S* so that $\sum_{S=0}^{N_S-1} p_S = 1$, N_S was the total number of taxa belonging to the classification group being analyzed, TS_S was the expected target strength returned from an individual of taxon *S* (dB re 1 m^2), and s_v was the linear mean volume backscattering coefficient (m^2 m^{-3}).

In Eq. 3, target strengths (TS_S) used included -68 dB for *Chaoborus* larvae (estimated from Knudsen et al. 2006), -70 dB for chironomid larvae (Kubecka et al. 2000), -76.5 dB for amphipods (Trevorrow and Tanaka 1997), -80.1 dB for *M. diluviana* (Rudstam et al. 2008), -94.2 dB for *L. macrurus* and *E. lacustris* (Lavery et al. 2007), -120 dB for *Daphnia* spp. (Hembre and Megard 2003), and -123 dB for *Diaptomus* spp. and Cyclopoida (Megard et al. 1997). A sensitivity analysis was also conducted for lakes containing *Chaoborus* larvae using a range of published target strengths, including -59 dB (Godlewska and Jelonek 2006), -68 dB (estimated from Knudsen et al. 2006), and -73 dB (Eckmann 1998).

In Eq. 3, to estimate s_v (m^2 m^{-3}) we used the entire hydroacoustic dataset from each lake or location in Lake Superior (Table 1), excluding those data used to develop the mixed species regression model. To calculate p_s, density estimates (individuals m^{-3}) for each taxon were estimated from individual net tows and compared against total density estimates for the classification group.

Taxon-specific density estimates were summed according to the taxa represented in each of the three classification groups. Taxon-specific biomass estimates (mg m^{-3}) were made using published length-weight regressions (Table 3) coupled with taxon-specific density estimates, and then summed according to the taxa represented in each classification group.

Mixed species regression – Total biomass was estimated by the regression using the mean volume backscattering coefficient (S_v, dB re m^2 m^{-3}) form of the linear mean volume backscattering coefficient (s_v, m^2 m^{-3}, where $S_v = 10 \log s_v$) as was used above (*Species-specific target strengths*). Taxon-specific biomasses (mg m^{-3}) were estimated using proportional biomasses based on net tow data, then summed according to the taxa represented in each of the three classification groups.

Taxon-specific densities (individuals m^{-3}) were estimated from biomass data using taxon-specific weight conversions (Table 3) equivalent to those used to convert density to biomass above (*Species specific target strengths*). Taxon-specific density estimates were then summed according to the taxa represented in each of the three classification groups.

Nonparametric tests were conducted in SYSTAT (v. 13.00.05) to compare estimates between net tow data and each hydroacoustic method because the data on zooplankton biomass did not fulfill the requirements of normality needed for parametric tests.

Zooplankton and fish spatial analysis (Objective 4)

Patterns in spatial correlation between fish and zooplankton were determined by analyzing hydroacoustic data from two frequencies (430-kHz, 120-kHz) for three lakes, including two basins of Trout Lake (Table 2). We vertically analyzed the 430-kHz echo squared integration data in 2-m depth increments by applying a minimum threshold of -75 dB and a maximum threshold to minimize backscatter from fish (Table 5). Backscatter from the 430-kHz transducer was then integrated and converted to zooplankton biomass using the mixed species regression. We analyzed the 120-kHz hydroacoustic data in 2-m depth increments by integrating backscatter with depth-specific single target estimates unless fewer than 30 single targets were identified per depth layer in which case the overall mean target strength was applied. The thresholds applied to the 120-kHz hydroacoustic analysis are listed in Table 5.

We conducted a horizontal spatial analysis at the depth stratum at which zooplankton and fish were estimated at peak abundances (Table 5, also see Fig. 7). We conducted this discrete-depth analysis to compare patches of zooplankton with patches of

zooplanktivorous fish within the same depth stratum. Using a discrete-depth analysis also allowed us to avoid confounding abiotic factors such as bottom depth and temperature that might influence spatial correlations when integrating biomass and density across the entire water column. Because there were peak abundances of zooplankton biomass and fish density at two depths in the south and north basins of Trout Lake, the spatial analysis was conducted at dual strata in both basins. Areas of the hydroacoustic transects where the bottom depth was shallower than the maximum depth of the discrete-depth analysis were excluded from the horizontal spatial analysis. Data were partitioned into 25-m horizontal increments for Trout Lake and Sparkling Lake and 100-m increments in Lake Superior to reduce the frequency of zero fish density estimates. The same thresholds that were applied when analyzing the data vertically were applied to the horizontal analysis. Echo squared integration data from the 120-kHz transducer were used to estimate fish density by applying an overall mean target strength estimate from the discrete depth strata that were being analyzed (Table 5). Echo squared integration data from the 430-kHz transducer were converted to zooplankton biomass using the mixed species regression.

A geostatistical analysis was conducted on the horizontal spatial estimates of zooplankton biomass and fish density using GS+ 9.0 software (Gamma Design Software, Plainwell, Michigan). A natural log transformation was applied to fish density estimates to normalize the data. Variograms and correlograms were used to represent autocorrelation for zooplankton biomass and fish density, and cross-correlograms were used to determine whether the correlation between these trophic levels was positive or negative depending on the significance of Mantel and partial Mantel tests (see below). Sturge's Rule was applied to determine the appropriate number of distance classes (Legendre and Legendre 1998), and the number of distance classes multiplied by the lag distance was approximately half the distance of the two furthest data points (Table 6). The software GS+ was used to fit either a Gaussian, spherical, exponential, or linear model to each variogram (Table 6).

For zooplankton biomass and fish density in the horizontal analyses, the overall significance of the Moran's *I* correlograms was evaluated at the Bonferonni corrected significance level. If the overall correlogram was significant, then a progressive

Bonferroni correction was applied to test for the significance of each individual autocorrelation statistic (Legendre and Legendre 1998). The spdep package (v. 0.4-50, function moran.mc) was used in R statistical software (R 2.8.1, R Development Core Team 2009) to determine the expected value and variance of Moran's *I*. Mantel tests were used to determine spatial correlations between zooplankton biomass, fish density, and "space", which represented the effect of unknown factors creating spatial structure in the data. Partial Mantel tests were used to determine correlations between two of these variables while controlling for the effect of the third variable (Legendre and Legendre 1998). The ecodist package (v. 1.2.2, function mantel) was used in R statistical software (R 2.8.1, R Development Core Team 2009) to calculate Mantel and partial Mantel statistics using 10,000 permutations.

Results

Hydroacoustic backscatter – mixed species biomass regression (Objective 1)

The mixed species regression between zooplankton biomass in net tows and 430-kHz hydroacoustic backscatter across all lakes was highly significant ($p<0.001$, Fig. 2). The strength of the regression ($R^2=0.90$) indicated that it was possible to estimate zooplankton dry weight biomass using hydroacoustic backscatter in a variety of lakes even when the zooplankton taxonomic composition varied greatly (Fig. 3). When conducting the regression analysis, sampling locations near Michigan Island and Long Island in Lake Superior were combined into two data points (Lake Superior spring and Lake Superior autumn) because zooplankton biomass was indistinguishable between sampling locations (ANOVA, $p>0.05$), but there was a statistical difference between sampling dates (ANOVA, $p<0.05$).

Evaluation of the mixed species regression (Objective 2)

Evaluation of the mixed species regression indicated that there was no significant difference in overall mean zooplankton biomass predicted by hydroacoustic backscatter compared with net tows (Wilcoxon signed-rank test, $p>0.05$, Fig. 4). However, hydroacoustics provided a significantly lower estimate of the standard deviation around

the mean when compared with net tows (Wilcoxon signed-rank test, $p<0.05$, Fig. 4). There was a significant positive relationship between the overall mean biomass estimated by hydroacoustics and the overall mean estimated from net tows (Spearman rank correlation coefficient, $\rho=0.96$, $p<0.01$).

Comparing the mixed species regression to species-specific target strength estimates (Objective 3)

Fig. 5 displays density and biomass estimates based on net tows, published species-specific target strengths, and our mixed species regression for three classification groups (large scatterers, large scatterers and large copepods, and all scatterers). For comparisons between net tows and the mixed species regression approaches, no significant differences were detected in density or biomass estimates for any of the three classification groups (Wilcoxon signed-rank tests, $p>0.05$). In contrast, for comparisons between net tows and the species-specific target strength approaches, there were significant differences detected in density estimates for two classification groups (large scatterers and large copepods, and all scatterers, Wilcoxon signed-rank tests, $p<0.05$) and biomass estimates for all three classification groups (Wilcoxon signed-rank tests, $p<0.05$).

Comparisons were made between the mean volume backscattering coefficient (S_v, dB re m^2 m^{-3}) from hydroacoustic transects and both density (individuals m^{-3}) and biomass (mg m^{-3}) estimates from net tows for the three classification groups. The strongest relationship existed between S_v and zooplankton biomass for all scatterers (Spearman rank correlation coefficient, $\rho=0.98$, $p<0.01$), and the second strongest relationship existed between S_v and zooplankton density for all scatterers (Spearman rank correlation coefficient, $\rho=0.87$, $p<0.01$).

Analysis of the species-specific target strength method indicated that when *Chaoborus* larvae were present, they were one of the most important scatterers because of their large estimated target strength. A sensitivity analysis was conducted using a range of published target strength estimates for *Chaoborus* larvae. Results indicated that density and biomass estimates could vary by as much as two orders of magnitude depending on the estimate of target strength that was applied (Fig. 6).

Zooplankton and fish spatial analysis (Objective 4)

The depth of peak biomass of zooplankton and peak density of zooplanktivorous fish overlapped in all study locations, including at dual depths in both basins of Trout Lake (Fig. 7). Moran's *I* spatial correlograms for zooplankton biomass indicated that there was strong autocorrelation at short distances for all sampling locations (Fig. 8). Additionally, zooplankton in Lake Superior and in the deep layers of the North and South Basins of Trout Lake displayed significant autocorrelation across the entire dataset. Only zooplankton in the shallow layer of the North and South Basins of Trout Lake reached a distance at which data were uncorrelated, at approximately 300 meters at both locations. Moran's *I* correlograms for zooplankton biomass also indicated the presence of a strong gradient in Lake Superior, Sparkling Lake, and the deep layer in the South Basin of Trout Lake, and the presence of patches in the deep layer in the North Basin of Trout Lake. The spatial structure in zooplankton biomass was well represented with variogram models in all cases except for the deep layer in the North Basin of Trout Lake (R^2=0.34, Table 6). The nugget effect was generally small for the zooplankton variograms at each location, except for in Sparkling Lake and the deep layer in the North Basin of Trout Lake (Table 6).

Moran's *I* spatial correlograms for fish density indicated no consistency in patterns of autocorrelation across multiple sampling locations (Fig. 8). For example, in Sparkling Lake, the correlogram indicated strong autocorrelation at distances of less than 200 meters but not thereafter (Fig. 8), while in both the deep and shallow layer of the South Basin of Trout Lake, fish density did not display significant patterns of autocorrelation (Fig. 8). Interestingly, in both these layers in the South Basin of Trout Lake, the spatial structure in fish density could be described reasonably well using a variogram model (R^2=0.73, R^2=0.68, respectively), although the nugget effect was approximately 50% in both cases (Table 6). In contrast, Moran's *I* correlograms of fish density in the shallow and deep layers in the North Basin of Trout Lake demonstrated small, but significant, positive autocorrelation at distances less than approximately 200 meters (Fig. 8). A linear variogram model was used to predict fish density in the shallow layer in the North Basin of Trout Lake with some success (R^2=0.62) although there was a

large nugget effect, similar to patterns observed in the South Basin of Trout Lake (Table 6). Fish density in the deep layer of the North Basin of Trout Lake was more difficult to model accurately with a variogram (R^2=0.36), even though Moran's *I* correlogram suggested significant positive autocorrelation at distances less than 200 m (Fig. 8).

Results of partial Mantel tests for the six depth strata analyzed among the three lakes are given in Table 7. "Space" in this study represents the effects of unknown factors creating spatial structure in the data. Results indicated that in each case, when controlling for fish density, there was a strong effect of "space" on zooplankton biomass. When controlling for "space", there was a significant correlation between zooplankton biomass and fish density in Lake Superior, the deep layer in the North Basin of Trout Lake, and Sparkling Lake, although the relationship in Sparkling Lake was weak (partial Mantel statistic=0.10, Table 7). In all three layers, cross-correlograms indicated that the relationship between these trophic levels was positive. When controlling for zooplankton biomass, partial Mantel tests indicated a significant effect of "space" on fish density in Sparkling Lake, and both the shallow and deep layers in the North Basin of Trout Lake, although these relationships tended to be weak (Table 7). Graphical models depicting the relationships between zooplankton biomass, fish density, and "space" in each of the six depth strata are displayed in Fig. 9.

Discussion

Hydroacoustic backscatter – mixed species biomass regression (Objective 1)

Our results indicate that it is possible to apply a general regression to convert hydroacoustic backscatter to zooplankton dry weight biomass in a variety of lakes with mixed species zooplankton assemblages (Fig. 2). Our results were consistent despite wide differences in zooplankton taxonomic composition (Fig. 3), lake area, and Secchi transparency. Prior research has shown that specific taxonomic groups scatter sound differently depending on their body size and morphology (Stanton et al. 1994, Stanton et al. 1996, Stanton and Chu 2000). The strength of our regression (R^2=0.90), however, indicated that freshwater zooplankton likely scattered sound in proportion to their dry

weight. Our findings are strengthened by our inclusion of several sites where at least one genus of large zooplankter (*Chaoborus* or *M. diluviana*) was present, one site in which both were present, and two sites in which neither was present.

Evaluation of the mixed species regression (Objective 2)

Using our regression (Fig. 2), we have shown that net tow data and hydroacoustic assessments provide similar estimates of mean zooplankton dry weight biomass across the lakes we studied, although estimates of the standard deviation provided by hydroacoustics were significantly lower (Fig. 4). This result is not altogether surprising given the large amount of water that is integrated when collecting data with hydroacoustics. To achieve the same level of precision with net tows, we would have needed to collect roughly twice as many samples at locations with the lowest zooplankton densities in our study (Downing et al. 1987). These results are consistent with prior research on Lake Superior zooplankton populations that determined hydroacoustics provided lower estimates of variance compared with net tows (Holbrook et al. 2006). There also were very large standard deviations around the mean detected with net tows in two lakes in our study (Silver and Whitefish Lakes). Both lakes have multiple basins and replicate samples at three sites appear to have been inadequate to define the mean. Therefore, in instances of low productivity and bathymetrically complex lakes, our data suggests that more sampling with nets was needed but that hydroacoustic technology may provide a more accurate measure of the mean particularly if time or sampling constraints limit the number of net tows that can be conducted.

A potential source of error in our hydroacoustic analysis was the application of a maximum threshold to reduce backscatter from fish echoes. This maximum threshold was employed when comparing whole-lake estimates of net tows with hydroacoustics, evaluating biomass and density estimates predicted using published estimates of target strength and our mixed species regression, and conducting a spatial analysis to assess the correlation between zooplankton biomass and fish density. Manually removing fish targets, as we did when developing the mixed species regression, is a tedious task when analyzing large amounts of hydroacoustic data. The application of a maximum threshold, however, may have resulted in preserving backscatter from the edges of fish traces,

inflating estimates of zooplankton biomass. Using a maximum threshold can also eliminate some backscatter from large zooplankton such as *M. diluviana* and *Chaoborus* spp. if the threshold is set too low. An alternative approach would be to construct a fish removal mask using the 120-kHz data, but there was not enough overlap in the 430-kHz and 120-kHz beams at the shallower depths in most of our study lakes because the transducers were mounted approximately 0.5 m apart. A more rigorous alternative would be to apply a cross-filter detector to create a fish removal mask (Balk and Lindem 2000, Rudstam et al. 2008), but we were unable to apply this approach using our technology.

Comparing the mixed species regression to species-specific target strength estimates (Objective 3)

We compared the relationship between the mean volume backscattering coefficient from hydroacoustics with biomass and density estimates from net tows for the three classification groups (large scatterers, large scatterers and large copepods, and all scatterers) for lakes in Table 1 and determined the two strongest correlations were when all scatterers were included. This result suggests that although large zooplankton such as *Chaoborus,* chironomids, *M. diluviana*, and amphipods likely return the greatest amount of energy, other taxonomic groups also make a detectable contribution to the overall backscatter. Although it has been hypothesized that cladocerans and copepods are insignificant scatterers (Wagner-Döbler and Jacobs 1988, Knudsen et al. 2006), our results agree with Lavery et al. (2007) who found that 420-kHz backscatter in marine systems was dominated by return echoes from copepods rather than taxonomic groups such as siphonophores and pneumatophores that contributed the majority of backscatter at lower frequencies.

Applying our mixed species regression (Fig. 2) and then scaling it to estimate mean density or biomass for the three classification groups provided estimates more similar to net tows than applying the species-specific target strength method (Fig. 5). One of the greatest disadvantages of applying estimates of target strength particularly in mixed zooplankton assemblages is that very few estimates have been published for various species of freshwater zooplankton. Because target strengths are frequency-dependent (Stanton et al. 1996, Rudstam et al. 2008), it is important to apply estimates

for freshwater zooplankton measured at a frequency similar to that employed for the data where it is being adapted. In our case, estimates at 430-kHz frequency exist only for *M. diluviana* (-80.1 dB, Rudstam et al. 2008) and *Chaoborus* (-59 dB, Godlewska and Jelonek 2006), although our sensitivity analysis indicated that this target strength estimate for *Chaoborus* may have been high (Fig. 6). Target strength estimates for the other freshwater zooplankton taxonomic groups were measured at frequencies ranging from 120-kHz to 198-kHz, so the accuracy in applying these estimates to scale backscatter collected at 430-kHz was unknown and may have been a large source of the variation from net tow estimates that we measured. It is also important to note that we applied a marine estimate of -95 dB for large copepods including *L. macrurus* and *E. lacustris* (Lavery et al. 2007). This target strength estimate was measured at a frequency of 420-kHz, but it is unknown whether freshwater copepods scatter sound similarly to marine copepods, particularly *E. lacustris* which was smaller on average (~1.6 mm) than the marine copepods used in the study (~2 mm).

In contrast to most freshwater zooplankton groups, there have been a number of published target strength estimates for *Chaoborus* (e.g. Eckmann 1998, Godlewska and Jelonek 2006, Knudsen et al. 2006). However, these estimates range considerably from -54 dB (Godlewska and Jelonek 2006) to -75 dB (Eckmann 1998). This variability may be due to three factors: the frequency at which data are collected, the length distribution of *Chaoborus* at the time data are collected, and acoustic interference from other zooplankton. Because *Chaoborus* resonates at 200 kHz, target strength estimates at this frequency should be higher than estimates at other frequencies as long as the size distribution remains unchanged (Knudsen et al. 2006). Our study indicates that other zooplankton taxonomic groups also contribute backscatter at high frequencies and this may inflate estimates of target strength for *Chaoborus*. Indeed, backscatter contributions by other zooplankton groups may explain why some of the highest published target strength estimates for *Chaoborus* were measured at 420 kHz (Godlewska and Jelonek 2006).

Variation in target strength estimates for *Chaoborus* is particularly problematic because the equation used to calculate volumetric zooplankton density (Eq. 3) is sensitive to species with large target strength estimates, which changes the amount of backscatter

allocated to other zooplankton taxonomic groups. As a result, density estimates vary greatly depending on the target strength estimate that is used (Fig. 6). Our sensitivity analysis suggests that an appropriate target strength estimate for *Chaoborus* in our lakes was likely between -68 dB and -73 dB. However, until there is stronger consensus on the most appropriate target strength for *Chaoborus* at multiple frequencies and for individuals of various lengths, our data indicate that calculating zooplankton density and biomass by applying estimates of target strength may be prone to substantial bias in lakes where *Chaoborus* is present.

Zooplankton and fish spatial analysis (Objective 4)

A strong effect of "space" representing the effects of unknown factors creating spatial structure on zooplankton biomass was observed for all six depth strata where a spatial analysis was conducted (Table 7, Fig. 9). Additionally, Moran's *I* correlograms indicated that these spatial patterns in zooplankton biomass were broad in scale (Fig. 8). Although we did not measure variables other than fish density that could have accounted for this spatial structure in zooplankton biomass, our results are consistent with other studies that have found a strong effect of abiotic factors such as wind-induced water movement on the spatial distribution of zooplankton abundance (Thackeray et al. 2004, Blukacz et al. 2009, Rinke et al. 2009). Overall, the spatial autocorrelation patterns for zooplankton biomass suggest that gradients and patches frequently exist at scales of 10s to 100s of meters, and that it may be difficult to assume statistical independence when collecting zooplankton samples at discrete locations within that spatial scale in north temperate lakes.

In contrast to the consistent effect of "space" on zooplankton biomass, the effect of "space" on fish density was variable (Table 7, Fig. 9). There was a significant effect of "space" on fish density in three of our study locations, but partial Mantel statistics indicated that the relationship tended to be weaker than the influence of "space" on zooplankton. The absence of a consistent relationship between "space" and fish density suggests that a wider variety of abiotic and biotic processes may regulate spatial patterns in fish density compared to zooplankton biomass. In addition to broad-scale abiotic processes such as temperature, light, and water clarity that influence feeding behavior and

growth rates, the spatial distribution of zooplanktivorous fish may also be influenced by fine-scale biotic interactions such as food availability, swimming capability, competition, and predator avoidance (Tyler and Rose 1994, Giske et al. 1998).

Even in situations where we observed strong spatial structure in one of these potential factors, fish may not respond in a predictable spatial arrangement. For example, in both the shallow and deep depth strata in the South Basin of Trout Lake, there was strong spatial structure in the distribution of zooplankton biomass, yet fish density was distributed nearly randomly (Fig. 8). This random distribution in fish density may be the result of collecting acoustic data at night when zooplanktivorous fish lose their schooling behavior and become dispersed (Appenzeller and Leggett 1992, Milne et al. 2005). The distribution of zooplanktivorous fish would likely become patchier during the day when schools form; however acoustic estimates of fish abundance are also prone to greater bias during the day (Appenzeller and Leggett 1992). In addition, many of the fish species contained in these lakes such as cisco (*Coregonus artedi*) and yellow perch (*Perca flavescens*) continue to feed at night and should potentially respond to aggregations of plankton (Hrabik 1999).

We detected significant spatial correlations between zooplankton biomass and fish density in Lake Superior, Sparkling Lake, and the North Basin of Trout Lake. Cross-correlograms indicated a positive correlation in these three locations, suggesting a bottom-up effect where fish concentrated in areas of higher zooplankton biomass. In contrast, we did not detect any negative correlations between fish density and zooplankton biomass, suggesting that fish density did not have a top-down effect on structuring zooplankton biomass.

There are two main explanations for why we did not detect a significant correlation between fish density and zooplankton biomass at the other three sites, all in Trout Lake. First, fish may have been responding to zooplankton patches at distances < 25 m, which is the increment we used for all sites other than Lake Superior. The fact that variogram models for fish densities had high nugget effects (except for Sparkling Lake) is evidence that spatial dynamics occurred at scales smaller than we measured (Table 6). As long as local means and variances do not change over the sampling space, the nugget effect can result from spatial variability occurring at distances less than the minimum lag

distance and/or experimental error (Rossi 1992). Analyzing fish density data at sampling increments < 25 m, however, failed to improve the nugget effect and caused the overall error of the variogram model to increase. We also attempted to manipulate the minimum lag size, but that approach did little to improve the nugget effect. Based on these results, it is possible that the large nugget effect in the fish density variogram models may be the result of local means and variances that changed throughout the hydroacoustic transect. This hypothesis is supported by the Mantel *I* correlograms, which generally indicated a shorter distance of autocorrelation than that estimated by variogram models.

A second possible reason that we did not detect more consistent correlations between zooplankton biomass and fish density in Trout Lake is that zooplankton biomass may not always accurately represent the prey that fish consume. As visual feeders, zooplanktivorous fish often select the largest, most visible zooplankters (Hrbacek et al. 1961, Brooks and Dodson 1965, O'Brien et al. 1976). It is difficult to determine spatial distribution patterns of individual zooplankton species with 430-kHz hydroacoustic frequency because of the likelihood that numerous zooplankton taxonomic groups contribute backscatter, unless this technology is used in conjunction with frequent net tows or optical plankton counters. One reason that we did not detect a top-down influence of fish predation on the spatial structure of zooplankton biomass as has been observed in other freshwater studies (George and Winfield 2000, Masson et al. 2001, Romare et al. 2003) may be because we were unable to assess species-specific interactions between large zooplankters and the fish species that preyed upon them. Our results were more consistent with Rinke et al. (2009) who found a bottom-up positive correlation between a general measure of zooplankton abundance and fish density.

There is a strong need for continued research examining broad scale spatial relationships between zooplankton and fish trophic levels. Our results indicate that positive associations can be anticipated based on our findings in three different lakes (Table 7, Fig. 9); however, significant correlations occurred in only 50% of the depth strata analyzed. More generally, it is possible that pelagic fish positively associate with overall zooplankton biomass (bottom-up) but then cause local depletion of their selected prey resources (top-down). Hence, when zooplankton assemblages are mixed and contain the species preferred by fish, using overall zooplankton biomass may be more

appropriate for predicting areas of greatest foraging potential for zooplanktivorous fish rather than using species-specific zooplankton abundance estimates.

In summary, we determined that a general regression to convert 430-kHz hydroacoustic backscatter to zooplankton dry weight biomass was applicable to mixed zooplankton species assemblages in a variety of lakes, ranging from highly oligotrophic to highly eutrophic. The results of our analysis demonstrated that it would be feasible to quickly estimate, assess, and map overall zooplankton dry weight biomass in a variety of lakes. This methodology provided density and biomass estimates that were more similar to net tows than when applying species-specific estimates of target strength. We also applied the regression to three different spatial data sets and were able to detect a significant, positive, bottom-up influence of zooplankton biomass on the spatial distribution of fish density at half of the depth strata that we analyzed. In the future, combining zooplankton hydroacoustics with other sampling technologies such as optical plankton counters would enable the assessment of both general and taxon-specific spatial distribution interactions between zooplankton and zooplanktivorous fish and further refinement of predictive models.

Table 1. Lakes that were sampled to correlate zooplankton biomass estimated from net tows with 430-kHz hydroacoustic backscatter (Objective 1), sorted by lake area. Locations in Lake Superior include: MI=Michigan Island, LI=Long Island, and CB=Chequamegon Bay. Maximum threshold was the threshold applied to hydroacoustic data other than at the site of zooplankton net tows to evaluate the mixed species regression (Objective 2). Separate thresholds were applied to the hydroacoustic data collected at different sampling dates and locations in Lake Superior. Separate thresholds were also applied in the south and north basins of Whitefish Lake.

Lake Name	Sampling Location (Lat ºN, Lon ºW)	Area (ha)	Z max (m)	Secchi Depth (m)	Sampling Date(s)	Maximum threshold (dB)
Superior – MI	46.91, -90.43	8210000	406	12.0	28 May 04, 14 Sep 04	-60, -63
Superior – LI	46.72, -90.69	8210000	406	12.0	29 May 04, 17 Sep 04	-57, -56
Superior – CB	46.66, -90.88	16660	23	6.5	16 Jul 04	-56
Island	47.03, -92.15	3283	29	2.0	5 Aug 03	-38
Trout	46.03, -89.66	1544	36	5.0	28 June 06	-52
Big Muskellunge	46.02, -89.62	376	21	4.5	28 Jun 06	-38
Whitefish	46.22, -91.87	337	31	6.5	17 Aug 06	-50 S, -40 N
Sparkling	46.01, -89.70	51	20	6.0	27 Jun 06	-61
Silver	44.07, -87.74	28	13	1.0	12 Jul 06	-33

Table 2. Lakes that were sampled to determine the within-lake spatial correlations between zooplankton and fish populations (Objective 4), sorted by lake area. The location in Lake Superior that was sampled was the Western Arm (W).

Lake Name	Sampling Location (Lat ºN, Lon ºW)	Area (ha)	Z max (m)	Secchi Depth (m)	Sampling Date	Distance Sampled (km)
Superior – W	47.46, -90.51	8210000	406	13.0	31 Aug 06	65.3
Trout S	46.03, -89.67	1030	36	5.0	26 Jul 04	1.9
Trout N	46.06, -89.66	514	27	5.0	26 Jul 04	2.1
Sparkling	46.01, -89.70	51	20	6.0	22 Jul 03	5.9

Table. 3. Length-weight regressions (right column) used to convert volumetric zooplankton density (individuals m^{-3}) of taxa in our samples (left column) to volumetric zooplankton biomass (mg m^{-3}).

Species	Length-Weight Regression
Acanthocyclops vernalis	Culver et al. 1985
Alona spp.	Culver et al. 1985 (*Chydorus sphaericus*)
Diacyclops thomasi	Culver et al. 1985
Diporeia hoyi	Winnell and White 1984
Bosmina longirostris	Culver et al. 1985
Bythotrephes longimanus	Makarewicz and Jones 1990 (reported as *B. cederstroemi*)
Chaoborus spp.	Lasenby et al. 1994 (*C. americanus*)
Chironomidae	Johnston and Cunjak 1999
Chydorus spp.	Culver et al. 1985 (*C. sphaericus*)
Daphnia spp. (except *D. pulicaria*)	Dumont et al. 1975 (*D. galeata)*
Daphnia pulicaria	O'Brien and deNoyelles 1974 (*D. pulix*)
Diaphanosoma birgei	Dumont et al. 1975 (*D. brachyurum*)
Diaptomus spp.	Culver et al. 1985 (*D.* copepodites)
Epischura lacustris	Culver et al. 1985 (*Diaptomus* copepodites)
Holopedium gibberum	Lawrence et al. 1987
Latona setifera	Rosen et al. 1981 (*Sida crystalline*)
Leptodora kindtii	Culver et al. 1985
Limnocalanus macrurus	Conway 1977
Macrothricidae	Guntzel et al. 2003 (*Macrothrix flabelligera)*
Mesocyclops edax	Culver et al. 1985
Mysis diluviana	Johannsson 1992 (*M. relicta*)

Table 4. Configurations of the hydroacoustic transducers used in this study.

Frequency (kHz)	Type of Beam	Beam-width (º)	Source level at 1 m (dB re 1 µPa)	Pulse duration (ms)	Receive Sensitivity (dB)	Pulse rate (pps)
120	Split	7.3 x 7.3	220.0	0.4	-51.2	1-2
430	Split	6.5 x 6.5	219.0	0.2	-54.0	1-2

Table 5. Thresholds used in the analysis of spatial correlations between zooplankton biomass and fish density (Objective 4). The 430-kHz maximum threshold was used to reduce backscatter from fish targets. The 120-kHz mean target strength (TS) was calculated for the portion of the water column that was analyzed in the discrete-depth analysis and was used to estimate fish density.

Sampling Location	Discrete depth analysis (m)	430-kHz S_v Min Threshold (dB)	430-kHz S_v Max Threshold (dB)	120-kHz S_v Min Threshold (dB)	120-kHz Single Target Min Threshold (dB)	120-kHz Mean TS (dB)
Superior	10-30	-75	-63	-65	-55	-42.1
Trout S Shallow	7-13	-75	-58	-60	-55	-52.6
Trout S Deep	16-24	-75	-54	-60	-55	-42.3
Trout N Shallow	7-12	-75	-59	-60	-55	-51.7
Trout N Deep	16-22	-75	-55	-60	-55	-39.0
Sparkling	4-8	-75	-62	-65	-55	-51.7

Table 6. Data points, distance classes, and lag sizes used to develop variogram models and Moran's *I* correlograms (Fig. 8). The variogram models for zooplankton biomass and fish density are listed for each study location. Variograms were fitted with either a Gaussian model (Gaus), a spherical model (Sph), an exponential model (Exp), or a linear function (Linear).

Sampling Location	Data points	Distance Classes	Lag size (m)	Zooplankton Biomass					Ln Fish Density				
				Model	Nugget	Sill	Range	R^2	Model	Nugget	Sill	Range	R^2
Superior	294	16	915	Gaus	1.1	33.5	8383	0.98	Sph	1.05	3.46	11140	0.99
Sparkling	151	14	42	Sph	1.3	5.5	1732	0.87	Gaus	0.01	0.62	217	0.90
Trout S Shallow	83	13	67	Exp	1.4	45.6	1152	0.88	Exp	0.52	1.04	363	0.73
Trout S Deep	74	12	73	Gaus	11.2	107.0	977	0.99	Sph	0.10	0.20	446	0.68
Trout N Shallow	82	13	67	Exp	1.2	18.8	522	0.89	Linear	0.66	1.04	836	0.62
Trout N Deep	74	12	73	Sph	4.4	16.3	272	0.34	Exp	0.13	0.32	309	0.36

Table 7. Simple Mantel statistics (above the diagonal, comparing two variables) and partial Mantel statistics (below the diagonal, comparing two variables while controlling for the third variable). Only significant values have been reported. NS = not significant. Values in bold are significant at $P < 0.001$. Mantel and partial Mantel tests were significant at the Bonferroni-corrected probability level of 0.05/3 = 0.017. Zooplankton = zooplankton biomass, Fish = fish density.

		Zooplankton	Fish	Space
Superior	Zooplankton	-	**0.43**	**0.45**
	Fish	**0.39**	-	**0.20**
	Space	**0.41**	NS	-
Sparkling	Zooplankton	-	**0.15**	**0.37**
	Fish	0.10	-	**0.18**
	Space	**0.35**	**0.13**	-
Trout S Shallow	Zooplankton	-	NS	**0.57**
	Fish	NS	-	NS
	Space	**0.57**	NS	-
Trout S Deep	Zooplankton	-	NS	**0.35**
	Fish	NS	-	0.12
	Space	**0.35**	NS	-
Trout N Shallow	Zooplankton	-	NS	**0.33**
	Fish	NS	-	**0.24**
	Space	**0.31**	**0.21**	-
Trout N Deep	Zooplankton	-	**0.35**	**0.18**
	Fish	**0.36**	-	NS
	Space	**0.21**	-0.10	-

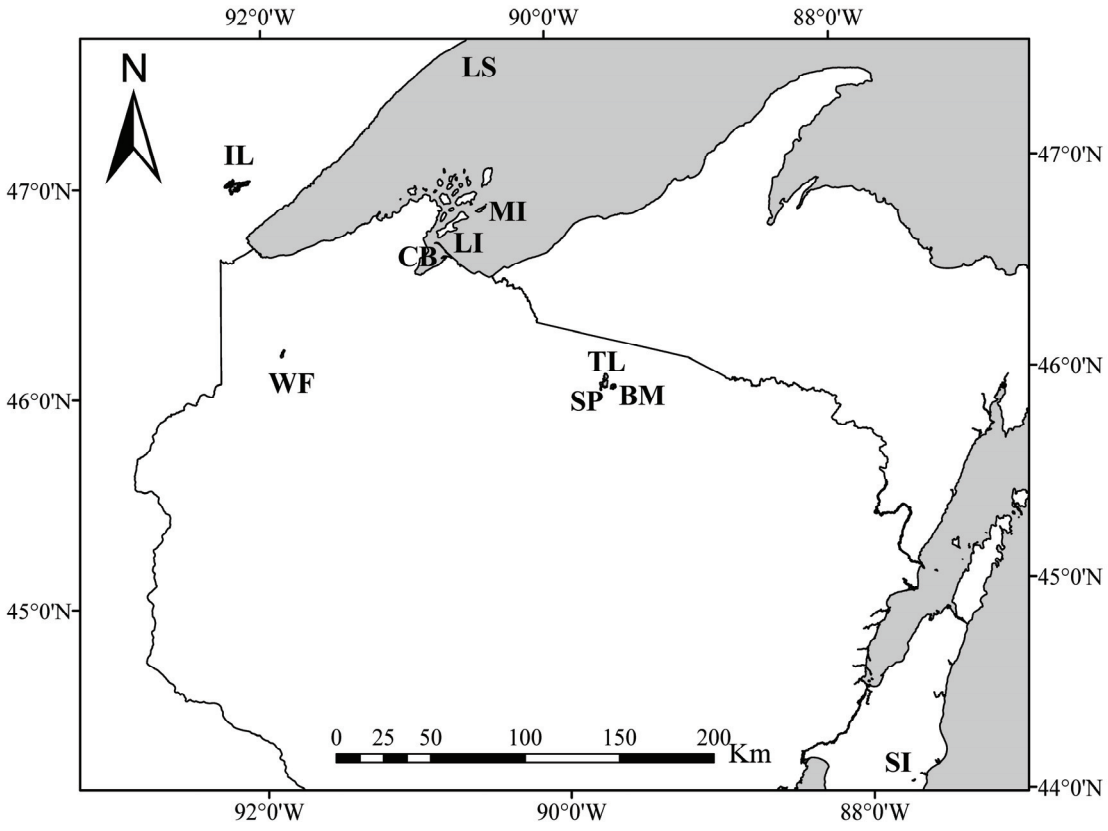

Fig. 1. Sites sampled as: IL=Island Lake Reservoir, LS=Western Arm of Lake Superior, MI=Michigan Island in Lake Superior, LI=Long Island in Lake Superior, CB=Chequamegon Bay in Lake Superior, WF=Whitefish Lake, TL=Trout Lake, SP=Sparkling Lake, BM=Big Muskellunge Lake, and SI=Silver Lake. See Table 1 and Table 2 for more details on each lake.

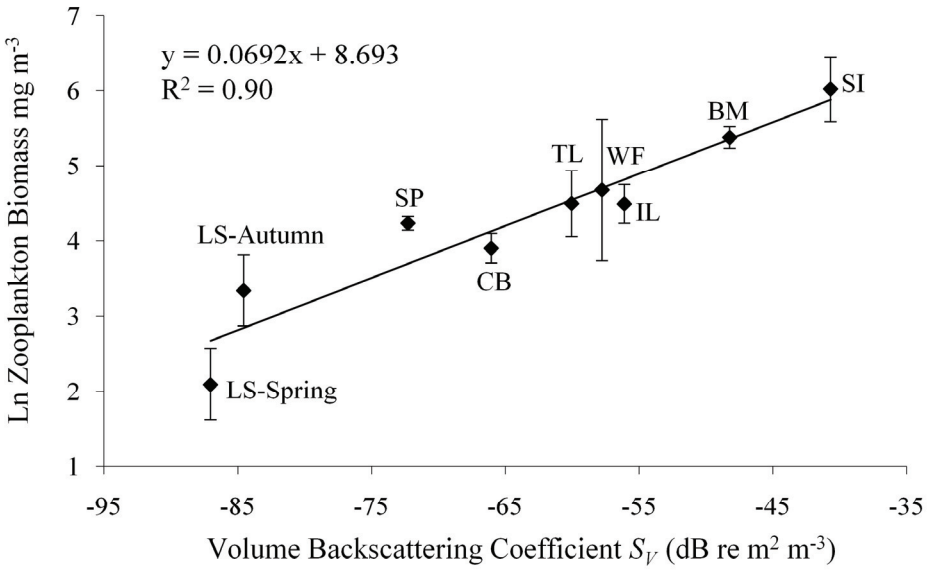

Fig. 2. The relationship between site specific 430-kHz mean volume backscattering coefficient (S_v, dB re m^2 m^{-3}) and the natural log of volumetric zooplankton dry weight biomass from net tows (mg m^{-3}). The solid line represents the ordinary least squares regression. Data from the Michigan Island sites and Long Island sites in Lake Superior were statistically indistinguishable and combined into Lake Superior spring and Lake Superior autumn data points (see text). Error bars are ± SD. See Fig. 1 for lake codes.

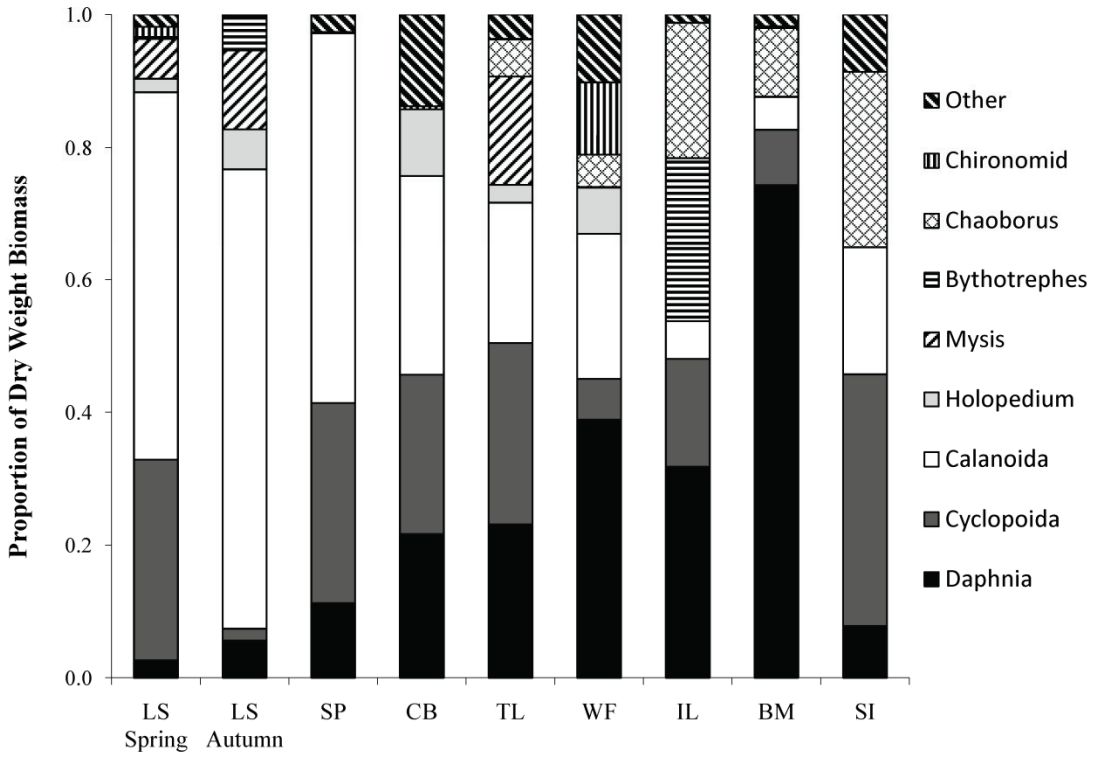

Fig. 3. The relative proportion of zooplankton taxonomic groups that comprised the dry weight biomass in the lakes used to develop the regression between 430-kHz hydroacoustic backscatter and zooplankton dry weight biomass from net tows. See Fig. 1 for lake codes.

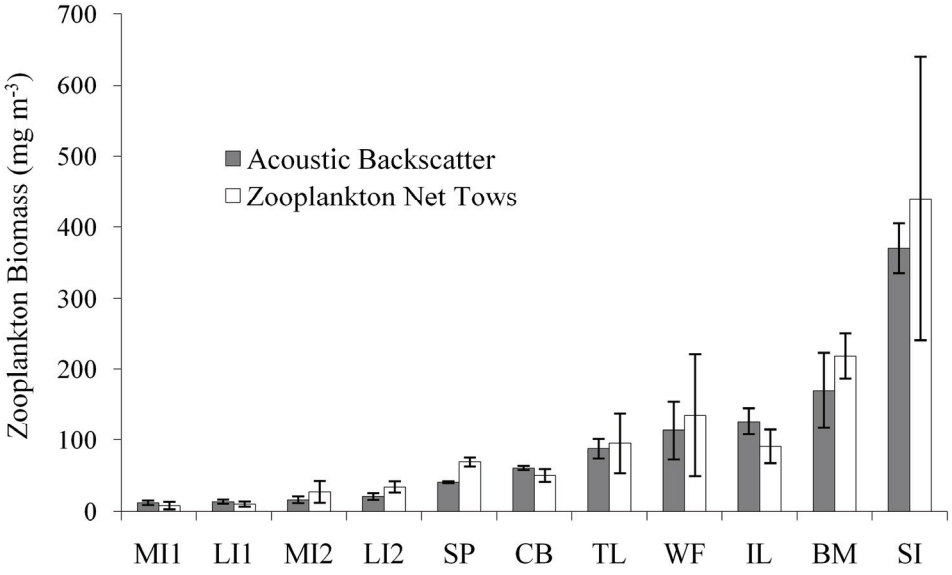

Fig. 4. Mean zooplankton dry weight biomass (mg m^{-3}) calculated from the entire 430-kHz hydroacoustic dataset, excluding the zooplankton net tow sampling sites, compared with corresponding mean zooplankton dry weight biomass estimates from net tows (mg m^{-3}). Lake codes are the same as in Fig. 1. except that sites on Lake Superior are listed separately by season as MI1=Michigan Island spring, LI1=Long Island spring, MI2=Michigan Island autumn, LI2=Long Island autumn. Error bars are ± SD.

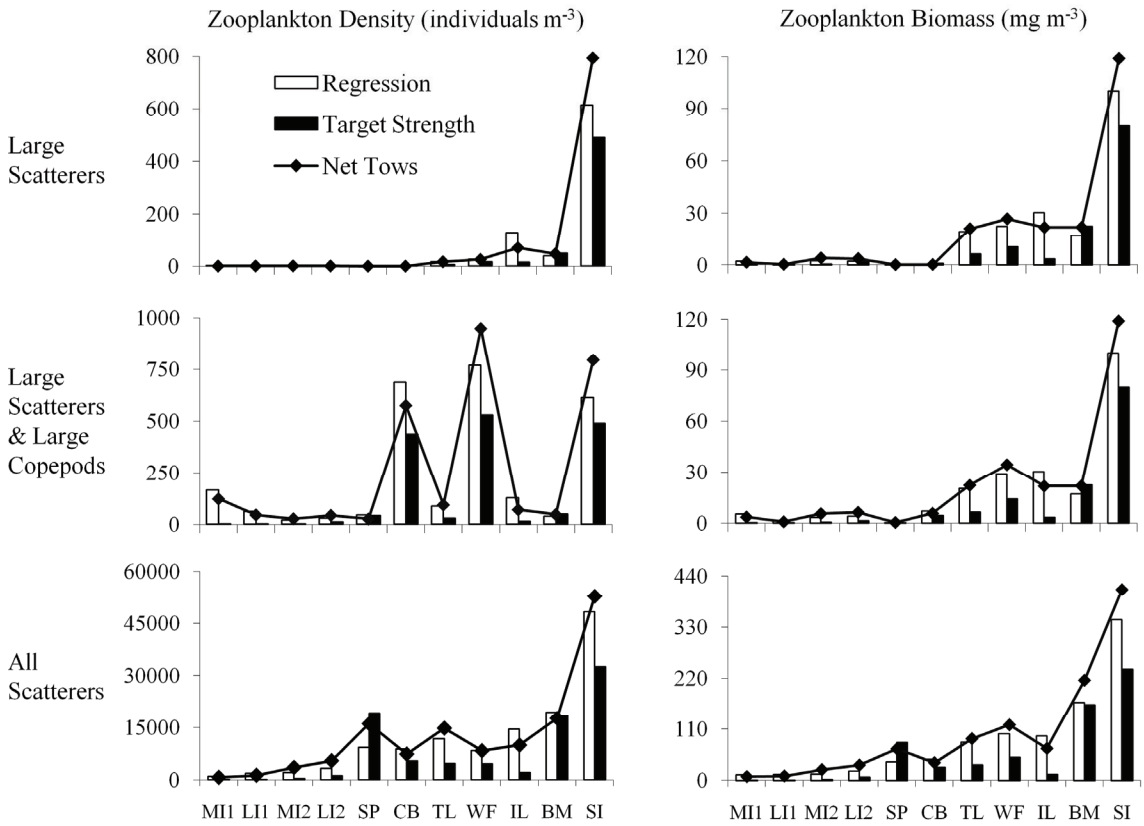

Fig. 5. Estimates of zooplankton density (individuals m^{-3}, left panels) and biomass (dry weight mg m^{-3}, right panels) for the three classification groups using three sampling methods: net tows, our mixed species regression, and published estimates of species-specific target strength. Lake codes are the same as in Fig. 4.

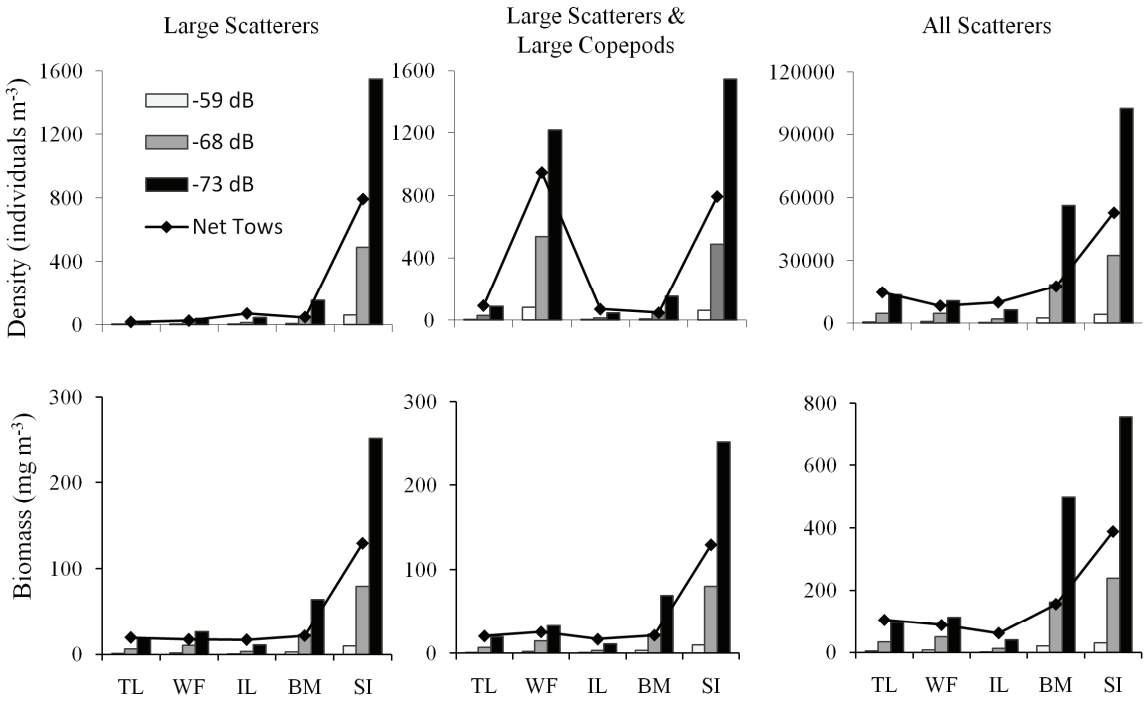

Fig. 6. Zooplankton density (individuals m^{-3}) and biomass (mg m^{-3}) estimates for the three classification groups in lakes that contain *Chaoborus* spp. larvae. Three different published estimates of target strength for *Chaoborus* larvae were used in the calculations: -59 dB (Godlewska and Jelonek 2006), -68 dB (estimated from Knudsen et al. 2006), and -73 dB (Eckmann 1998). See Fig. 1 for lake codes.

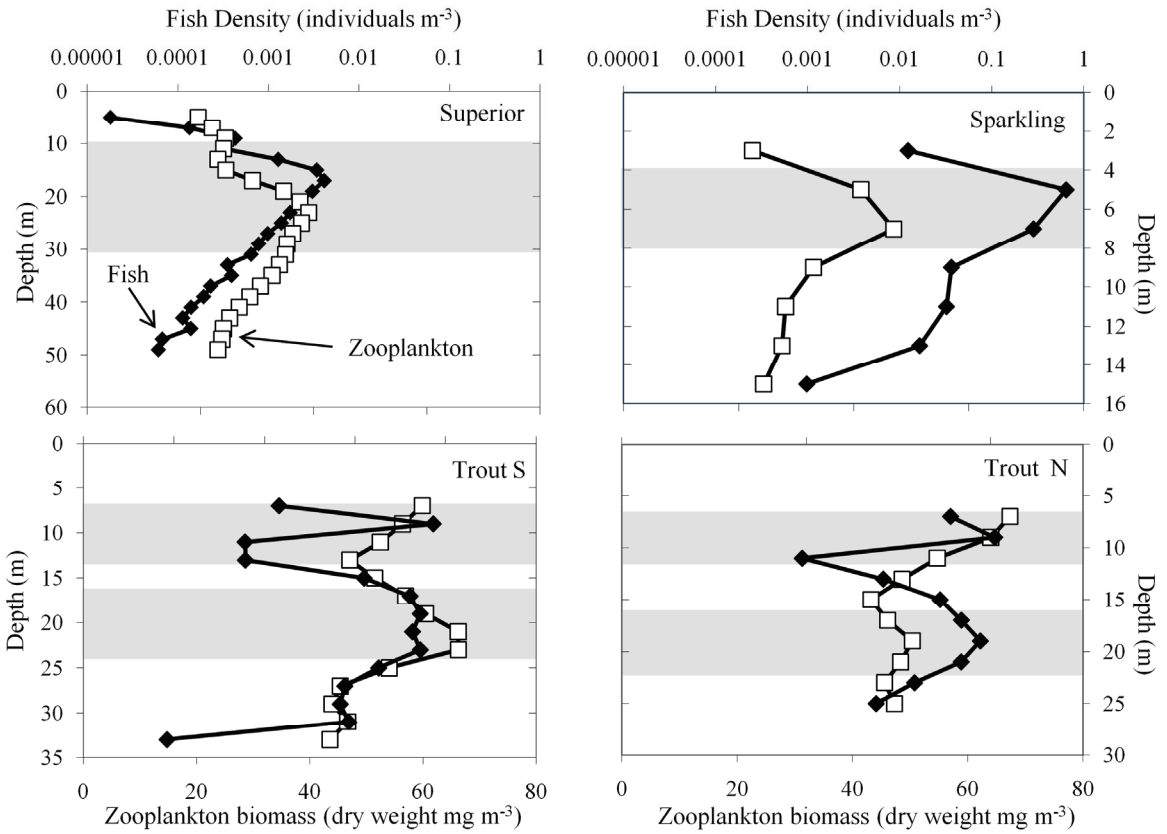

Fig. 7. The vertical distribution of zooplankton biomass (mg m^{-3}) and fish density (individuals m^{-3}) at each study location. Shaded areas represent depth strata analyzed in the spatial analysis (see text).

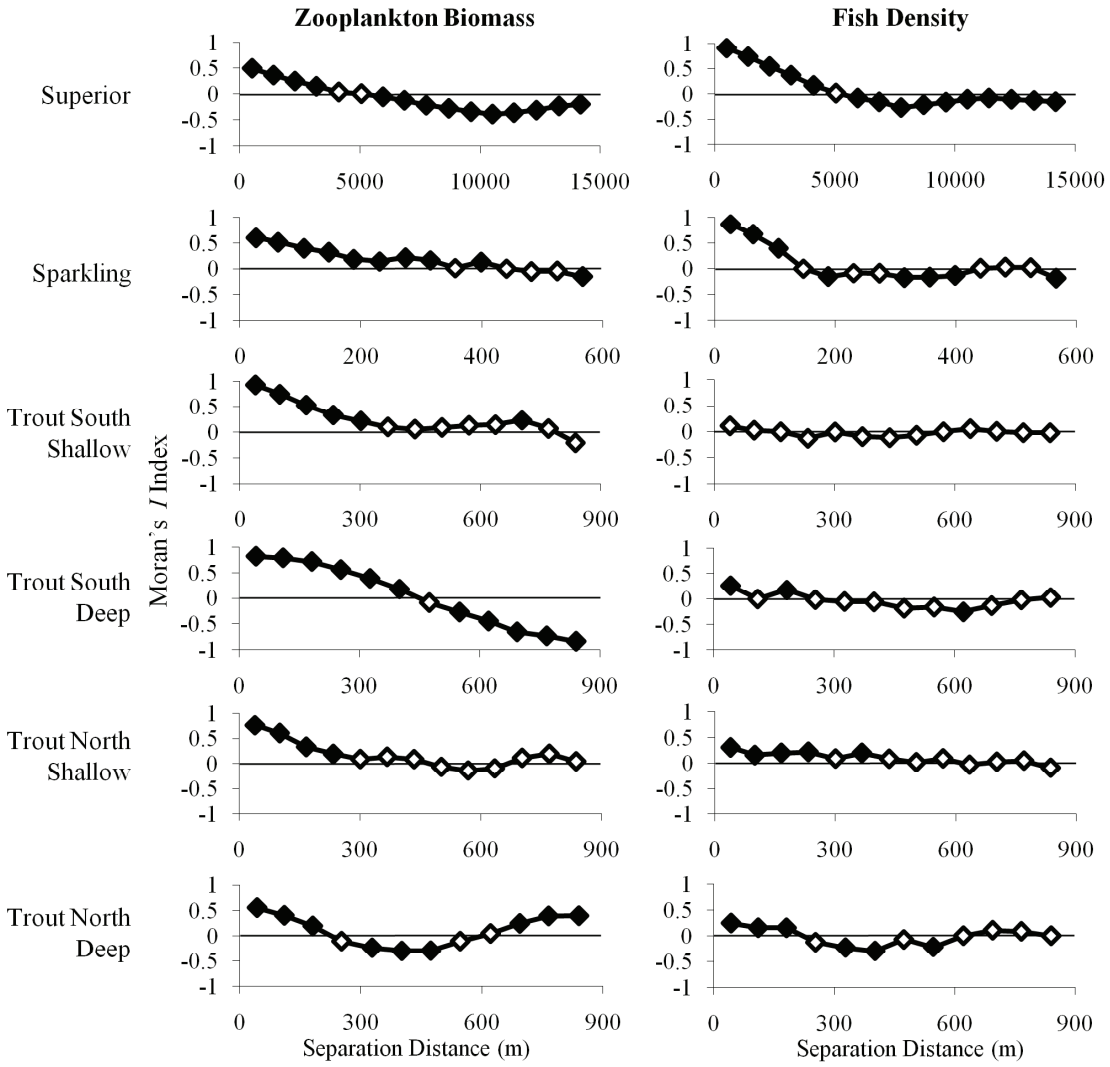

Fig. 8. Moran's *I* spatial correlograms of the vertical discrete-depth analysis for each of the study locations. Closed circles represent individual autocorrelation statistics that were significant based on a progressive Bonferroni correction and open circles represent autocorrelation statistics that were not significant based on a progressive Bonferroni correction.

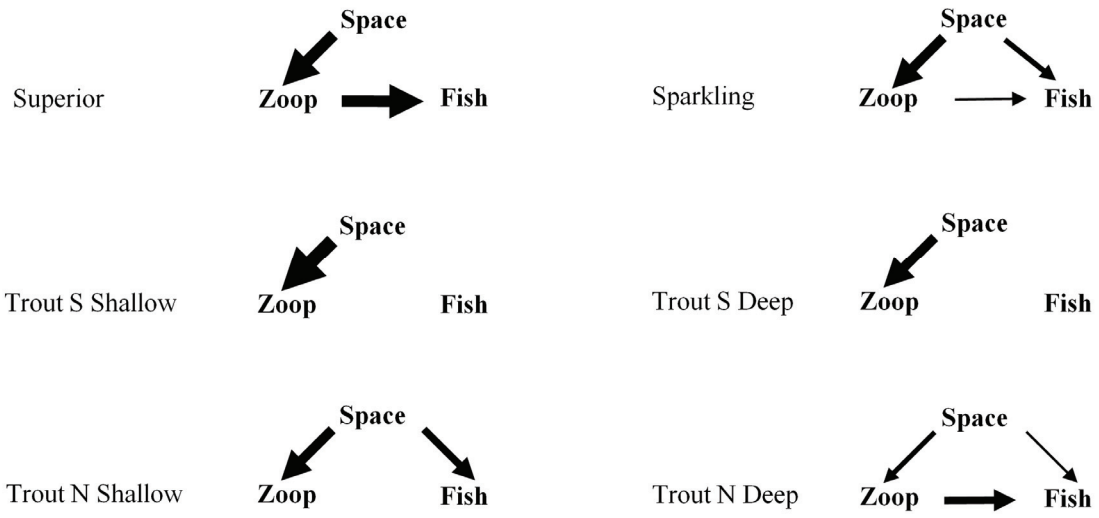

Fig. 9. Graphical models depicting relationships determined by Mantel analyses (see Table 7) and cross-correlograms. The models represent relationships between zooplankton biomass, fish density, and "space" which represented the effects of unknown factors creating spatial structure in the data. Zooplankton biomass was assumed to influence fish density (bottom-up) if the partial Mantel statistic was significant and cross-correlograms indicated a positive correlation. Fish density was assumed to influence zooplankton biomass (top-down) if the partial Mantel statistic was significant and cross-correlograms indicated a negative correlation. The weight of an arrows represents the strength of the partial Mantel statistic.

Chapter 5: Multi-trophic level interactions associated with upwelling and mesoscale eddies in a large lake

---

Introduction

Large lakes (greater than 500 km^{-2}) are unique and important ecosystems because they contain the vast majority of the total surface area of freshwater held in all lakes throughout the world (Herdendorf 1984) and because they experience physical processes such as upwellings and eddies that are similar to those found in marine systems. These physical processes may be important for delivering nutrients from inorganic-rich sources in the hypolimnion to euphotic surface waters, thereby enhancing primary productivity. In nearshore regions influenced by upwelling, there is evidence in both marine and freshwater ecosystems that this infusion of nutrients propagates up the food web to influence productivity at higher trophic levels (Ryther 1969, Mann 2000, O'Reilly et al. 2003). In offshore regions of the open ocean, there also are evidence that the majority of productivity may be the result of nutrient delivery by cyclonic mesoscale eddies (McGillicuddy et. al. 1998). Although smaller in scale, mesoscale temperature anomalies have been identified in large lakes (Ralph 2002), which may be the result of prevailing currents and lake bottom topography (Bennington et al. 2010). However, the potential influence of mesoscale eddies on the phytoplankton, zooplankton, and fish communities in large lakes has not been investigated.

The influence of hydrologic processes such as upwellings and eddies have been largely unexplored in large lakes, in part because technologies such as satellite data, hydroacoustics, and conductivity-temperature-depth (CTD) sensors have only recently enabled the rapid assessment of large volumes of water at relatively fine scales to assess simultaneous distributions of biomass and abiotic conditions. In marine systems, satellite-derived sea surface temperature (SST) data have been used successfully to identify upwelling and eddies and to correlate these temperature anomalies with *in-situ* biological variables such as chlorophyll-*a* concentrations, zooplankton biomass, and fish

recruitment (e.g. Santos et al. 2001, Perry et al. 2008, Keister et al. 2009). Satellite-derived data also are ideal for identifying these types of physical processes in large lakes because of their large spatial and temporal coverage and frequency of data collection (e.g. Ralph 2002).

SST can be used as a proxy for water temperature, which can influence organisms in two ways: 1) as an indication of physical processes that influence water column stability; and 2) as a bioenergetic driver for metabolic processes. As a result of these processes, biota may respond in complex manners to temperature gradients. For example, SST was positively correlated with phytoplankton abundance in the North Pacific when waters were cool and presumably nutrient-rich, but negatively correlated with phytoplankton abundance when waters were warm and presumably more stable and nutrient-poor (Richardson and Shoeman 2004). In Lake Superior, although concentrations of soluble nutrients in the metalimnion are low (Baehr and McManus 2003, Anagnostou and Sherrell 2008), C:P ratios of biota there also are low (Barbiero and Tuchman 2004) suggesting that P subsidy may occur. Entrainment of metalimnetic waters to nearer surface with stronger light could be a mechanism by which mesoscale eddies affect spatial distributions of productivity in Lake Superior.

Similarly, zooplankton populations may be influenced in complex ways by water temperature. Birth and growth rates of zooplankton are highly sensitive to temperature (Huntley and Lopez 1992, Rinke and Petzoldt 2003), which may result in positive correlations between measures of near-surface biomass and water temperature in large lakes (Watson and Wilson 1978, Zhou et al. 2001). However, in areas of coastal upwelling, negative correlations have also been detected between surface temperature and zooplankton biomass as a result of increased planktonic food resources for cold-water zooplankton species and currents that kept warm-water zooplankton species offshore (Keister et al. 2009). In addition to being influenced by temperature, zooplankton also have been positively correlated with chlorophyll-*a* and corresponding rates of primary production, as may be expected for a resource-consumer relationship (McQueen et al.1989, Richard and Shoeman 2004, Ware and Thompson 2005).

Temperature-driven changes in lower trophic levels also may influence higher trophic levels such as fish communities through bottom up processes. Positive spatial relationships between chlorophyll-*a,* zooplankton biomass, and fish abundance have been identified in both marine and freshwater ecosystems (Ware and Thomson 2005, Chassot et al. 2007, Rinke et al. 2009). However other limnological and marine studies have detected a negative spatial correlation between zooplankton and planktivorous fish, indicating top-down control through predation (i.e., George and Winfield 2000, Worm and Meyers 2003). It appears there may be a host of complex bottom-up and top-down processes associated with mesoscale temperature variability in large aquatic ecosystems.

The objectives of this research were to use SST data to identify areas of upwellings and mesoscale eddies within a study site on a large lake and to determine the influence of these hydrologic processes on the spatial arrangement of phytoplankton, zooplankton, and fish. We assumed that physical processes influencing SST would most strongly affect organisms within the mixed layer, particularly if temperature gradients and surface anomalies were relatively persistent, which would allow biota time to respond to the physical conditions in the lake. Therefore, our purposes for this study were twofold: 1) to determine the influence of upwelling and mesoscale eddies as determined by satellite-derived measurements on the spatial distribution of epilimnetic chlorophyll-*a* concentrations, zooplankton biomass, and fish density; and 2) to determine spatial coupling between these trophic levels within the mixed layer.

Methods

Study site

Data were collected at night (1 h after sunset, 2 h before sunrise) aboard the R/V Blue Heron in the western arm of Lake Superior on 22 Aug through 26 Aug 2005, and on 28 Aug through 1 Sept 2006 (Fig. 1). Transects were established approximately 50 km in

length in 2005, and 30 km in length in 2006 (Fig. 1). Only night data were collected to accommodate fish and zooplankton participating in diel vertical migration and to avoid the inhibition of photosynthetic cells during daylight hours (Kiefer 1973) that would influence data collected with the fluorometer. Wind data immediately preceding and during sampling dates were downloaded from station 45006 of the National Oceanic and Atmospheric Administration's National Data Buoy Center (http://www.ndbc.noaa.gov). Wind rose graphs were created using WRPLOT View 6.5.2 (Lakes Environmental, Waterloo, Ontario).

Bottom depths were relatively constant at approximately 170 m throughout the transects. A Triaxus underwater towbody was pulled behind the vessel at 13 km h^{-1}, undulating continuously between 5 m and 50 m depth to sample water both vertically and horizontally. Triaxus measurements included temperature (ºC), depth (Seabird 911 plus CTD), and chlorophyll-*a* concentration (Wetlabs fluorometer, mg m^{-3}). Data collected with the Triaxus towbody were georeferenced using the vessel's global positioning system (GPS). However, the towbody trailed the vessel at a distance varying between 130 m and 200 m, so the cruise track was imported into a geographic information system (GIS, ESRI ArcMap 9.3), which was used to offset the GPS of the Triaxus towbody based on the navigation log.

The depth of the epilimnion was estimated by analyzing vertical temperature profiles collected by Triaxus in approximately 30 minute increments. If there was a substantial difference in the depth of the epilimnion within that time frame, then smaller increments of time were used to estimate the epilimnion depth until vertical temperature profiles were similar. Measurements of temperature and chlorophyll-*a* were averaged each time the epilimnion was sampled and assigned a GPS tag for the midpoint.

Hydroacoustic data

Data on fish and zooplankton density and distribution were collected using hydroacoustic technology. Alternating pulse transmissions were used for two high-

frequency hydroacoustic units with separate, non-overlapping frequencies (Zooplankton: Biosonics 430 kHz split-beam echosounder DT6000; Fish: Biosonics 120 kHz split-bean echosounder DT6000). Transducers were mounted on a towbody that was towed alongside the research vessel so data were collected concurrently while the Triaxus towbody was deployed. Both hydroacoustic units were periodically calibrated using standard tungsten-carbide spheres, and their target strengths never varied significantly (<±1 dB) from the known target strength of the spheres. Configurations of the transducers are listed in Table 1. Hydroacoustic data were georeferenced using the vessel's GPS.

All hydroacoustic data were analyzed using Echoview 4.10 (Myriax Software Pty., Hobart, Tasmania). Hydroacoustic data were partitioned in 100 m increments in 2005 and 200 m increments in 2006 to correlate with the average distance that the Triaxus towbody traveled through the epilimnion during each sampling year. Georeferenced epilimnion depths from Triaxus were imported into Echoview and applied to both the echo squared integration data and single target data so that only zooplankton and fish in the epilimnion were analyzed. The top 2-m of the water column were not analyzed to eliminate backscatter from air bubbles caused by wave action and turbulence.

The 430-kHz acoustic data were analyzed for zooplankton biomass distribution (mg m^{-3}) based on the methodology described by Holbrook et al. (2006). A minimum threshold of -85 dB was applied to echo squared integration data and a maximum threshold was applied to eliminate backscatter from fish targets (2005: -54 dB; 2006: -60 dB). Hydroacoustic backscatter was then converted to zooplankton dry weight biomass (mg m^{-2}) using the regression developed by Holbrook et al. (2006) and divided by the depth of the epilimnion to determine zooplankton volumetric biomass (mg m^{-3})

The 120-kHz acoustic data were analyzed for fish density distribution (individuals m^{-3}). An overall average mean target strength (TS) was estimated by conducting a split-beam analysis of single targets using a -55 dB threshold and single target detection parameters described by Yule et al. (2006). The average single target size was -43.8 dB in 2005 (n=394) and -40.1 dB in 2006 (n=2591), which was applied to echo squared

integration data to estimate fish density (Yule et al. 2006). A minimum threshold value of -65 dB was applied during post-processing analysis of the echo squared integration data (Hrabik et al. 2006). Hydroacoustic data were imported into GIS and a spatial join function was used with the GPS to match the closest hydroacoustic increment with the midpoint of the epilimnion sampled by the Triaxus towbody.

Satellite data

Satellite-derived sea surface temperature (SST) data from Advanced Very High Resolution Radiometer (AVHRR; resolution: 1.1 km) were used to identify temperature patterns and mesoscale anomalies. Mostly cloud-free nighttime AVHRR SST images that corresponded with *in-situ* sampling were averaged for the cruise dates. Using the methodology described in Ralph (2002), a smooth field was created by replacing each pixel of the composite SST data with the median SST value within a 20 km x 20 km box centered at the pixel. The smooth field was subtracted from the composite SST data to determine mesoscale temperature anomalies indicative of warm and cold eddies and then trimmed to the sampling location.

Statistical analysis

A regression tree analysis was conducted using the rpart package (v. 3.1-48) within the R environment (R 2.11.1, R Development Core Team 2011) to evaluate the most significant variables predicting the abundance of chlorophyll-*a*, zooplankton biomass, and fish density. The regression tree statistical method is a nonparametric approach that is well-suited for models that include complex interactions among variables (McCune and Grace 2002). The regression tree technique involved recursively partitioning the data into increasingly homogenous subsets. The first step involved growing a maximal tree and the second step involved pruning the tree to avoid overfitting. We used a cost-complexity criterion (cp) and 10-fold cross-validation to prune the tree to an optimum size (Therneau and Atkinson 1997). The one-standard error rule was used to select the least complex tree whose cross-validated error did not differ

by more than one standard error compared with the minimum cross-validated error (Breiman et al. 1984). Variables entered into the analysis included: SST (ºC), surface anomaly (ºC), chlorophyll-*a* concentration (mg m^{-3}), zooplankton biomass (mg m^{-3}), and fish density (individuals m^{-3}). SST was used instead of *in situ* epilimnetic temperatures to keep methodology consistent with Ralph et al. (2002) who used SST to identify mesoscale eddies as persistent features in Lake Superior.

Mantel tests were used to evaluate correlations among the preceding variables and including "space", which represented the effect of unmeasured factors creating spatial structure in the data. Partial Mantel tests were used to determine correlations between two variables while controlling for the effect of a third variable (Legendre and Legendre, 1998). Variables that were not normally distributed were transformed using either a $\log_{10}(x+1)$ transformation or Box-Cox transformation prior to conducting the tests. The significance of the Mantel test and Partial Mantel Tests were evaluated at the Bonferonni corrected significance level. The ecodist package (v. 1.2.3, function mantel) was used in R statistical software to calculate Mantel and partial Mantel statistics using 1,000 permutations. If the Mantel statistics indicated a significant correlation between two variables, cross-correlograms were conducted using GS+ 9.0 software (Gamma Design Software, Plainwell, Michigan) to determine the directionality of the relationship.

We also compared two prominent, proximate cold- and warm-water eddies that were transected during the 2005 sampling cruise. Both eddies were located outside the upwelling zone approximately 30 km offshore. A one-way ANOVA was conducted to detect significant ($p<0.05$) differences in chlorophyll-*a* concentrations, zooplankton biomass, and fish density within these two eddies. We displayed means from the eddies with means from the upwelling zone for comparison, but data from the upwelling zone were not included in the ANOVA analysis because of complex eddy interactions within this zone.

Results

The maximum depth of the epilimnion averaged 7.5 m in 2005 and 16 m in 2006, although measurements as deep as 38 m were recorded alongshore in 2006. The increased depth of the epilimnion in 2006 coincided with strong easterly and northeasterly winds recorded during sampling dates (Fig. 2). In both years, the average temperature of the epilimnion was significantly correlated with SST (Spearman rank correlation coefficient; 2005: $\rho=0.84$, $p<0.01$, $n=293$; 2006: $\rho=0.57$, $p<0.01$, $n=105$).

There was no overlap in SST between the two years of this study (Fig. 3). SST ranged from 11.0 – 16.2 ºC in 2005 and 16.3 – 17.6 ºC in 2006. There was also greater variability in chlorophyll-*a* and zooplankton biomass in 2005 compared with 2006 (Fig. 3). In 2005, maps of SST overlaid with distributions of chlorophyll-*a* concentrations, zooplankton biomass, and fish density indicated colder temperatures nearshore (Fig. 4) as a result of upwelling due to offshore winds immediately preceding the sampling cruise (Fig. 2). Chlorophyll-*a* concentrations were highly clumped and located in one nearshore region, while zooplankton biomass was distributed mostly evenly across the study site and fish density showed no detectable pattern (Fig. 4). In 2006, the number of transects were limited due to poor weather conditions (Fig. 1), but chlorophyll-*a* concentrations and zooplankton biomass were clumped, while fish density showed no detectable pattern (Fig. 5). Fig. 4 and Fig. 5 also display maps of surface anomalies overlaid with distributions of chlorophyll-*a* concentrations, zooplankton biomass, and fish density. In 2005, there was a strong presence of both warm and cold eddies that were not strongly correlated with patterns in SST (Fig. 4). In 2006, maps of surface anomalies were very similar to maps of SST and eddies could not be easily identified (Fig. 5).

Regression tree analysis indicated that in 2005, 63% of the variability in chlorophyll-*a* was explained by SST and zooplankton biomass (Fig. 6) The first split explained 54% of the variability in chlorophyll-*a* concentration, and the second split explained an additional 9%. Lower SST corresponded with greater chlorophyll-*a* concentrations, mostly within the cold SST region nearshore (Fig. 4). Lower concentrations of zooplankton biomass also corresponded with greater chlorophyll-*a*

concentration within this cold-water SST region (Fig. 6). Regression tree analysis did not select any significant predictors of zooplankton biomass or fish density in 2005.

Regression tree analysis indicated that in 2006, 52% of the variability in chlorophyll-*a* was explained by zooplankton biomass (Fig. 6). Similar to 2005, lower concentrations of zooplankton biomass corresponded with greater chlorophyll-*a* concentrations. The pruned tree models also indicated that in 2006, 54% of the variability in zooplankton biomass was explained by chlorophyll-*a*, with lower concentrations of chlorophyll-*a* correlated to higher abundances of zooplankton biomass (Fig. 6). Regression tree analysis did not select any significant predictors of fish density in 2006.

Mantel statistics indicated that in 2005, variables that were significantly correlated included SST and surface anomaly, SST and chlorophyll-*a*, SST and zooplankton biomass, and surface anomaly and chlorophyll-*a* (Table 2). However, partial Mantel tests indicated that the correlation between surface anomaly and chlorophyll-*a* concentration was not significant once the effects of SST were removed. Simple Mantel statistics also indicated the presence of spatial autocorrelation in SST, chlorophyll-*a* concentration, and zooplankton biomass (Table 2), but partial Mantel statistics indicated that the autocorrelation in chlorophyll-*a* concentration and zooplankton biomass was largely due to the spatial structure present within SST data. When the effects of SST were removed, there was no longer significant spatial structure in chlorophyll-*a* concentrations or zooplankton biomass (Table 2).

Mantel statistics indicated that in 2006, variables that were significantly correlated included SST and surface anomaly, chlorophyll-*a* and zooplankton biomass, and SST and chlorophyll-*a* (Table 3). However, partial Mantel tests indicated that the correlation between SST and chlorophyll-*a* was not significant when the spatial effect was removed. Simple Mantel statistics also indicated the presence of spatial autocorrelation in SST, surface anomaly, chlorophyll-*a* concentration, and zooplankton biomass (Table 3). However, simple Mantel tests indicated that spatial autocorrelation in surface anomaly and chlorophyll-*a* concentration was largely due to the spatial structure

present within SST data. When the effect of SST was removed, there was no significant spatial autocorrelation in either of these data sets. However, significant spatial autocorrelation remained within zooplankton biomass data even when removing the effects of SST (Table 3).

Average chlorophyll-*a* concentration, zooplankton biomass, and fish density were compared between two prominent proximate eddies (Fig. 7) that were transected while sampling (Fig. 4). The means from the upwelling zone are also shown (Fig. 7), although the significance was not tested because of the confounding effects of a prominent warm-water eddy and possible cold-water eddies within this upwelling zone (Fig. 4). Moran's *I* correlograms indicated autocorrelation in chlorophyll-*a* and zooplankton biomass data collected within each eddy. If data were considered to be independent, chlorophyll-*a* concentration was significantly higher in the cold-water eddy (ANOVA, F=13.7, $p<0.01$), and zooplankton biomass was significantly lower in the cold-water eddy (ANOVA, F=6.3, $p<0.05$) compared with the warm-water eddy (Fig. 7). However, when we accounted for autocorrelation by calculating an effective sample size (Fortin and Dale 2005), there were no significant differences between chlorophyll-*a* and zooplankton biomass at the $p=0.05$ significance level. There also were no significant differences in fish density (ANOVA, $p>0.05$). Patterns of higher concentrations of chlorophyll-*a*, lower abundances of zooplankton, and higher densities of fish were consistent between the cold-water eddy and the upwelling zone.

Five representative down and up temperature and chlorophyll-*a* profiles within each eddy are displayed in Fig. 8. Vertical profiles within the cold-water eddy were characterized by colder surface temperatures, higher concentrations of chlorophyll-*a* near-surface, and a shallower chlorophyll maximum at approximately 18 m depth. Vertical profiles within the warm-water eddy were characterized by warmer surface temperatures, lower concentrations of chlorophyll-*a* near-surface, a deeper chlorophyll maximum at approximately 28 m depth, and higher concentrations of chlorophyll-*a* deeper in the water column (Fig. 8).

Discussion

The only primary finding that was consistent among the two years of this study was the strong, significant presence of spatial structure in SST data (Tables 2, 3). However, temperature gradients varied substantially from one year to the next presumably as a result of circulation patterns related to prevailing winds. In 2005, offshore westerly winds were dominant during the two days prior to the sampling dates (Fig. 2), leading to upwelling along the western shore of Lake Superior. As a result, the study site was characterized by cold SST nearshore and warm SST offshore (Fig. 4). In 2006, strong easterly and northeasterly winds coincided with our sampling dates (Fig. 2), limiting the spatial coverage of the sampling cruise (Fig. 1), and presumably pushing warmer surface waters nearshore, tilting the thermocline, and causing increased vertical mixing. This scenario is supported by our data, including a higher SST on average in 2006 compared with 2005 (Fig. 2), more variability in nearshore-offshore SST gradients in 2006 (Fig. 5), a less pronounced eddy field in 2006 (Fig. 5), and greater epilimnion depths nearshore in 2006. Therefore, although we found that SST was significantly correlated with mean epilimnion temperature during both years of this study, the weaker relationship in 2006 was likely due to greater thermal mixing subsurface.

We expected the influence of SST and surface anomalies to be more pronounced in 2005, given the relative stability of the thermal regime and the strength of the eddy field, which would have given time for biota to respond to upwelling that occurred prior to the research cruise. In contrast, we expected to find little influence of SST and surface anomalies on the biota in 2006, given the volatility of wind conditions and thermal mixing that occurred during the research cruise. The relationship between SST and chlorophyll-*a* supported this hypothesis, with regression tree analysis, Mantel statistics, and cross-correlograms all indicating a strong negative relationship between SST and chlorophyll-*a* in 2005. However, there was no effect of surface anomalies on chlorophyll-*a* concentrations in 2005. In 2006, simple Mantel statistics and cross-

correlograms indicated a weak positive relationship between SST and chlorophyll-*a*, but partial Mantel statistics indicated that this relationship was not significant when the spatial effect was removed. There was no effect of surface anomalies on chlorophyll-*a* in 2006.

On average, epilimnetic chlorophyll-*a* concentrations were higher in 2006 compared to 2005, although the highest values were observed in 2005 in association with the coldest SST (Fig. 3). Hydrodynamic processes may explain both trends. In 2005, upwelling in the days prior to our sampling dates likely may have caused an increase in epilimnetic chlorophyll-*a* concentration through three possible mechanisms: 1) mixing of phosphorus from near-shore or sub-surface waters to near-surface waters; 2) mixing of phytoplankton from the deep chlorophyll layer (DCM) to near-surface waters; or 3) upward movement of water reducing sedimentation rates and causing greater retention of phosphorus within the epilimnion. In Lake Superior, phytoplankton growth is P-limited and Fe-deficient (Sterner et al. 2004), so increased P availability near-surface would likely cause increased phytoplankton growth. There is some evidence that near-shore phosphorus may be more reactive than offshore phosphorus (Baehr and McManus 2003), which could have enhanced phytoplankton growth in the near-shore upwelling zone. Additionally, sub-surface nutrient delivery could have enhanced phytoplankton growth further offshore. Although there is no evidence that soluble reactive phosphorus (SRP) or total dissolved phosphorus (TDP) concentrations increase at depth in Lake Superior (Baehr and McManus 2003; Anagnostou and Sherrell 2008), phosphorus made available through processes such as mineralization and grazing may be utilized too quickly to be detected in water concentrations (Barbiero and Tuchman 2004). Phosphorus enrichment may also explain the lower C:P ratios of phytoplankton in the DCM compared with phytoplankton in the epilimnion (Barbiero and Tuchman 2004), although light limitation could also be a cause (Barbiero and Tuchman 2004, Sterner 2010). Alternatively, the upward movement of water may push phytoplankton from the DCM into near-surface waters causing an increase in abundance of phytoplankton containing high chl:C ratios (Sterner 2010), or it may reduce nutrient loss within the epilimnion causing enhanced

phytoplankton growth. In areas of our study area unaffected by upwelling, calm winds during sampling in 2005 (Fig. 2) may have enhanced water column stability, depleting nutrients and causing a reduction in phytoplankton growth. In 2006, easterly and northeasterly winds (Fig. 2) may have resulted in higher chlorophyll-*a* concentrations offshore as a result of increased thermal mixing, which may have brought sub-surface nutrients or phytoplankton to near-surface waters, or reduced sedimentation rates that increased phosphorus retention within the epilimnion, similar to mechanisms that may explain higher chlorophyll concentrations within the upwelling zone in 2005.

In addition to the relationship between SST and chlorophyll-*a* concentrations, we also detected a weak, positive relationship between SST and epilimnetic zooplankton biomass in 2005 (Mantel r=0.12). This relationship was much weaker than the r^2=0.54 correlation observed by Zhou et al. (2001), who compared the average temperature in the upper 10 m of the water column with the natural log of zooplankton bio-volume in Lake Superior. For comparison, the correlation between average epilimnetic temperature and the natural log of zooplankton biomass in our data was r^2=0.07 in 2005 and r^2=0.26 in 2006. Interestingly, the relationship in 2006 was negative and stronger than the relationship in 2005, even though Mantel statistics indicated that there was no significant relationship between SST and zooplankton biomass in 2006, which may indicate that SST is not an accurate proxy for subsurface temperatures during large mixing events.

One of the primary differences in this study compared with that conducted by Zhou et al. (2001) was the timing of the sampling. Zhou et al. (2001) conducted an offshore to nearshore transect in mid-July, so the relationship between near-surface temperature and zooplankton biomass may have been influenced by seasonal warming trends. The second primary difference between this study and that conducted by Zhou et al. (2001) is that we used hydroacoustic technology to sample the zooplankton community rather than an optical plankton counter (OPC). There is strong evidence that 430-kHz backscatter is highly correlated with zooplankton biomass from 250 µm net tows (Holbrook et al. 2006, Holbrook 2011). At this frequency, large zooplankton likely scatter the greatest proportion of sound, although small zooplankton can be important

contributors if their biomass is highly concentrated (Holbrook 2011). In contrast to hydroacoustic technology, the OPC is non-discriminative and samples zooplankton down to 250 – 300 μm (Sprules et al. 1998). Our data suggest that the relationship between temperature and near-surface zooplankton biomass may be weaker for larger zooplankton that are more mobile and capable of horizontal and vertical migration.

We propose two mixing schemes (Fig. 9) to describe patterns in SST and chlorophyll-*a* concentrations, based on similar scenarios proposed in other studies (Svensson 1978, George and Winfield 2000). In 2005, offshore winds prior to sampling caused upwelling alongshore, resulting in cooler SST and vertical profiles that were characterized by the presence of a chlorophyll maximum within the mixed layer. Offshore vertical profiles were characterized by warmer SST and vertical profiles that were characterized by the presence of a chlorophyll maximum below the thermocline (Fig. 9). In 2006, onshore winds caused warm surface water to pile up nearshore, resulting in vertical profiles characterized by an increased depth of the mixed layer and low concentrations of chlorophyll-*a* in the epilimnion. Offshore, vertical profiles were characterized by a shallower thermocline and the presence of a chlorophyll maximum near the top of the thermocline.

The mixing schemes that we propose in Fig. 9 would also explain the strong, negative correlation between chlorophyll-*a* and zooplankton biomass that we observed in 2006 (Table 3). In the northwest corner of the study site, high chlorophyll-*a* concentrations were observed offshore and high abundances of zooplankton biomass were observed nearshore, although low abundances of zooplankton were found immediately nearshore (Fig. 5). Northeasterly and easterly winds may have transported epilimnetic zooplankton along with warm surface waters nearshore (Fig. 9), where downwelling may have caused a decrease in zooplankton biomass closest to the shore (Fig. 5). Meanwhile, boundary mixing may have caused sub-surface nutrients or phytoplankton to be transported offshore via return epilimnetic currents and brought closer to the surface along the tilted thermocline (Fig. 9). Alternatively, increased mixing

may have resulted in reduced nutrient loss rates within the epilimnion, causing enhanced phytoplankton growth.

Alternatively, the inverse relationship between chlorophyll-*a* and zooplankton biomass in 2006 could have been the result of zooplankton grazing on phytoplankton. However, Rinke et al. (2009) determined that biological interactions were strongest when the strength of external forcing such as wind-induced currents was lowest, so this hypothesis seems less likely given the instability of circulation patterns in 2006 and the limited time the biota had to respond to these conditions during our sampling dates. More likely, biological interactions could explain the weak negative relationship between zooplankton and phytoplankton within the cold SST region in 2005 (Fig. 6). While the two mixing schemes that we proposed (Fig. 9) may explain several of the trends that we observed during the years of this study, the small amount of data that we collected in the southeast corner of the study area in 2006 suggests that mid-lake circulation patterns were much more complex than nearshore circulation patterns when wind-induced mixing was high.

In contrast to spatial patterns in SST, chlorophyll-*a*, and zooplankton biomass, we did not detect any spatial structure in fish density during either year of this study (Tables 2, 3). Epilimnetic fish density was very low and showed no detectable pattern across the sampling site during both 2005 and 2006 (Figs. 4, 5). Although there were differences in the mean target strength during the two years of this study (2005: -43.8 dB, 2006: -40.1 dB), targets of these sizes located in the epilimnion of Lake Superior were likely primarily rainbow smelt (*Osmerus mordax*) based on Yule et al. (2009). We also did not detect any correlations between lower trophic levels and the fish community, which is in contrast to some marine and freshwater research which has detected positive correlations between trophic levels (Ware and Thomson 2005, Chassot et al. 2007, Rinke et al. 2009). In our study, epilimnetic fish densities may have been too low to adequately detect relationships with lower trophic levels. Alternatively, because rainbow smelt undergo diel vertical migration (Appenzeller and Leggett 1995), it is possible that the relatively

short duration of time that they were in the epilimnion at night did not allow for them to concentrate in areas of greatest prey abundance.

This study represents a first attempt to determine whether the presence of mesoscale surface anomalies in Lake Superior may have an important bottom-up influence on the spatial distribution of phytoplankton, zooplankton, and fish. We did not detect broad-scale influences of mesoscale eddies on the distribution of chlorophyll-*a* concentration, zooplankton biomass, or fish density during either year of this study (Tables 2, 3, Fig. 6). Comparisons between two proximate prominent warm- and cold-water eddies in 2005 (Fig. 4) were inconclusive (Fig. 7). When accounting for autocorrelation in the data by calculating an effective sample size (Fortin and Dale 2005), there were no significant differences between eddies when using an ANOVA analysis. However, there are challenges to this approach, particularly when applied to a small sample size such as in this case (Fortin and Dale 2005). However, the patterns that we observed in our data were consistent with marine studies that have found cyclonic cold-water eddies to have higher concentrations of chlorophyll-*a* compared with surrounding waters (McGillicuddy et al. 1998, Benitez-Nelson et al. 2007, Nencioli et al. 2008). In marine systems, the relationship between zooplankton biomass and cyclonic eddies is more variable, but there is evidence that the core of cold-water eddies may be associated with lower abundances of zooplankton biomass (Hernández-León et al. 2001, McGillicuddy et al. 2007). Vertical profiles within the cold-water eddy were characterized by a shallower depth of the chlorophyll maximum (Fig. 8), which is also characteristic of marine cold-water cyclonic eddies (McGillicuddy et al. 2007, Benitez-Nelson et al. 2007, Nencioli et al. 2008). Although our data suggest that cold-water mesoscale eddies may potentially contribute to near-surface primary production, our conclusions are far from definitive. Additionally, the effects of cold-water eddies appear to be substantially weaker than the effects of upwelling (Fig. 8).

A closer investigation of the surface anomalies from our 2005 data indicated that the eddies were approximately 5-8 km in size and frequently oscillated in position, although averaging the eddy field over the course of the sampling dates indicated that

warm- and cold-water eddies tended to stay within a 10- to 15-km region. The frequent fluctuations of these eddies within these regions may make it difficult to detect effects on the biotic community. Additionally, because we sampled without prior information and without knowing where eddies were positioned, we transected the edges of many of the most prominent eddies (Fig. 4) where the effect may have been less pronounced (Allen et al. 1996). That we transected so few eddies may explain why we were unable to detect a broad-scale influence of surface anomalies, but we were able to detect significant differences in chlorophyll concentration and zooplankton biomass between the two eddies that we examined more closely (Figs. 7, 8). In the future, a targeted approach may allow the biological influence of these eddies to be more thoroughly addressed. Satellite images could be downloaded on-ship in near-real time and quickly analyzed to determine where sampling should be focused.

Assessing the biological influence of temperature gradients, upwellings, and surface anomalies is timely given evidence of increased wind speeds over Lake Superior as a result of climate change (Desai et al. 2009). The results of our study indicate that patterns in chlorophyll-*a* concentration and zooplankton can be strongly influenced by wind-driven circulation patterns. For example, an increase in the frequency and intensity of northeasterly and easterly winds may result in greater concentrations of zooplankton biomass nearshore when transported with warm surface waters (Fig. 5). Alternatively, an increase in frequency and intensity of westerly winds may result in increased upwelling along the western shore of Lake Superior, causing increased chlorophyll-*a* concentrations in the epilimnion. However, the impacts of upwelling may be reduced by warming surface temperatures that increase the depth of the mixed layer and limit the upward movement of water (Desai et al. 2009, Roemmich and McGowan 1995).

In summary, we determined that hydrologic processes associated with prevailing winds created spatial structure in SST and influenced the distribution of epilimnetic chlorophyll-*a* and zooplankton biomass. In 2005, upwelling as a result of westerly winds that preceded sampling dates caused an increase in the concentration of chlorophyll-*a* within the mixed layer. We also detected a weak negative relationship between

chlorophyll-*a* and zooplankton biomass within this cold, upwelling-influenced region. In 2006, downwelling as a result of easterly and northeasterly winds during our sampling dates resulted in warm surface waters piling up nearshore, causing tilting of the thermocline, low concentrations of chlorophyll-*a*, and high concentrations of zooplankton. Offshore, we detected high concentrations of chlorophyll-*a* in the epilimnion, perhaps as a result of sub-surface turbulent mixing and epilimnetic currents, or reduced nutrient loss within the epilimnion. We were unable to detect any broad-scale biological influence of surface anomalies, but we did detect significant differences in chlorophyll-*a* concentration and zooplankton biomass between two prominent proximate warm- and cold-water eddies in 2005. We also did not detect any correlations between fish density and SST or lower trophic levels, although epilimnetic fish density was very low during both years of this study. In conclusion, our data indicate that circulation patterns in Lake Superior create a dynamic environment that structures the spatial distribution of phytoplankton and zooplankton.

Table 1. Configurations of the hydroacoustic transducers used in this study.

Frequency (kHz)	Type of Beam	Beam-width (º)	Source level at 1 m (dB re 1 µPa)	Pulse duration (ms)	Receive Sensitivity (dB)	Pulse rate (pps)
120	Split	7.3 x 7.3	220.0	0.4	-51.2	1-2
430	Split	6.5 x 6.5	219.0	0.2	-54.0	1-2

Table 2. Simple (upper right) and partial (lower left) Mantel statistics for 2005 data. Significant values were reported at the Bonferroni-corrected probability (simple: 0.003; partial: 0.0008). *NS* = tests that were not significant. Partial Mantel statistics tested the correlation between two variables while controlling for the effects of a third variable: SST (*T*), anomaly (*A*), chlorophyll-*a* (*C*), zooplankton (*Z*), fish (*F*), and space (*S*). "Space" represented the strength of spatial autocorrelation.

	SST (ºC)	Anomaly (ºC)	Chlorophyll-*a* (mg m^{-3})	Zooplankton (mg m^{-3})	Fish (# m^{-3})	Space
SST (ºC)	_	0.20	0.39	0.12	NS	0.55
Anomaly (ºC)	-C: 0.17 -Z: 0.20 -F: 0.20 -S: 0.21	_	0.11	NS	NS	NS
Chlorophyll-*a* (mg m^{-3})	-A: 0.38 -Z: 0.39 -F: 0.39 -S: 0.31	-T: NS -Z: 0.11 -F: 0.11 -S: NS	_	NS	NS	0.26
Zooplankton (mg m^{-3})	-A: 0.12 -C: 0.12 -F: 0.12 -S: 0.10	-T: NS -C: NS -F: NS -S: NS	-T: NS -A: NS -F: NS -S: NS	_	NS	0.07
Fish (# m^{-3})	-A: NS -C: NS -Z: NS -S: NS	-T: NS -C: NS -Z: NS -S: NS	-T: NS -A: NS -Z: NS -S: NS	-T: NS -A: NS -C: NS -S: NS	_	NS
Space	-A: 0.56 -C: 0.51 -Z: 0.55 -F: 0.55	-T: NS -C: NS -Z: NS -F: NS	-T: NS -A: 0.25 -Z: 0.25 -F: 0.26	-T: NS -A: 0.07 -C: NS -F: 0.07	-T: NS -A: NS -C: NS -Z: NS	_

Table 3. Simple (upper right) and partial (lower left) Mantel statistics for 2006 data. Significant values were reported at the Bonferroni-corrected probability (simple: 0.003; partial: 0.0008). *NS* = tests that were not significant. Partial Mantel statistics tested the correlation between two variables while controlling for the effects of a third variable: SST (*T*), anomaly (*A*), chlorophyll-*a* (*C*), zooplankton (*Z*), fish (*F*), and space (*S*). "Space" represented the strength of spatial autocorrelation.

	SST (ºC)	Anomaly (ºC)	Chlorophyll-*a* (mg m^{-3})	Zooplankton (mg m^{-3})	Fish (# m^{-3})	Space
SST (ºC)	_	0.91	0.14	NS	NS	0.49
Anomaly (ºC)	-C: 0.91 -Z: 0.91 -F: 0.91 -S: 0.89	_	NS	NS	NS	0.46
Chlorophyll-*a* (mg m^{-3})	-A: NS -Z: NS -F: 0.14 -S: NS	-T: NS -Z: NS -F: NS -S: NS	_	0.45	NS	0.11
Zooplankton (mg m^{-3})	-A: NS -C: NS -F: NS -S: NS	-T: NS -C: NS -F: NS -S: NS	-T: 0.45 -A: 0.45 -F: 0.45 -S: 0.44	_	NS	0.21
Fish (# m^{-3})	-A: NS -C: NS -Z: NS -S: NS	-T: NS -C: NS -Z: NS -S: NS	-T: NS -A: NS -Z: NS -S: NS	-T: NS -A: NS -C: NS -S: NS	_	NS
Space	-A: 0.18 -C: 0.48 -Z: 0.48 -F: 0.49	-T: NS -C: 0.46 -Z: 0.46 -F: 0.46	-T: NS -A: NS -Z: NS -F: NS	-T: 0.19 -A: 0.19 -C: 0.18 -F: 0.21	-T: NS -A: NS -C: NS -Z: NS	_

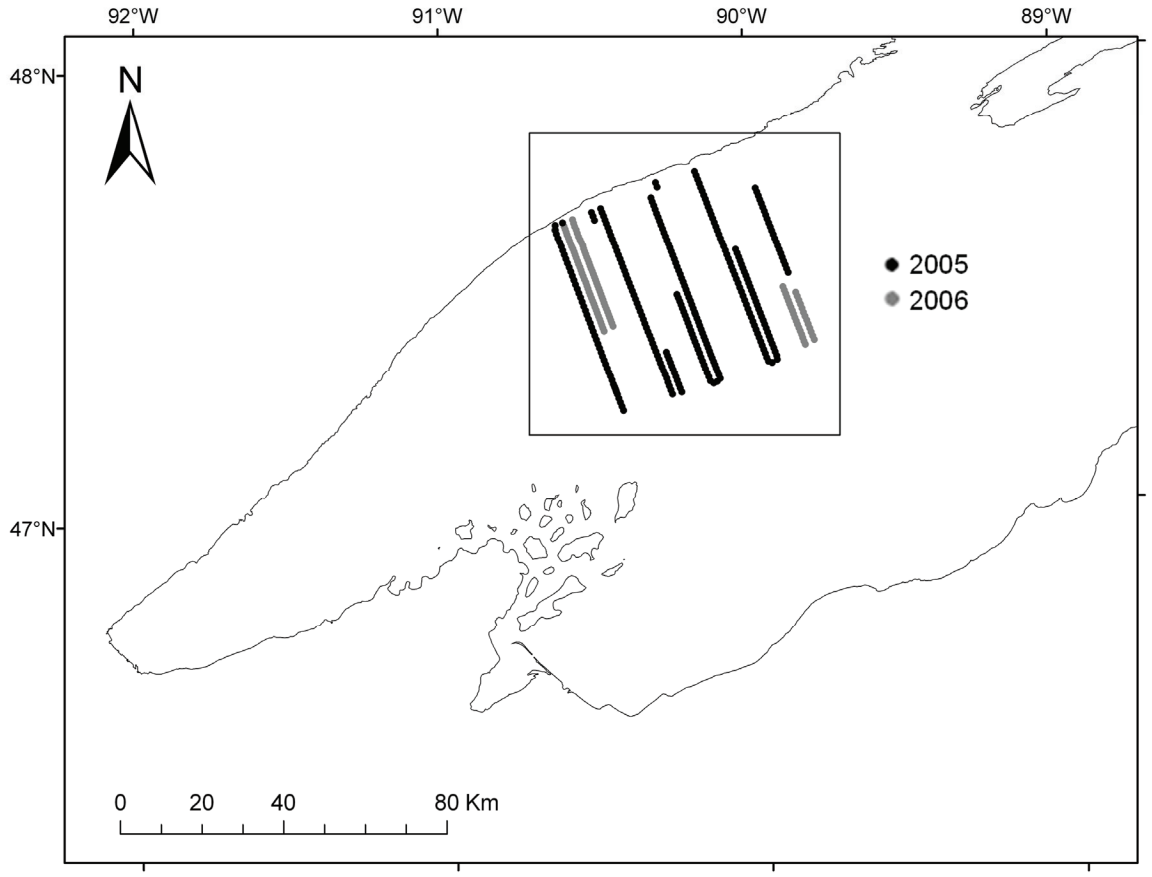

Fig. 1. Sampling location for this study (box). Transects were conducted in 2005 (black circles) and 2006 (gray circles).

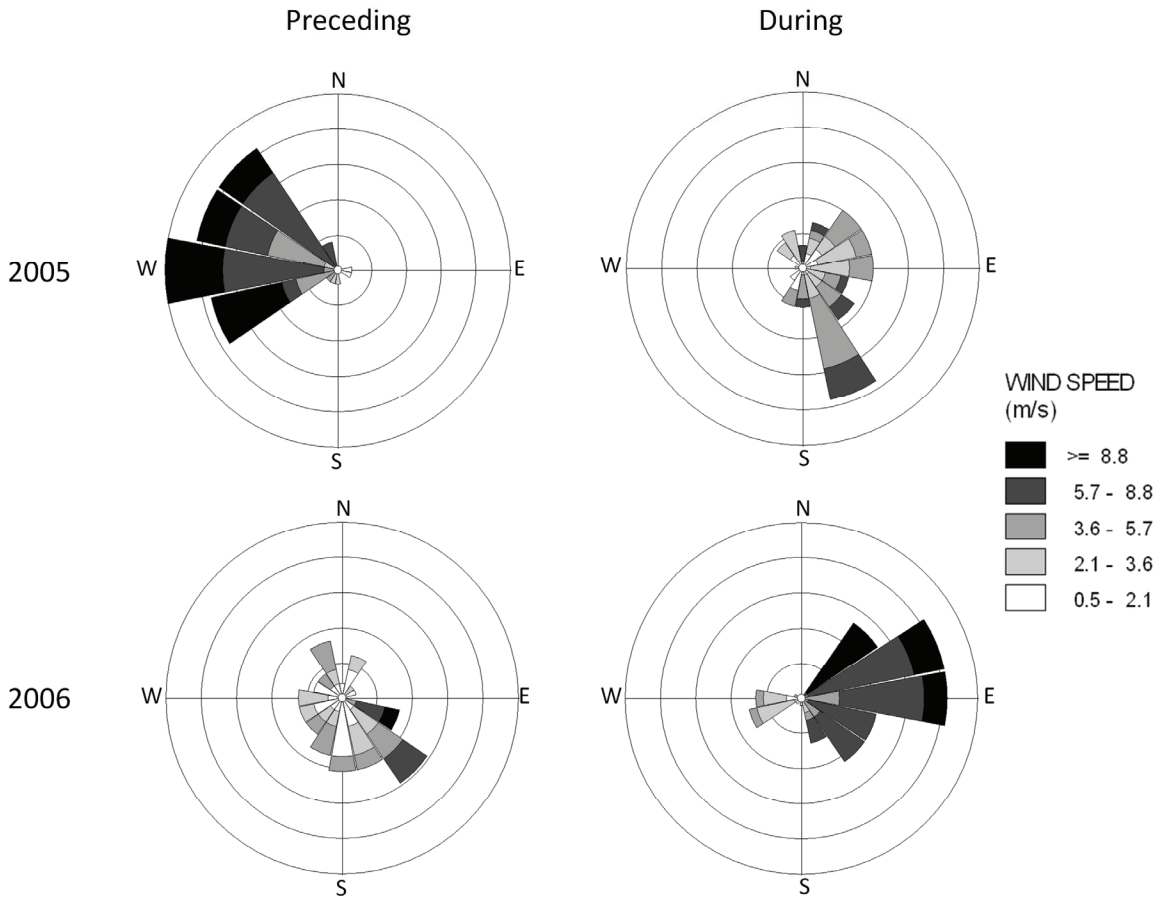

Fig. 2. Wind rose plots showing wind duration, direction, and speed two days prior to and during the sampling dates for both 2005 and 2006. Shading represents the wind speed (m s^{-1}) and concentric circles (5% increments) represent the amount of time that the wind blew from a particular direction.

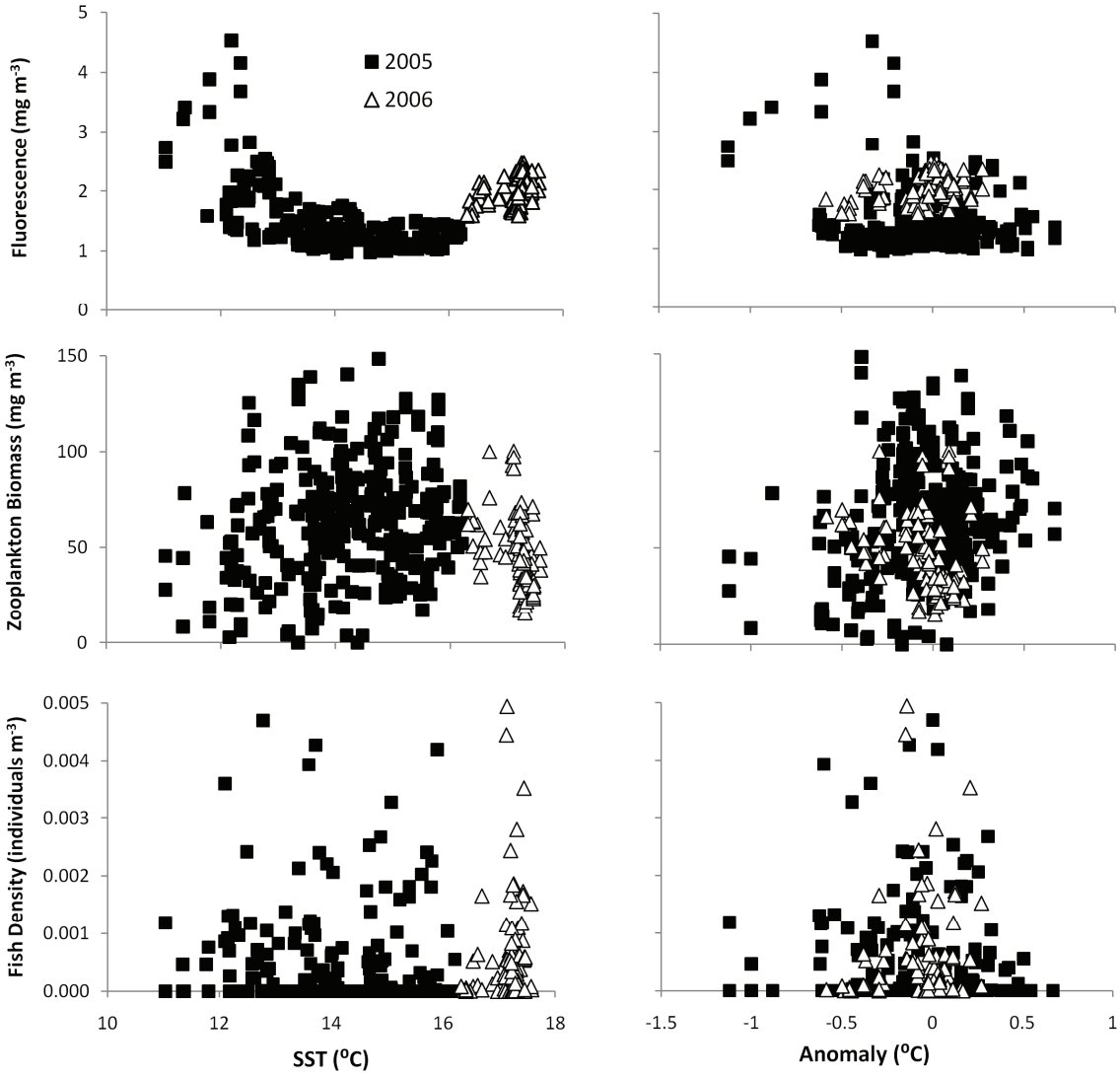

Fig. 3. Scatterplots of fluorescence (mg m^{-3}), zooplankton biomass (mg m^{-3}), and fish density (individuals m^{-3}) compared with SST (ºC, left panels) and surface anomaly (ºC, right panels) for the two years of this study.

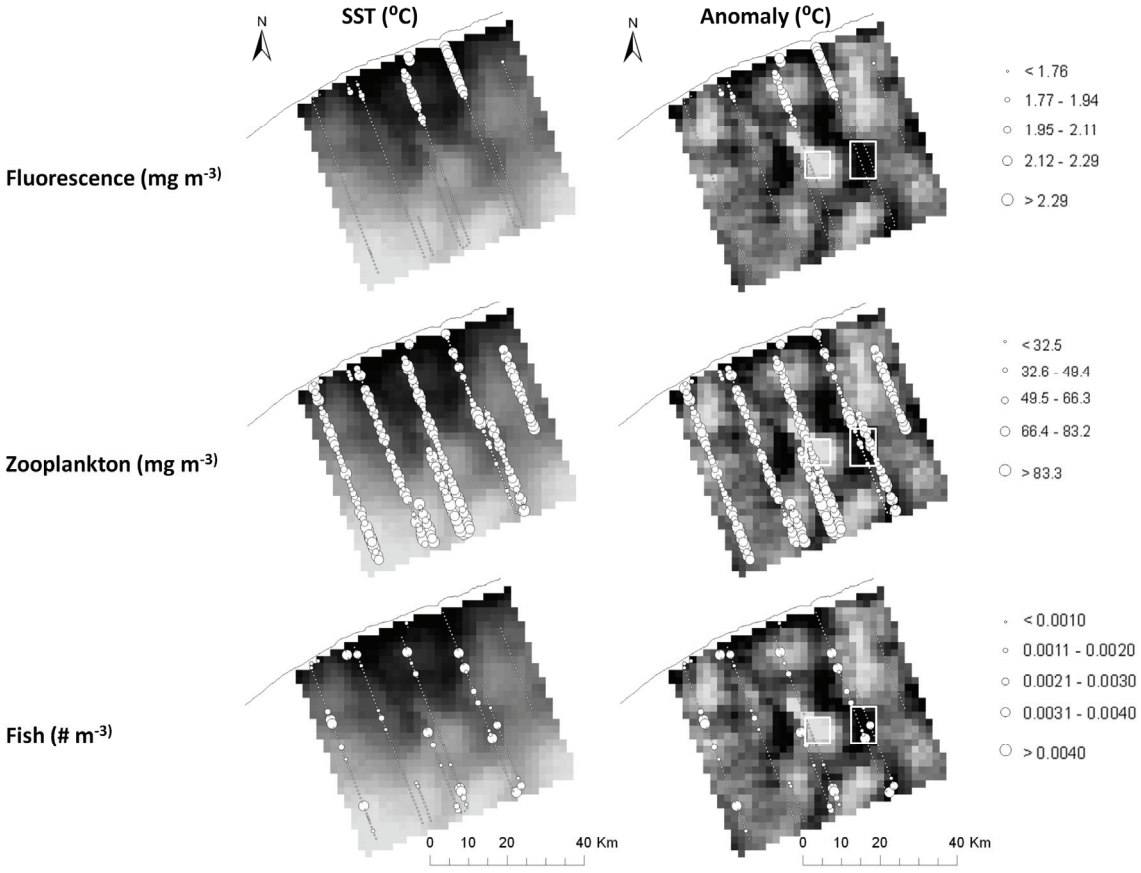

Fig. 4. Spatial maps displaying chlorophyll-*a* concentration (mg m^{-3}), zooplankton biomass (mg m^{-3}), and fish density (individuals m^{-3}) compared with SST (ºC, left maps) and surface anomaly (ºC, right maps) for 2005 data. SST was displayed using stretched values from 12ºC to 16ºC. Surface anomaly was displayed using stretched values from -0.5ºC to 0.5ºC. Graduated symbols were used to display chlorophyll-*a* concentration, zooplankton biomass, and fish density. The white boxes represent comparisons made between a warm-water eddy (left box) and a cold-water eddy (right box) that were transected while sampling.

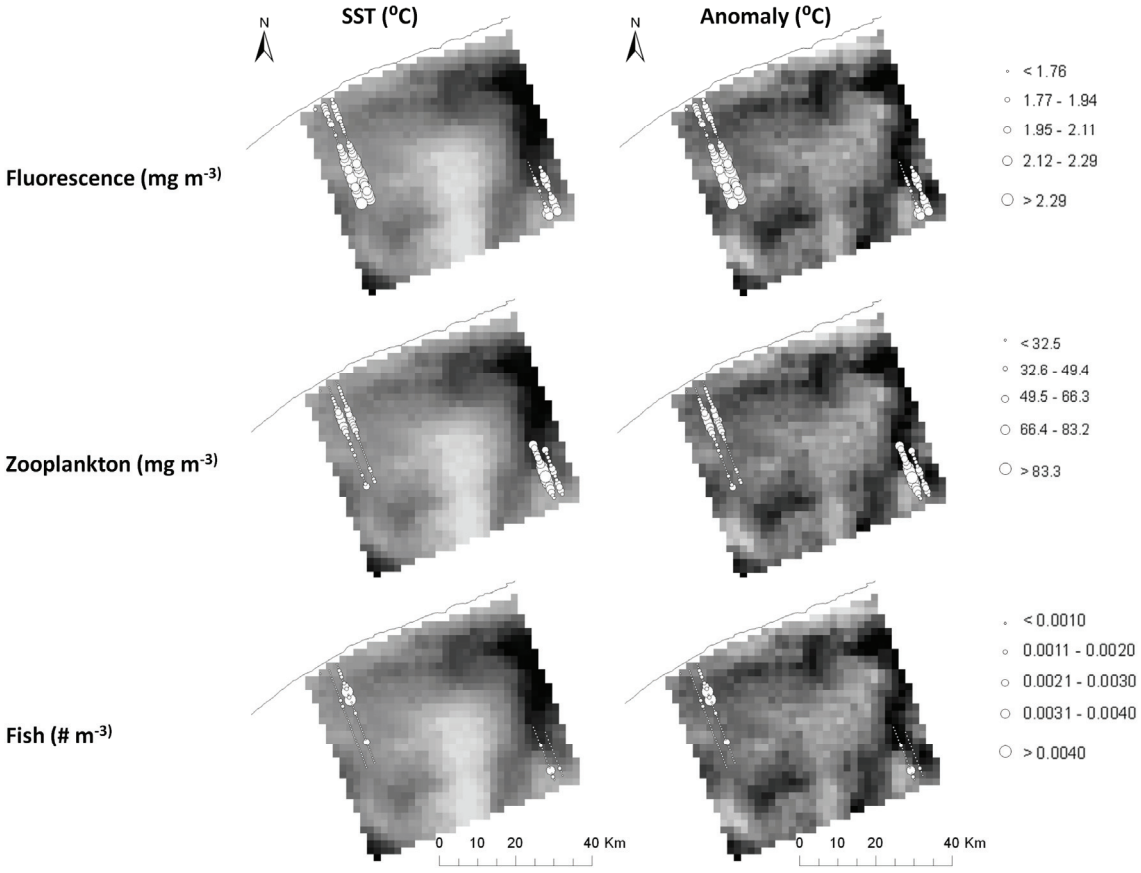

Fig. 5. Spatial maps displaying chlorophyll-*a* concentration (mg m^{-3}), zooplankton biomass (mg m^{-3}), and fish density (individuals m^{-3}) compared with SST (ºC, left maps) and surface anomaly (ºC, right maps) for 2006 data. SST was displayed using stretched values from 16ºC to 18ºC. Surface anomaly was displayed using stretched values from -0.5ºC to 0.5ºC. Graduated symbols were used to display chlorophyll-*a* concentration, zooplankton biomass, and fish density. Graduated symbols were used to display chlorophyll-*a* concentration, zooplankton biomass, and fish density.

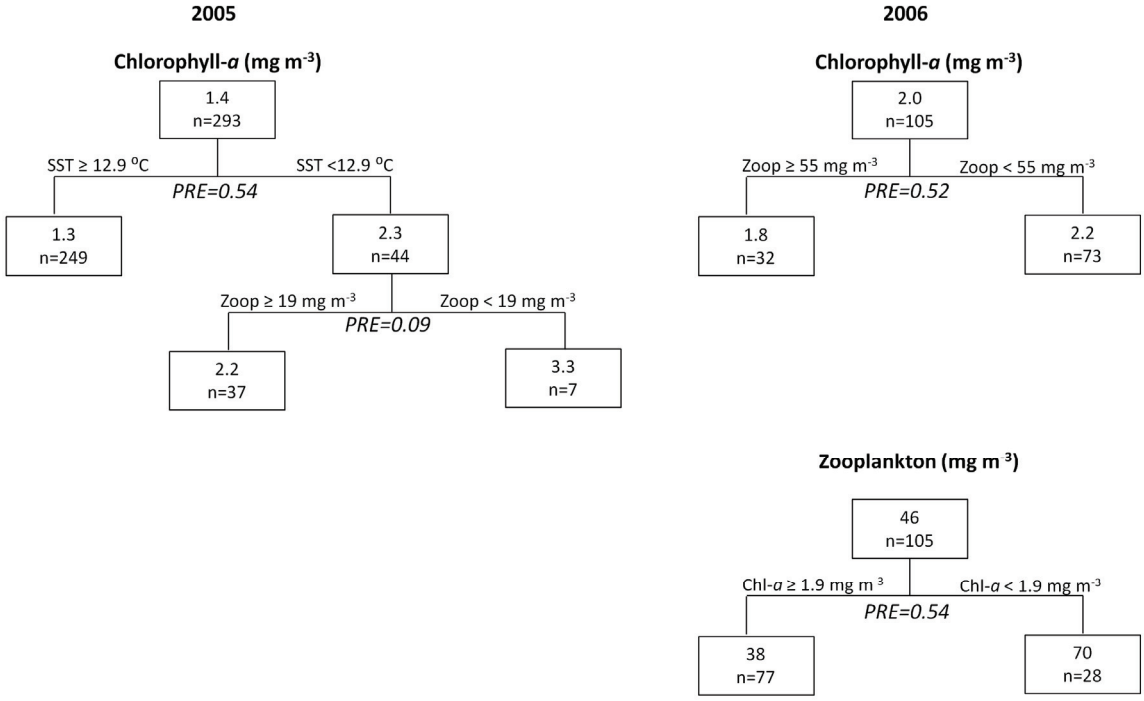

Fig. 6. Regression tree models predicting chlorophyll-*a* concentration (mg m^{-3}) in 2005 (top left panel) and in 2006 (top right panel) and zooplankton biomass (mg m^{-3}) in 2006 (bottom right panel).

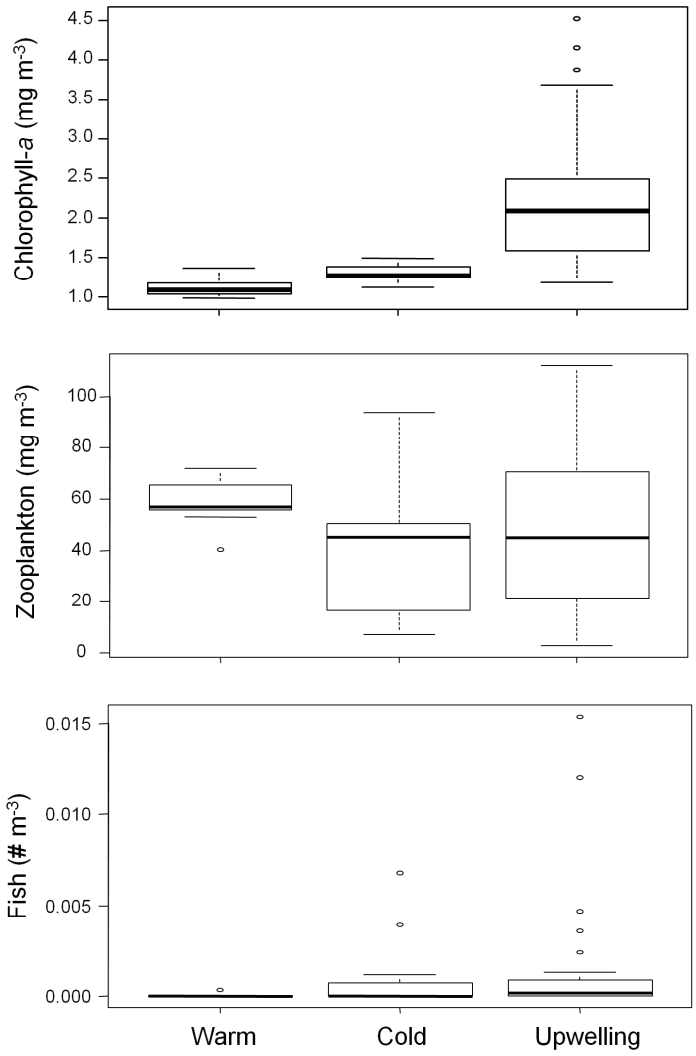

Fig. 7. Box and whisker plot comparing chlorophyll-*a* concentration, zooplankton biomass and fish density between prominent proximate cold- and warm-water eddies and the upwelling zone from the 2005 cruise.

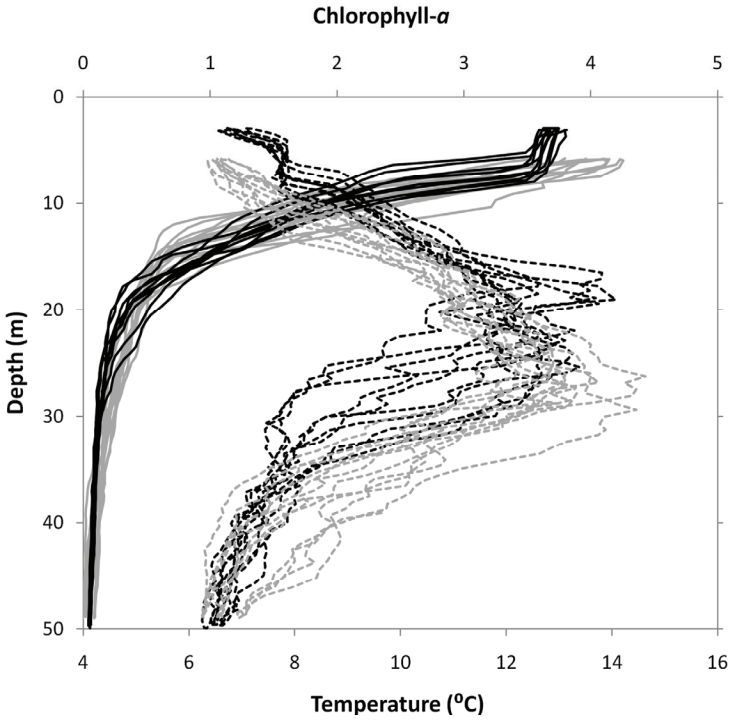

Fig. 8. Vertical profiles of temperature (solid line) and chlorophyll-*a* concentration (dashed line) comparing a cold-water eddy (black line) and a warm-water eddy (gray line) from the 2005 cruise. A representative sample of five down and up vertical Triaxus profiles within each eddy are displayed.

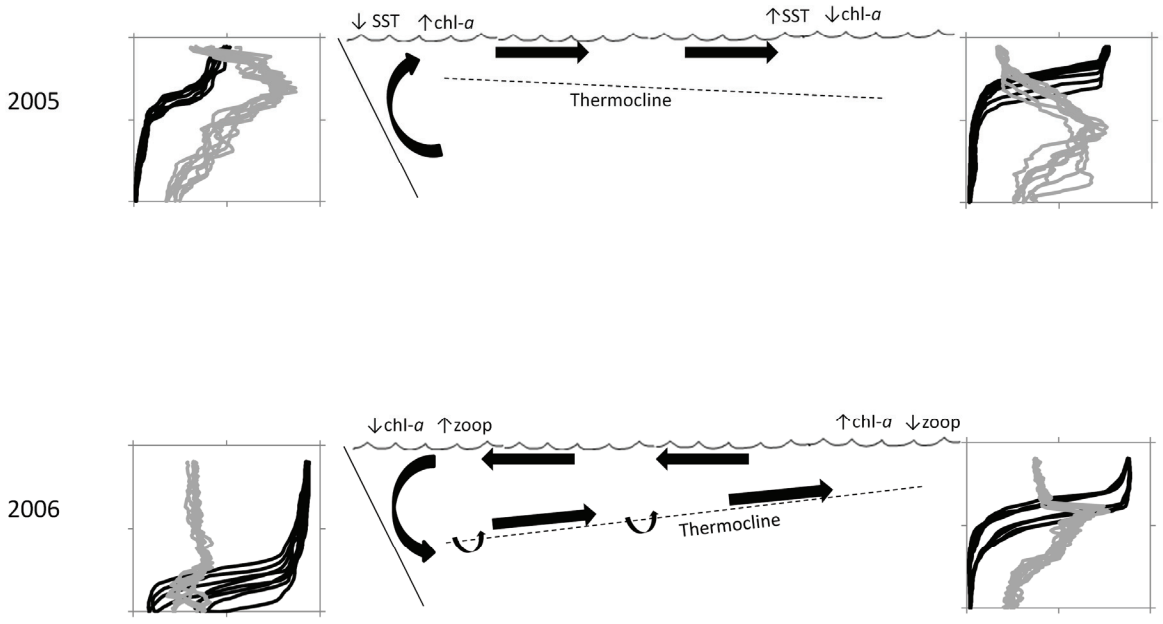

Fig. 9. Schematic drawings showing hypothetical epilimentic circulation patterns as a result of westerly winds preceding the 2005 cruise and resulting in upwelling (top panel) and as a result of easterly and northesterly winds during the 2006 cruise resulting in downwelling (bottom panel). A representative sample of eight down and up vertical Triaxus profiles from nearshore and offshore regions are also displayed, with depth on the y-axis (0-50 m), temperature on the primary x-axis (black lines, 4-18ºC), and chlorophyll-*a* on the secondary x-axis (gray lines, 0-6 mg m^{-3}).

References

Abbott, M.R., Denman, K.L., Powell, T.M., Richerson, P.J., Richards, R.C., and Goldman, C.R. 1984. Mixing and the dynamics of the deep chlorophyll maximum in Lake Tahoe. Limnol. Oceanogr. 29: 862-878.

Allen, C.B., Kandat, J., and Laws, E.A. 1996. New production and photosynthetic rates within and outside a cyclonic mesoscale eddy in the North Pacific subtropical gyre. Deep-Sea Res. I 43:917-936.

Anagnostou, E., and Sherrell, R., 2008. A MAGIC method for sub-nanomolar orthophosphate determination in freshwater. Limnol. Oceanogr.: Methods 6: 64-74.

Appenzeller, A.W., and Leggett, W.C. 1992. Bias in hydroacoustic estimates of fish abundance due to acoustic shadowing: evidence from day-night surveys of vertically migrating fish. Can. J. Fish. Aquat. Sci. 49: 2179-2189.

Avois, C., Legendre, P., Masson, S., and Pinel-Alloul, B. 2000. Is the sampling strategy interfering with the study of spatial variability of zooplankton communities? Can. J. Fish. Aquat. Sci. 57: 1940-1956.

Baehr, M.M., and McManus, J. 2003. The measurement of phosphorus and its spatial and temporal variability in the western arm of Lake Superior. J. Great Lakes Res. 29: 479-487.

Benitez-Nelson, C.R., Bidigare, R.R., Dickey, T.D., Landry, M.R., Leonard, C.L., Brown, S.L., Nencioli, F., Rii, Y.M., Maiti, K., Becker, J.W., Bibby, T.S., Black, W., Cai, W.-J., Carlson, C.A., Chen, F., Kuwahara, V.S., Mahaffey, C., McAndrew, P.M., Quay, P.D., Rappé, M.S., Selph, K.E., Simmons, M.P., Yang, E.J. 2007. Mesoscale eddies drive increased silica export in the subtropical Pacific Ocean. Science 316: 1017-1021.

Balk, H., and Lindem, T. 2000. Improved fish detection in data from split-beam sonar. Aquat. Living Resour. 13: 297-303.

Barbiero, R.P., and Tuchman, M.L. 2004. The deep chlorophyll maximum in Lake Superior. J. Great Lakes Res. 30(Suppl. 1): 256-268.

Bascompte, J., and Solé, R.V. 1995. Rethinking complexity: modeling spatiotemporal dynamics in ecology. Trends Ecol. Evol. 10: 361-366.

Bennington, V., McKinley, G.A., Kimura, N., and Wu, C.H. 2010. General circulation of Lake Superior: Mean, variability, and trends from 1979 to 2006. J. Geophys. Res. 115: C12015.

Bergstedt, R.A., Eshenroder, R.L., Bowen II, C., Seelve, J.G., and Locke, J.C. 1990. Mass-marking of otoliths of lake trout sac fry by temperature manipulation. *In* Fish-marking techniques. Edited by N.C. Parker, A.E. Giorgi, R.C. Heidinger, D.B. Jester Jr., E.D. Prince, and G.A. Winans. American Fisheries Society, Bethesda, M.D. pp. 216-223.

Blukacz, E.A., Shuter, B.J., and Sprules, W.G. 2009. Towards understanding the relationship between wind conditions and plankton patchiness. Limnol. Oceanogr. 54: 1530-1540.

Bollache, L., Kaldonski, N., Troussard, J.-P., Lagrue, C., and Rigaud, T. 2006. Spines and behavior as defences against fish predators in an invasive freshwater amphipod. Anim. Behav. 72: 627-633.

Bowers, J.A. 1988. Diel vertical migration of the opossum shrimp *Mysis-relicta* in Lake Superior - observations and sampling from the Johnson-Sea-Link II submersible. Bull. Mar. Sci. 43: 730-738.

Breiman, L., Friedman, J., Olshen, R., and Stone, C. 1984. Classification and Regression Trees, CRC Press, Boca Raton, F.L.

Bronte, C.R., Schram, S.T., Selgeby, J.H., and Swanson, B.L. 1995. Density-independent survival of wild lake trout in the Apostle Islands area of Lake Superior. J. Great Lakes Res. 21(Suppl. 1): 246-252.

Bronte, C.R., Ebener, M.P., Schreiner, D.R., DeVault, D.S., Petzold, M.M., Jensen, D.A., Richards, C., and Lozano, S.J. 2003. Fish community change in Lake Superior, 1970-2000. Can. J. Fish. Aquat. Sci. 60: 1552-1574.

Breck, J.E. 1993. Foraging theory and piscivorous fish: Are forage fish just big zooplankton? Trans. Am. Fish. Soc. 122: 902-911.

Brentnall, S.J., Richards, K.L., Brindley, J., and Murphy, E. 2003. Plankton patchiness and its effect on larger-scale productivity. J. Plankton Res. 25: 121-140.

Brooks, J.L., and Dodson, S.I. 1965. Predation, body size, and composition of zooplankton. Science 150: 28-35.

Brothers, E.R. 1990. Otolith marking. American Fisheries Society Symposium 7: 183-202.

Carvalho, P.S.M., Tillitt, D.E., Zajicek, J.L, Claunch, R.A., Honeyfield, D.C., Fitzsimons, J.D., and Brown, S.B. 2009. Thiamine deficiency effects on the vision and foraging ability of lake trout fry. J. Anim. Aquat. Health 21: 315-325.

Chassot, E., Melin, F., LePape, O., and Gascuel, D. 2007. Bottom-up control regulates fisheries production at the scale of eco-regions in European seas. Mar. Ecol. Prog. Ser. 343: 45-55.

Christie, W. J. 1974. Changes in the fish species composition of the Great Lakes. J. Fish Res. Board Can. 31: 827-854.

Ciannelli, L., Brodeur, R.D., Swartzman, G.L., and Salo, S. 2002. Physical and biological factors influencing the spatial distribution of age-0 walleye Pollock (*Theragra chalcogramma*) around the Pribilof Islands, Bering Sea. Deep-Sea Res. 49: 6109-6126.

Claramunt, R.M., Jonas, J.L., Fitzsimons, J.D., and Marsden, J.E. 2005. Influences of spawning habitat characteristics and interstitial predators on lake trout egg deposition and mortality. Trans. Amer. Fish. Soc. 134: 1048-1057.

Confer, J.L., Howick, G.L., Corzette, M.H., Kramer, S.L., Fitzgibbon, S., and Landesberg, R. 1978. Visual predation by planktivores. Oikos 31: 27-37.

Conway, J.B. 1977. Seasonal and depth distribution of *Limnocalanus macrurus* at a site on Western Lake Superior. J. Great Lakes Res. 3: 15-19.

Cooper, W.E. 1965. Dynamics and Production of a Natural Population of a Fresh-Water Amphipod, *Hyalella azteca*. Ecol. Monogr. 35: 377-394.

Culver, D.A., Boucherle, M.M., Bean, D.J., and Fletcher, J.W. 1985. Biomass of freshwater crustacean zooplankton from length-weight regressions. Can. J. Fish. Aquat. Sci. 42: 1380-1390.

Cummins, K. W., and Wuycheck, J. C. 1971. Caloric equivalents for investigations in ecological energetics. International Association of Theoretical and Applied Limnology Communication, No. 18.

Daly, R., Hacker, V.A., and Wiegert, L. 1962. The lake trout: its life history, ecology, and management. Wis. Conserv. Dep. Publ. No. 233.

Davies, J. 1985. Evidence for a diurnal horizontal migration in *Daphnia hyaline lacustris* Sars. Hydrobiologia 120: 103-105.

DeRoche, S.E. 1969. Observations on the spawning habits and early life history of lake trout. Prog. Fish-Cult. 31: 109-113.

Desai, A.R., Austin, J.A., Bennington, V., and McKinley, G.A. 2009. Stronger winds over a large lake in response to weakening air-to-lake temperature gradient. Nature Geosci. 2: 855-858.

Downing, G., and Litvak, M.K. 2001. The effect of light intensity and spectrum on the incidence of first feeding by larval haddock. J. Fish Biol. 59: 1566-1578.

Downing, J.A., and Rigler, F.H. 1984. A manual on methods for the assessment of secondary productivity in fresh waters. Blackwell Scientific Publications, Oxford, England.

Downing, J.A., Perusse, M., and Frenette, Y. 1987. Effects of interreplicate variance on zooplankton sampling design and data analysis. Limnol. Oceanogr. 32: 673-680.

Dumont, H.J., Van de Velde, I., and Dumont, S. 1975. The dry weight estimate of biomass in a selection of cladocera, copepod, and rotifer from the plankton, periphyton and benthos of continental waters. Oecologia 19: 75-97.

Eckmann, R. 1998. Allocation of echo integrator output to small larval insect (*Chaoborus* sp.) and medium-sized (juvenile fish) targets. Fish. Res. 35: 107-113.

Edsall, T.A., Manny, B.A., and Kennedy, G.W. 2003. Starvation resistance in lake trout fry. J. Great Lakes Res. 29: 375-382.

Fitzsimons, J.D. 1995. Assessment of lake trout spawning habitat and egg deposition in Lake Ontario. J. Great Lakes Res. 21(Suppl. 1): 337–347.

Fitzsimons, J.D., Jonas, J.L., Claramunt, R.M., Williston, B., Williston, G., Marsden, J.E., Ellrott, B.J., and Honeyfield, D.C. 2007. Influence of egg predation and physical disturbance on lake trout *Salvelinus namaycush* egg mortality and implications for life-history theory. J. Fish Biol. 71: 1–16.

Fitzsimons, J.D., Brown, S.B., Williston, B., Williston, G., Brown, L.R., Moore, K., Honeyfield, D.C., and Tillitt, D.E. 2009. Influence of thiamine deficiency on lake trout larval growth, foraging, and predator avoidance. J. Aquat. Anim. Health 21: 302-314.

Folt, C.L., and Burns, C.W. 1999. Biological drivers of zooplankton patchiness. Trends Ecol. Evol. 14: 300-305.

Fortin, M.-J., and Dale, M.R.T. 2005. Spatial Analysis. Cambridge, Cambridge University Press, UK.

Franklin, J.F. 2005. Spatial pattern and ecosystem function: reflections on current knowledge and future directions. *In* Ecosystem function in heterogeneous landscapes. *Edited by* G.M. Lovett, M.G. Turner, C.G. Jones and K.C. Weathers. K.C. Springer Press, New York, N.Y. pp. 427-442.

Gabriel, W., and Thomas, B. 1988. Vertical migration of zooplankton an evolutionary stable strategy. Am. Nat. 132:199-216.

Gal, G., Loew, E.R., Rudstam, L.G., and Mohammadian, A.M. 1999. Light and diel vertical migration: spectral sensitivity and light avoidance by *Mysis relicta*. Can. J. Fish. Aquat. Sci. 56: 311-322.

Gerritsen, J., and Strickler, J.R. 1977. Encounter probabilities and community structure in zooplankton: a mathematical model. J. Fish. Res. Board Can. 34: 73-82.

Giske, J., Huse, G., and Fiksen, O. 1998. Modelling spatial dynamics of fish. Rev. Fish Biol. Fish. 8: 57-91.

Godlewska, M., and Jelonek, M. 2006. Acoustical estimates of fish and zooplankton distribution in the Piaseczno reservoir, Southern Poland. Aquat. Ecol. 40: 211-219.

Güntzel, A.M., Matsumura-Tundisi, T., and Rocha, O. 2003. Life cycle of *Macrothrix flabelligera* Smirnov, 1992 (Cladocera, Macrothricidae), recently reported in the Neotropical region. Hydrobiologia 490: 87-92.

Hamilton, D.P., O'Brien, K.R., and Burford, M.A. 2010. Vertical distributions of chlorophyll in deep, warm monomictic lakes. Aquat. Sci. 72: 295-307.

Hanski, I. 1981. Coexistence of competitors in patchy environment with and without predation. Oikos 37: 306-312.

Hanson, P., Johnson, T., Kitchell, J., and Schindler, D.E. 1997. Fish bioenergetics (v. 3.0) University of Wisconsin, Sea Grant Institute, Madison, Wisconsin, USA.

Hansson, S., De Stasio, B.T., Gorokhova, E., and Mohammadian, M.A. 2001. Ratio-dependent functional responses—tests with the zooplanktivore *Mysis mixta*. Mar. Ecol. Prog. Ser. 216: 181-189.

Hassinger, R.L., and T.L. Close. 1984. Interaction of lake trout and rainbow smelt in two northeastern Minnesota lakes. St. Paul, MN: Minn. Dept. Nat. Res. Sect. Fish. Invest. Rep. 379.

Hastings, A. 2001. Transient dynamics and persistence of ecological systems. Ecol. Lett. 4: 215-220.

Hedrick, T.L. 2008. Software techniques for two- and three-dimensional kinematic measurements of biological and biomimetic systems. Bioinspir. Biomim. 3: 034001.

Hembre, L.K., and Megard, R.O. 2003. Seasonal and diel patchiness of a *Daphnia* population: an acoustic analysis. Limnol. Oceanogr. 48: 2221-2233.

Henderson, B.A., and Nepszy, S.J. 1992. Comparison of catches in mono- and multifilament gill nets in Lake Erie. N. Am. J. Fish. Manage. 12: 618–624.

Herdendorf, C. E. 1984. Inventory of the morphometric and limnologic characteristics of the large lakes of the world. Ohio Sea Grant College Program Technical Bulletin OHSU-TB-017.

Hernández-León, S., Almeida, C., Gómez, M., Torres, S., Montero, I., and Portillo-Hahnefeld, A. 2001. Zooplankton biomass and indices of feeding and metabolism in island-generated eddies. J. Mar. Syst. 30: 51-66.

Hobbs, N.T. 2006. Large herbivores as sources of disturbance in ecosystems. *In* Large Herbivore Ecology, Ecosystem Dynamics and Conservation. *Edited by* K. Danell, R. Bergstrom, P. Duncan and J. Pastor. Cambridge University Press, Cambridge, U.K. pp. 261-288.

Holbrook, B.V., Hrabik, T.R., Branstrator, D.K., Yule, D.L., and Stockwell, J.D. 2006. Hydroacoustic estimation of zooplankton biomass at two shoal complexes in the Apostle Island Region of Lake Superior. J. Great Lakes Res. 32: 680–696.

Holbrook, B.V. 2011. Spatial and temporal variability in zooplankton-fish interactions in freshwater communities. Ph.D. thesis, University of Minnesota, Minneapolis, Minnesota.

Holey, M.E., Rybicki, R.W., Eck, G.W., Brown Jr., E.H., Marsden, J.E., Lavis, D.S., Toneys, M.L., Trudeau, T.N., and Horall, R.M. 1995. Progress toward lake trout restoration in Lake Michigan. J. Great Lakes Res. 21(Suppl. 1): 128-151.

Holmes, R.A., and Gibson, R.N. 1986. Visual cues determining prey selection by the turbot, *Scophthalmus maximus* L. J. Fish Biol. 29: 49-58.

Howick, G.L., and O'Brien, W.J. 1983. Piscivorous Feeding Behavior of Largemouth Bass: An Experimental Analysis. Trans. Am. Fish. Soc. 112: 508-516.

Hrabik, T.R., Magnuson, J.J., and McLain, A.S. 1998. Predicting the effects of rainbow smelt on native fishes in small lakes: evidence from long-term research on two lakes. Can. J. Fish. Aquat. Sci. 55: 1364–1371.

Hrabik, T.R. 1999. Factors influencing fish distribution and condition within lakes and across landscapes. Ph.D. thesis, University of Wisconsin, Madison, Wisconsin.

Hrabik, T.R., Jensen, O.P., Martell, S.J.D., Walters, C.J., and Kitchell, J.F. 2006. Diel vertical migration in the Lake Superior pelagic community. I. Changes in vertical migration of coregonids in response to varying predation risk. Can. J. Fish. Aquat. Sci. 63: 2286–2295.

Hrbacek, J., Dvorakova, M., Korinek, V., and Prochazkova, L. 1961. Demonstration of the effect of the fish stock on the species composition of zooplankton and the intensity of metabolism of the whole plankton assemblage. Verh. Int. Ver. Theor. Angew. Limnol. 14: 192-195.

Hudson, P.L., Savino, J.F., and Bronte, C.R. 1995. Predator-prey relations and competition for food between age-0 lake trout and slimy sculpins in the Apostle Island Region of Lake Superior. J. Great Lakes Res. 21(Suppl. 1): 445-457.

Huntley, M. E., and Lopez, M. D. 1992. Temperature-dependent production of marine copepods: a global synthesis. Am. Nat. 140:201-242

Janiczcek, P.M.J., and DeYoung, A.J. 1987. Computer programs for sun and moon illuminance with contingent table and diagram. U.S. Naval Observatory Circular 171.

Johannsson, O. 1992. Life history and productivity of *Mysis relicta* in Lake Ontario. J. Great Lakes Res. 18: 154-168.

Johnson, T.B., Mason, D.M., Schram, S.T., and Kitchell, J.F. 1999. Ontogenetic and seasonal patterns in the energy content of piscivorous fishes in Lake Superior. J. Great Lakes Res. 25: 275-281.

Johnston, T.A., and Cunjak, R.A. 1999. Dry mass-length relationships for benthic insects: a review with new data from Catamaran Brook, New Brunswick, Canada. Fresh. Biol. 41: 53-674.

Jones, M.L., Eck, G.W., Evans, D.O., Fabrizio, M.C., Hoff, M.H., Hudson, P.L., Janssen, J., Jude, D., O'Gorman, R., and Savino, J.F. 1995. Limitations to lake trout (*Salvelinus namaycush*) rehabilitation in the Great Lakes imposed by biotic interactions occurring at early life stages. J. Great Lakes Res. 21(Suppl. 1): 505-517.

Keister, J. E., Peterson, W. T., and Pierce, S. D. 2009. Zooplankton distribution and cross-shelf transfer of carbon in an area of complex mesoscale circulation in the northern California Current. Deep-Sea Res. I 56: 212-231.

Kitchell, J.F., Stewart, D.F., and Weininger, D. 1977. Applications of a bioenergetics model to yellow perch (*Perca flavescens*) and walleye (*Stizostedion vitreum*). J. Fish. Res. Board Can. 34: 1922-1935.

Knudsen, F.R., Larsson, P., and Jakobsen, P.J. 2006. Acoustic scattering from a larval insect (*Chaoborus flavicans*) at six echosounder frequencies: implication for acoustic estimates of fish abundance. Fish. Res. 79: 84-89.

Krauss, A., and Neumeyer, C. 2003. Wavelength dependence of the optomotor response in zebrafish (*Danio rerio*). Vision Res. 43: 1273-1282.

Krebs, J.R. 1978. Optimal foraging: decision rules for predators. *In* Behavior ecology, an evolutionary approach. *Edited by* J.R. Krebs and N.B. Davies. Sinauer Associates, Sunderland, M.A. pp. 23-63.

Krueger, C.C., Perkins, D.L., Mills, E.L., and Marsden, J.E. 1995. Predation by alewives on lake trout fry in Lake Ontario: role of an exotic species in preventing restoration of a native species. J. Great Lakes Res. 21(Suppl. 1): 458-469.

Kubecka, J., Frouzová, J., Cech, M., Peterka, J., Ketelaars, H.A.M., Wagenwoort, A.J., and Papácek, M. 2000. Hydroacoustic assessment of pelagic stages of freshwater insects. Aquat. Living Resour. 13: 361-366.

Lasenby, D.C., Yan, N.D., and Futter, M.N. 1994. Changes in body dimensions of larval *Chaoborus* in ethanol and formalin. J. Plankton Res. 16: 1601-1608.

Lavery, A.C., Wiebe, P.H., Stanton, T.K., Lawson, G.L., Benfield, M.C., and Copley, N. 2007. Determining dominant scatterers of sound in mixed zooplankton populations. J. Acoust. Soc. Am. 122: 3304-3325.

Lawrence, S.G., Malley, D.F., Findlay, W.J., Maclver, M.A., and Delbaere, I.L. 1987. Method for estimating dry weight of freshwater planktonic crustaceans from measures of length and shape. Can. J. Fish. Aquat. Sci. 44: 264-274.

Lawrie, A.H., and Rahrer, J.F. 1972. Lake Superior: effects of exploitation and introductions on the salmonid community. J. Fish Res. Board Can. 29: 765-776.

Legendre, P., and Legendre, L. 1998. Numerical Ecology. Elsevier, Amsterdam.

Loftus, D. H., and Hulsman, P.F. 1986. Predation on larval lake whitefish (*Coregonus clupeaformis*) and lake herring (*C. artedii*) by adult rainbow smelt (*Osmerus mordax*). Can. J. Fish. Aquat. Sci. 43: 812–818.

Lorke, A., McGinnis, D.F., Spank, P., and Wuest, W. 2004. Acoustic observations of zooplankton in lakes using a Doppler current profiler. Fresh. Biol. 49: 1280-1292.

Love, R.H. 1977. Target strength of an individual fish at any aspect. J. Acoust. Soc. Am. 62: 1397-1403.

Ludovisi, A., Minozzo, M., Pandofi, P., and Taticchi, M.-I. 2005. Modelling the horizontal spatial structure of planktonic community in Lake Trasimeno (Umbria, Italy) using multivariate geostatistical methods. Ecol. Modelling 181: 247-262.

Lythgoe, J.N. 1984. Visual pigments and environmental light. Vision Res. 24: 1539-1550.

Makarewicz, J.C., and Jones, H.D. 1990. Occurrence of *Bythotrephes cederstroemi* in Lake Ontario offshore waters. J. Great Lakes Res. 16: 143-147.

Malinen, T., Horppila, J., and Liljendahl-Nurminen, A. 2001. Langmuir circulations disturb the low-oxygen refuge of phantom midge larvae. Limnol. Oceanogr. 46: 689–692.

Malone, B.J., and McQueen, D.J. 1983. Horizontal patchiness in zooplankton populations in two Ontario kettle lakes. Hydrobiologia 99: 101-124.

Mann, K.H. 2000. Ecology of coastal waters, with implications for management, 2nd ed. Blackwell Science, Boston, M.A.

Martin, L.V., Stanton, T.K., Wiebe, P.H., and Lynch, J.F. 1996. Acoustic classification of zooplankton. ICES J. Mar. Sci. 53: 217-224.

Masson, S., Angeli, N., and Guillard, J. 2001. Diel vertical and horizontal distribution of crustacean zooplankton and young of the year fish in a sub-alpine lake: an approach based on high frequency sampling. J. Plankton Res. 23: 1041-1060.

Mazur, M.M., and Beauchamp, D.A. 2003. A comparison of visual prey detection among species of piscivorous salmonids: effects of light and low turbidities. Environ. Biol. Fishes 67: 397-405.

McCune, B., and Grace, J.B. 2002. Analysis of ecological communities. MjM Software Design, Gleneden Beach, O.R.

McGillicuddy, D.J., Robinson, A.R., Siegel, D.A., Jannasch, H.W., Johnson, R., Dickey, T.D., McNeil, J., Michaels, A.F., and Knap, A.H. 1998. Influence of mesoscale eddies on new production in the Sargasso Sea. Nature 394: 263-266.

McGillicuddy, D.J., Anderson, L.A., Bates, N.R., Bibby, T. Buesseler, K.O., Carlson, C.A., Davis, C.S., Ewart, C., Falkowski, P.G., Goldthwait, S.A., Hansell, D.A., Jenkins, W.J., Johnson, R., Kosnyrev, V.K., Ledwell, J.R., Li, Q.P., Siegel, D.A., and Steinberg, D.K. 2007. Eddy/wind interactions stimulate extraordinary mid-ocean plankton blooms. Science 316: 1021-1026.

McQueen, D.J., Johannes, M.R., Post, J.R., Stewart, T.J., and Lean, D.R. 1989. Bottom-up and top-down impacts on freshwater pelagic community structure. Ecol. Monogr. 59: 289-309.

Megard, R.O., Kuns, M.M., Whiteside, M.C., and Downing, J.A. 1997. Spatial distributions of zooplankton during coastal upwelling in western Lake Superior. Limnol. Oceanogr. 42: 827-840.

Miller, D.M. 1984. Reducing transformation bias in curve fitting. Am. Stat. 38: 124-126.

Milne, S.W., Shuter, B.J., and Sprules, W.G. 2005. The schooling and foraging ecology of lake herring (*Coregonus artedi*) in Lake Opeongo, Ontario, Canada. Can. J. Fish. Aquat. Sci. 62: 1210-1218.

Morbey, Y.E., Anderson, D.M., and Henderson, B.A. 2008. Progress toward the rehabilitation of lake trout (*Salvelinus namaycush*) in South Bay, Lake Huron. J. Great Lakes Res. 34: 287-300.

Myers, J.T., Jones, M.L., Stockwell, J.D., and Yule, D.L. 2009. Reassessment of the predatory effects of rainbow smelt on ciscoes in Lake Superior. Trans. Am. Fish. Soc. 138: 1352-1368.

Negus, M.T. 1999. Thermal marking of otoliths in lake trout sac fry. N. Am. J. Fish. Manage. 19: 127–140.

Nencioli, F., Kuwahara, V.S., Dickey, T.D., Rii, Y.M., and Bidigare, R.R. 2008. Physical dynamics and biological implications of a mesoscale eddy in the lee of Hawai'i: Cyclone Opal observations during E-Flux III. Deep-Sea Res. II 55: 1252-1274.

Nero, R.W., and Magnuson, J.J. 1992. Effects of changing spatial scale on acoustic observations of patchiness in the Gulf Stream. Landscape Ecol. 6: 279-291.

O'Brien, D.P. 1987. Description of escape responses of krill (Crustacea: Euphausiacea), with particular reference to swarming behaviour and the size and proximity of the predator. J. Crustacean Biol. 7: 449-457.

O'Brien, D.P., and Ritz, D.A. 1988. Escape responses of gregarious mysids (Crustacea: Mysidacea): towards a general classification of escape responses in aggregated crustaceans. J. Exp. Mar. Biol. Ecol. 116: 257-272.

O'Brien, W.J., and deNoyelles, F. 1974. Relationship between nutrient concentration, phytoplankton density, and zooplankton density in nutrient enriched experimental ponds. Hydrobiologia 44: 105-125.

O'Brien, W.J., Slade, N.A., and Vinyard, G.L. 1976. Apparent size as the determinant of prey selection by bluegill sunfish (*Lepomis macrochirus*). Ecology 57: 1304-1310.

O'Reilly, C.M., Alin, S.R., Plisnier, P.-D. Cohen, A.S., and McKee, B.A. 2003. Climate change decreases aquatic ecosystem productivity of Lake Tanganyika, Africa. Nature 424: 766-768.

Peck, J.W. 1982. Extended residence of young-of-the-year lake trout in shallow water. Trans. Amer. Fish. Soc. 111: 775-778.

Perkins, D.L., and Krueger, C.C. 1995. Dynamics of reproduction by hatchery-origin lake trout (*Salvelinus namaycush*) at Stony Island Reef, Lake Ontario. J. Great Lakes Res. 21(Suppl. 1): 400-417.

Perry, M. J., Sackmann, B. S., Eriksen, C. C., and Lee, C. M. 2008. Seaglider observations of blooms and subsurface chlorophyll maxima off the Washington coast. Limnol. Oceanogr. 53: 2169-2179.

Pinel-Alloul, B., Downing, J.A., Perusse, M., and Cotin-Bluwer, G. 1988. Spatial heterogeneity in freshwater zooplankton: systematic variation with body size, depth, and sampling scale. Ecology 69: 1393-1400.

Pinel-Alloul, B. 1995. Spatial heterogeneity as a multiscale characteristic of zooplankton community. Hydrobiologia 300-301: 17-42.

Pinel-Alloul, B., Guay, C., Angeli, N., Legendre, P., Dutilleul, P., Balvay, G., Gerdeaux, D., and Guillard, J. 1999. Large-scale spatial heterogeneity of macrozooplankton in Lake of Geneva. Can. J. Fish. Aquat. Sci. 56: 1437-1451.

Pycha, R. L. 1962. Relative efficiency of nylon and cotton gillnets for taking lake trout in Lake Superior. J. Fish. Res. Board Can. 19: 1085–1094

R Development Core Team. 2009. R: A language and environment for statistical computing. R Foundation for Statistical Computing, Vienna, Austria. http://www.R-project.org.

R Development Core Team. 2011. R: A language and environment for statistical computing. R Foundation for Statistical Computing, Vienna, Austria. http://www.R-project.org.

Rademacher, K., and Kils, U. 1996. Predator prey dynamics of fifteen-spined stickleback (*Spinachia spinachia*) and the mysid (*Neomysis integer*). Arch. Fish. Mar. Res. 43: 171-181.

Ralph, E.A. 2002. Scales and structures of large lake eddies. Geophys. Res. Lett. 29: doi:IO.1029/200lGLOI4654

Reid, D.M., Anderson, D.M., and Henderson, B.A. 2001. Restoration of Lake Trout in Parry Sound, Lake Huron. N. Am. J. Fish. Manage. 21: 156-169.

RESTORE (International Conference on Restoration of the Lake Trout in the Laurentian Great Lakes). 1995. Conference proceedings. J. Great Lakes Res. 21(Suppl. 1).

Richardson, A.J., and Schoeman, D.S. 2004. Climate impact on plankton ecosystems in the Northeast Atlantic. Science 305: 1609-1612.

Richmond, H.E., Hrabik, T.R., and Mensinger, A.F. 2004. Light intensity, prey detection and foraging mechanisms of age 0 year yellow perch. J. Fish Biol. 65: 195-205.

Riley, S.C., He, J.X., Johnson, J.E., O'Brien, T.P., and Schaeffer, J.S. 2007. Evidence of widespread natural reproduction by lake trout *Salvelinus namaycush* in the Michigan waters of Lake Huron. J. Great Lakes Res. 33: 917-921.

Ringelberg, J. 1999. The photobehavior of *Daphnia* spp. as a model to explain diel vertical migration in zooplankton. Biol. Rev. 74: 397-423.

Rinke, K., and Petzoldt, T. 2003. Modelling the effects of temperature and food on individual growth and reproduction of *Daphnia* and their consequences on the population level. Limnologica 33: 293-304.

Rinke, K., Hübner, I., Petzoldt, T., Rolinski, S., König-Rinke, M., Post, J., Lorke, A., and Benndorg, J. 2007. How internal waves influence the vertical distribution of zooplankton. Fresh. Biol. 52: 137-144.

Rinke, K., Huber, A.M.R., Kempke, S., Eder, M., Wolf, T., Probst, W.N., and Rothhaupt, K.-O. 2009. Lake-wide distribution of temperature, phytoplankton, zooplankton, and fish in the pelagic zone of a large lake. Limnol. Oceanogr. 54: 1306-1322.

Roemmich, D., and McGowan, J. 1995. Climatic warming and the decline of zooplankton in the California Current. Science 267: 1324-1326.

Romare, P., Sorenberg, T.L., and Jeppesen, E. 2003. Spatial and temporal distribution of fish and zooplankton in a shallow lake. Fresh. Biol. 48: 1353-1362.

Rose, G.A., and Leggett, W.C. 1990. The importance of scale to predator-prey spatial correlations: an example of Atlantic fishes. Ecology 71: 33-43.

Roseman, E.J., Taylor, W.W., Hayes, D.B., Knight, R.L., and Hass, R.C. 2001. Removal of walleye eggs from reefs in western Lake Erie by a catastrophic storm. Trans. Amer. Fish. Soc. 130: 341–346.

Roseman, E.F., Stott, W., O'Brien, T.P., Riley, S.C., and Schaeffer, J.S. 2009. Heritage strain and diet of wild young of year and yearling lake trout in the main basin of Lake Huron. J. Great Lakes Res. 35: 620-626.

Rosen, R.A. 1981. Length-dry weight relationships of some freshwater zooplankton. J. Fresh. Ecol. 1: 225-229.

Rossi, R.E., Mulla, D.J., Journel, A.G., and Franz, E.H. 1992. Geostatistical tools for modeling and interpreting ecological spatial dependence. Ecol. Monogr. 63: 277-314.

Rovinsky, A.B., Adiwidjaja, H., Yakhnin, V.Z., and Menzinger, M. 1997. Patchiness and enhancement of productivity in plankton ecosystems due to the differential advection of predator and prey. Oikos 78: 101-106.

Rudstam, L.G. 1989. A bioenergetic model for Mysis growth and consumption applied to a Baltic population of *Mvsis mixta*. J. Plankton Res. 11: 971-983.

Rudstam, L.G., Parker, S.L., Einhouse, D.W., Witzel, L.D., Warner, D.M., Stritzel, J.L., Parrish, D.L., and Sullivan, P.J. 2003. Application of in situ target-strength estimations in lakes: examples from rainbow-smelt surveys in Lakes Erie and Champlain. ICES J. Mar. Sci. 60: 500-507.

Rudstam, L.G., Knudsen, F.R., Balk, H., Gal, G., Boscarino, B.T., and Axenrot, T. 2008. Acoustic characterization of *Mysis relicta* at multiple frequencies. Can. J. Fish. Aquat. Sci. 65: 2769-2779.

Ryther, J.H. 1969. Photosynthesis and fish production in sea. Science 166: 72–76.

Santos, A.M.P., Borges, M.F., and Groom, S. 2001. Sardine and horse mackerel recruitment and upwelling off Portugal. ICES J. Mar. Sci. 58: 589-596.

Saros, J.E., Interlandi, S.J., Doyle, S., Michel, T.J., and Williamson, C.E. 2005. Are the deep chlorophyll maxima in alpine lakes primarily induced by nutrient availability, not UV avoidance? Arct. Antarct. Alp. Res. 37: 557-563.

Schaerer, S., and Neumeyer, C. 1996. Motion detection in goldfish investigated with the optomotor response is "color blind". Vision Res. 36: 4025-4034.

Schram, S.T., Selgeby, J.H., Bronte, C.R., and Swanson, B.L. 1995. Population recovery and natural recruitment of lake trout at Gull Island Shoal, Lake Superior, 1964-1992. J. Great Lakes Res. 21(Suppl. 1): 225-232.

Shaver, G.R. 2006. Spatial heterogeneity: past, present, and future. *In* Ecosystem function in heterogeneous landscapes. *Edited by* G.M. Lovett, M.G. Turner, C.G. Jones and K.C. Weathers. Springer Press, New York, N.Y. pp. 443-450.

Sih, A. 1984. The behavioral response race between predator and prey. Am. Nat. 123: 143-150.

Sly, P.G. 1988. Interstitial water quality of lake trout spawning habitat. J. Great Lakes Res. 14: 301–315.

Smith, S.H. 1968. Species succession and fishery exploitation in the Great Lakes. J. Fish. Res. Board Can. 25: 667-693.

Smith, S.H. 1972. Factors of ecologic succession in oligotrophic fish communities of the Laurentian Great Lakes. J. Fish. Res. Board Can. 29: 717-730.

Sprules, W. G., Jin, E. H., Herman, A. W., and Stockwell, J. D. 1998. Calibration of an optical plankton counter for use in fresh water. Limnol. Oceanogr. 43: 726-733.

Stanton, T.K., Wiebe, P.H., Chu, D., Benfield, M.C., Scanlon, L., Martin, L.V., and Eastwood, R.L. 1994. On acoustic estimates of biomass. ICES J. Mar. Sci. 51: 505-512.

Stanton, T.K., Chu, D., and Wiebe, P.H. 1996. Acoustic scattering characteristics of several zooplankton groups. ICES J. Mar. Sci. 53: 289-295.

Stanton, T.K., and Chu, D. 2000. Review and recommendations for the modelling of acoustic scattering by fluid-like elongated zooplankton: euphausiids and copepods. ICES J. Mar. Sci. 57: 793–807.

Stauffer, T.M. 1981. Collecting gear for lake trout eggs and fry. Prog. Fish-Cult. 43: 186-193.

Sterner, R.W., Smutka, T.M., McKay, R.M.L., Xiaoming, Q., Brown, E.T., Sherrell, R.M. 2004. Phosphorus and trace metal limitation of algae and bacteria in Lake Superior. Limnol. Oceanogr. 49: 495–507.

Sterner, R.W. 2010. In situ-measured primary production in Lake Superior. J. Great Lakes Res. 36: 139-149.

Stewart, D.J., Weininger, D., Rottiers, D.V., and Edsall, T.A. 1983. An energetic model for lake trout, *Salvelinus namaycush*: Application to the Lake Michigan population. Can. J. Fish. Aquat. Sci. 40: 681-698.

Svensson, U. 1978. Examination of the summer stratification. Nord. Hydrol. 9: 105-120.

Swedberg, D.V., and Peck, J.W. 1984. Food of young of-the-year lake trout (*Salvelinus namaycush*) in Presque Isle Harbor, Lake Superior. J. Great Lakes Res. 10: 280-285.

Thackeray, S.J., George, D.G., Jones, R.I., and Winfield, I.J. 2004. Quantitative analysis of the importance of wind-induced circulation for the spatial structuring of planktonic populations. Fresh. Biol. 49: 1091-1102.

Therneau, T.M., and Atkinson, E.J. 1997. An introduction to recursive partitioning using the RPART routines. Mayo Clinic, section of statistics. Tech. report no. 61.

Tillitt, D.E., Zajicek, J.L., Brown, S.B., Brown, L.R., Fitzsimons, J.D., Honeyfield, D.C., Holey, M.E., and Wright, G.M. 2005. Thiamine and thiaminase status in forage fish of salmonines from Lake Michigan. J. Aquat. Anim. Health 17: 13-25.

Trevorrow, M.V., and Tanaka, Y. 1997. Acoustic and in situ measurements of freshwater amphipods (*Jesogammarus annandalei*) in Lake Biwa, Japan. Limnol. Oceanogr. 42: 121-132.

Turner, M.G., Gardner, R.H., and O'Neill, R.V. 2001. Landscape Ecology: In Theory and Practice. Springer-Verlag, New York, N.Y.

Turner, M.G., and Chapin, F.S. III. 2005. Causes and consequences of spatial heterogeneity in ecosystem function. *In* Ecosystem function in heterogeneous landscapes. *Edited by* G.M. Lovett, M.G. Turner, C.G. Jones and K.C. Weathers. K.C. Springer Press, New York, N.Y. pp. 9-30.

Tyler, J.A., and Rose, K.A. 1994. Individual variability and spatial heterogeneity in fish population models. Rev. Fish Biol. Fish. 4: 91-123.

Utne-Palm, A.C. 1999. The effect of prey mobility, prey contrast, turbidity and spectral composition on the reaction distance of *Gobiusculus flavescens* to its planktonic prey. J. Fish Biol. 54: 1244-1258.

Utne-Palm, A.C., and Bowmaker, J.K. 2006. Spectral sensitivity of the two-spotted goby *Gobiusculus flavescens* (Fabricius): a physiological and behavioural study. J. Exper. Biol. 209: 2034-2041.

Ventling-Schwank, A.R., and Livingstone, D.M. 1994. Transport and burial as a cause of whitefish (*Coregonus* sp.) egg mortality in a European lake. Can. J. Fish. Aquat. Sci. 51: 1908–1919.

Vogel, J.L., and Beauchamp, D.A. 1999. Effects of light, prey size, and turbidity on reaction distances of lake trout (*Salvelinus namaycush*) to salmonid prey. Can. J. Fish. Aquat. Sci. 68: 706-717.

Wagner-Döbler, I., and Jacobs, J. 1988. High frequency echography: quantitative relation between echogram density and vertical distribution of *Chaoborus* larvae. Arch. Hydrobiol. 112: 567-578.

Ware, D.M., and Thomson, R.E. 2005. Bottom-up ecosystem trophic dynamics determine fish production in the Northeast Pacific. Science 308: 1280-1284.

Watson, N.H., and Wilson, J.B. 1978. Crustacean zooplankton of Lake Superior. J. Great Lakes Res. 4: 481-496.

Wellborn, G.A. 1994. Size-biased predation and prey life histories: a comparative study of freshwater amphipod populations. Ecology 75: 2104-2117.

White, E.M., Church, S.C., Willoughby, L.J., Hudson, S.J., and Partridge, J.C. 2005. Spectral irradiance and foraging efficiency in the guppy, *Poecilia reticulata*. Anim. Behav. 69: 519-527.

White, E.P., and Brown, J.H. 2005. The template: patterns and processes of spatial variation. *In* Ecosystem function in heterogeneous landscapes. *Edited by* G.M. Lovett, M.G. Turner, C.G. Jones and K.C. Weathers. Springer Press, New York, N.Y. pp. 31-48.

Wiebe, P.H., Greene, C.H., Stanton, T.K., and Burczynski, J. 1990. Sound scattering by live zooplankton and micronekton: empirical studies with a dual-beam acoustical system. J. Acoust. Soc. Am. 88: 2346-2360.

Winberg, G.G. 1956. Rate of metabolism and food requirements of fishes. Belorussian Univ., Minsk. (Transl. by Fish. Res. Board Can. Transl. Ser. No. 164, 1960).

Winnell, M.H., and White, D.S. 1984. Ecology of shallow and deep water populations of *Pontoporeia hoyi* (Smith) (Amphipoda) in Lake Michigan. Fresh. Invert. Biol. 3: 118-138.

Worm, B., and Meyers, R.A. 2003. Meta-analysis of cod-shrimp interactions reveals top-down control in oceanic food webs. Ecology 84: 162-173.

Wright, D.I., and O'Brien, W.J. 1982. Differential location of *Chaoborus* larvae and *Daphnia* by fish: The importance of motion and visible size. Am. Midl. Nat. 108: 68-73.

Wright, D.I., and O'Brien, W.J. 1984. The development and field test of a tactical model of the planktivorous feeding of white crappie (*Pomoxis annularis*). Ecol. Monogr. 54: 65-98.

Yule, D.L., Stockwell, J.D., Cholwek, G.A., Evrard, L.M., Schram, S., Seider, M., and Symbal, M., 2006. Evaluation of methods to estimate lake herring spawner abundance in Lake Superior. Trans. Am. Fish. Soc. 135: 680–69.

Yule, D.L., Stockwell, J.D., Schreiner, D.R., Evrard, L.M., Balge, M., and Hrabik, T.R. 2009. Can pelagic forage fish and spawning cisco (*Coregonus artedi*) biomass in the western arm of Lake Superior be assessed with a single summer survey? Fish. Res. 96: 39-50.

Zhou, M., Zhu, Y., Putnam, S., and Peterson, J. 2001. Mesoscale variability of physical and biological fields in Southeastern Lake Superior. Limnol. Oceanogr. 46: 679-688.

Zimmerman, M.S., and Krueger, C.C. 2009. An ecosystem perspective on re-establishing native deepwater fishes in the Laurentian Great Lakes. N. Am. J. Fish. Manage. 29: 1352–1371.